



ERASMUS INTENSIVE PROGRAMME

OPTIMAX#2014

Radiation dose and image quality
optimisation in medical imaging

Lisbon, Portugal

Edited by Peter Hogg and Luis Lança



ERASMUS INTENSIVE PROGRAMME

OPTIMAX 2014 – radiation dose and image quality optimisation in medical imaging

L i s b o n , P o r t u g a l

Edited by Peter Hogg¹, and Luis Lança²

1) Professor of Radiography, University of Salford, Manchester, UK

2) Radiography Program Leader, Lisbon School of Health Technology (ESTeSL), Portugal



PUBLISHING INFORMATION

Open Source

Publisher



Attribution-NonCommercial-ShareAlike

CC BY-NC-SA

ISBN 978-1-907842-60-3

ACKNOWLEDGEMENTS

Siemens Healthcare Portugal

For the loan of essential equipment

Sumed Medical

For the loan of essential equipment

Coimbra Health School

For the loan of paediatric phantom

SAMS Hospital (Lisbon)

For facilitating CT images acquisition

ACKNOWLEDGEMENTS

We should like to thank the following people:

Carla Lança

Lecturer in Orthoptics

Orthoptic Department – Lisbon School of Health Technology, Polytechnic Institute of Lisbon

Lisbon, Portugal

For performing and analysing the visual acuity tests

Leslie Robinson

Senior Lecturer

School of Health Sciences

University of Salford

Manchester, United Kingdom

For delivering essential lectures on team theory and project management

Maria da Luz Antunes

Head Librarian

Lisbon School of Health Technology, Polytechnic Institute of Lisbon

Lisbon, Portugal

Editor advisory

Miguel Mendes

Wok Design

Designer

OPTIMAX Participants



C O N T E N T S

Foreword	6	Foreign bodies in orbits	53
Introduction	7	<i>Review article - X Radiation dose implications in screening patients with ferromagnetic IOFBs prior to MRI: A literary review</i>	53
Iterative Reconstruction in CT	9	<i>Experimental article - A balance between image quality and effective dose in orbital X-ray screening for ferromagnetic IOFBs: A Pilot Study</i>	59
<i>Review Article – An evaluation of SAFIRE’s potential to reduce the dose received by paediatric patients undergoing CT: a narrative review</i>	9	<i>Pressure mapping</i>	69
<i>Experimental article – Maintaining image quality for paediatric chest CTs while lowering dose: FBP versus SAFIRE</i>	15	<i>Review article - The effects of clinical support surfaces on pressure as a risk factor in the development of Pressure Ulcers, from a radiographical perspective - A narrative literature review.</i>	69
<i>Review article – The impact of Sinogram-Affirmed Iterative Reconstruction on patient dose and image quality compared to filtered back projection: a narrative review</i>	21	<i>Experimental article - An experimental study to compare the interface pressure and experience of healthy participants when lying still for 20 minutes in a supine position on two different imaging surfaces</i>	75
<i>Research article – A comparison of Sinogram Affirmed Iterative Reconstruction and filtered back projection on image quality and dose reduction in paediatric head CT: a phantom study</i>	27	<i>Paediatric pelvis - Cu filtration</i>	81
Cobb Angle	37	<i>Review article – A narrative review on the reduction of effective dose to a paediatric patient by using different combinations of kVp, mAs and additional filtration whilst maintaining image quality</i>	81
<i>Review article - Optimisation of exposure parameters for spinal curvature measurements in paediatric radiography</i>	37	<i>Experimental article - Reducing effective dose to a paediatric phantom by using different combinations of kVp, mAs and additional filtration whilst maintaining image quality.</i>	85
<i>Research article - Optimisation of paediatrics computed radiography for full spine curvature measurements using a phantom: a pilot study</i>	43		

Foreword

Following the successful OPTIMAX summer school held in Salford, 2013, we organised another OPTIMAX summer school in Lisbon during August, 2014. Sixty six people participated, comprising PhD, MSc and BSc students as well as tutors from the 5 European partners. Professional mix was drawn from engineering, medical physics / physics, radiography and occupational therapy. The summer school was hosted by the Lisbon School of Health Technology, Polytechnic Institute of Lisbon, Portugal. It was funded by Erasmus, aside one additional student who was funded by Nuffield. The summer school comprised of lectures and group work in which experimental research projects were conducted in six teams. Team project focus varied, with two concentrating on iterative reconstruction (CT), one into interface pressure

mapping (between human body and imaging couch) whilst the remaining three focused to determining ways to reduce dose whilst preserving image quality for different projection radiography procedures. The summer school culminated in a conference, in which each team presented two oral papers. One paper reviewed the literature on their area of interest, whilst the other considered their experimental findings. The oral papers were also presented in written format, in journal article style, and after editing they have been included within this book. At the time of editing this book, several of the experimental papers had been submitted to conferences and some lecturers have commenced development work in order to make them fit for submission to journals.

OPTIMAX 2014 Steering Committee

- Lança L, Lisbon School of Health Technology, Polytechnic Institute of Lisbon, Portugal
 - Buissink C, Department of Medical Imaging and Radiation Therapy, Hanze University of Applied Sciences, Groningen, The Netherlands
 - Jorge J, Haute École de Santé Vaud – Filière TRM, University of Applied Sciences and Arts of Western Switzerland, Lausanne, Switzerland
 - Sanderud A, Department of Life Sciences and Health, Oslo and Akershus University College of Applied Sciences, Oslo, Norway
 - Hogg P, School of Health Sciences, University of Salford, Manchester, United Kingdom
-

Introduction

Medical imaging is a powerful diagnostic tool. Consequently, the number of medical images taken has increased vastly over the past few decades. The most common medical imaging techniques use X-radiation as the primary investigative tool. The main limitation of using X-radiation is associated with the risk of developing cancers. Alongside this, technology has advanced and more centres now use CT scanners; these can incur significant radiation burdens compared with traditional X-ray imaging systems. The net effect is that the population radiation burden is rising steadily. Risk arising from X-radiation for diagnostic medical purposes needs minimising and one way to achieve this is through reducing radiation dose whilst optimising image quality.

All ages are affected by risk from X-radiation however the increasing population age highlights the elderly as a new group that may require consideration. Of greatest concern are paediatric patients: firstly they are more sensitive to radiation; secondly their younger age means that the potential detriment to this group is greater.

Containment of radiation exposure falls to a number of professionals within medical fields, from those who request imaging to those who produce the image. These staff are supported in their radiation protection role by engineers, physicists and technicians. It is important to realise that radiation protection is currently a major European focus of interest and minimum competence levels in radiation protection for radiographers have been defined through the integrated activities of the EU consortium called MEDRAPET. The outcomes of this project have been used by the European Federation of Radiographer Societies to describe the European Qualifications Framework levels for radiographers in radiation protection. Though variations exist between European countries radiographers and nuclear medicine technologists are normally the professional groups who are responsible for exposing screening populations

and patients to X-radiation. As part of their training they learn fundamental principles of radiation protection and theoretical and practical approaches to dose minimisation. However dose minimisation is complex – it is not simply about reducing X-radiation without taking into account major contextual factors. These factors relate to the real world of clinical imaging and include the need to measure clinical image quality and lesion visibility when applying X-radiation dose reduction strategies. This requires the use of validated psychological and physics techniques to measure clinical image quality and lesion perceptibility.

The OPTIMAX summer school allowed students and tutors to experience new ways of optimising dose and image quality. The summer school has radiation dose limitation and image quality as core themes and it draws on expertise in radiography, radiobiology, psychology and medical physics. The target groups for OPTIMAX include under- and post-graduate students of diagnostic radiography, nuclear medicine technology, biomedical science, engineering and physics. Indirect target groups include qualified staff, mainly physicists and radiographers.

Assessment of image quality (using physical or visual techniques) is a low order task as the results are commonly used to infer whether an image is fit for purpose. Image quality assessment cannot determine whether the image is fit for purpose or not, as higher order observer studies are required to determine this. Image quality analyses are therefore pseudo measures. Nevertheless image quality analyses are common within the literature and practice and OPTIMAX 2014 placed a particular emphasis on visual and to some extent physical techniques to assess image quality. Only one OPTIMAX 2014 study (Cobb Angle) addressed a high order task (observer performance), in which vertebral angles were assessed. Generally speaking the ROC methodologies have been used extensively for such purposes.

ITERATIVE RECONSTRUCTION IN CT

Review Article – An evaluation of SAFIRE's potential to reduce the dose received by paediatric patients undergoing CT: a narrative review

Synnøve Borge^a, Nina Campbell^b, Ana Gomes^c, Aysha M. Raszkowski^a, Jan Willem Rook^d, Audun Sanderud^a, Anique Vallinga^d, Audrey Vouillamoz^e, Carst Buissink^d

a) Department of Health, Radiography, Oslo and Akershus University College of Applied Sciences, Norway

b) School of Health Sciences, University of Salford, United Kingdom

c) Lisbon School of Health Technology (ESTeSL), Portugal

d) Department of Medical Imaging and Radiation Therapy, Hanze University of Applied Sciences, Groningen, The Netherlands

e) Haute École de Santé Vaud – Filière TRM, University of Applied Sciences and Arts of Western Switzerland, Lausanne, Switzerland



KEYWORDS

SAFIRE
Iterative Reconstruction CT
Paediatric
Patients
Chest
Radiation risk Dose reduction

ABSTRACT

Introduction: The purpose of this review is to gather and analyse current research publications to evaluate Sinogram-Affirmed Iterative Reconstruction (SAFIRE). The aim of this review is to investigate whether this algorithm is capable of reducing the dose delivered during CT imaging while maintaining image quality. Recent research shows that children have a greater risk per unit dose due to increased radiosensitivity and longer life expectancies, which means it is particularly important to reduce the radiation dose received by children.

Discussion: Recent publications suggest that SAFIRE is capable of reducing image noise in CT images, thereby enabling the potential to reduce dose. Some publications suggest a decrease in dose, by up to 64% compared to filtered back projection, can be accomplished without a change in image quality. However, literature suggests that using a higher SAFIRE strength may alter the image texture, creating an overly 'smoothed' image that lacks contrast. Some literature reports SAFIRE gives decreased low contrast detectability as well as spatial resolution. Publications tend to agree that SAFIRE strength three is optimal for an acceptable level of visual image quality, but more research is required. The importance of creating a balance between dose reduction and image quality is stressed. In this literature review most of the publications were completed using adults or phantoms, and a distinct lack of literature for paediatric patients is noted.

Conclusion: It is necessary to find an optimal way to balance dose reduction and image quality. More research relating to SAFIRE and paediatric patients is required to fully investigate dose reduction potential in this population, for a range of different SAFIRE strengths.

INTRODUCTION

Computed tomography (CT) is valuable for diagnostic insight. However, X-ray images taken during CT examinations expose the patient to a high dose of radiation, which has the potential to cause cancer.

Recent US cancer risk projections estimate 1 cancer per

1000 brain CT scans for patients under 5 years of age¹; it is therefore understandable that radiation dose has been a longstanding concern for paediatric patients, particularly when multiple scans are required.

One of the possible solutions for dose reduction is the use of iterative reconstruction instead of conventional filtered back projection (FBP). Sinogram Affirmed Iterative

Reconstruction (SAFIRE), developed by Siemens, is one of the newest available iterative algorithms. Based on its noise reduction capabilities, it is believed that this algorithm may have the potential to significantly reduce dose in children undergoing CT scans without sacrificing image quality.

This review attempts to discuss whether SAFIRE is suitable for dose reduction in patients undergoing CT. Our focus is to analyse whether dose can be reduced for paediatric patients whilst maintaining an image quality that is acceptable for diagnosis.

Literature search and review strategy

Literature searching was conducted on several computerised databases (ScienceDirect, PubMed), online journals and publishers were also utilised, such as AJR Online and Springer.

As SAFIRE is relatively new, published articles available are limited. English articles from all years of publishing were included in this literature review; dates ranged from 2012 to 2014. Keywords used whilst searching for literary references were: SAFIRE, paediatric, CT. Due to a small number of articles, research focussing on SAFIRE being used for adults was also considered for this review article.

Articles were excluded on the basis of not being related to: SAFIRE CT reconstruction, CT exposure for paediatric patients and the related risks, comparisons of SAFIRE with standard FBP. Most articles related to angiography were also excluded due to the use of high-contrast dyes. Ultimately, 21 articles were selected for inclusion in this review article.

DISCUSSION

CT for paediatric patients

Use of CT has increased in recent years and, according to studies by Shah and Brenner et al.²⁻³, in 2007 there were 62 million CT examinations taken in the USA; 7 million of which were children. This is a concern for paediatric patients and, unfortunately, this number is steadily increasing each year.

The risk per unit dose for paediatric patients is greater than for adults, and it is a concern that some institutions do not lower the exposure for younger patients⁴.

There are two reasons why children have a higher risk of developing cancer due to radiation exposure. Firstly, the

life expectancy is longer than in adults. Secondly, children have rapidly dividing cells which makes them more sensitive to radiation².

The radiosensitivity of children has been subject to debate and it is currently estimated that for 25% of cancer types, children are more susceptible than adults, and for 20% of tumour types the data is inconclusive⁵. It has been estimated that a one year old child is as much as ten times more susceptible to radiation-induced cancer than an adult⁴.

In recent years, based on the steadily increasing use of CT, more attention has been focussed on trying to reduce patient dose. Frush and McCollough et al.⁶⁻⁷ describe different strategies that are currently used or have been proposed to solve this problem, such as the use of different modalities or a reduction in acquisition parameters. Another possibility is the use of an iterative reconstruction (IR) algorithm instead of FBP.

FBP and IR

CT image reconstruction was a longstanding issue of debate, mostly because the images created with the original technique (back projection) did not have sufficient quality. Back projection created projections of the object from many angles and the end result was a blurry image. FBP was a development of back projection, which additionally filtered all of the raw data to minimize artefacts and give better overall image quality⁸. FBP is currently the most used reconstruction technique. Unfortunately, this algorithm has a trade-off between dose and image quality, which limits by how much the dose can be reduced⁹.

IR techniques generate images using several iterative steps to create images that are more precise¹⁰, meaning dose can be lowered. IR was used in first generation CTs, but despite its potential for dose reduction, it was dismissed due to too much data and too little computer power available¹¹.

In the past few years new and improved IR algorithms have emerged. Unfortunately there are concerns among some radiologists that IR creates a 'smeared' effect¹², which in turn could mean that pathology could go unnoticed. Equally there is a perception that there is not yet an IR technique which produces better visual (clinical) image quality than FBP for a lower dose¹³. However it is well known that physical measures of image quality (e.g., noise and CNR) improve when using IR.

One of the first generation IR algorithms to be introduced into daily practice was IRIS (Iterative Reconstruction

in Image Space, 2009). A study by Hu et al. noted that IRIS gave the possibility of 40% dose reduction while maintaining image quality. Unfortunately, the time needed to reconstruct the images was 4-5 times longer than for FBP¹⁴, making IRIS difficult to use clinically.

SAFIRE

The Sinogram-Affirmed Iterative Reconstruction algorithm is a new technique developed by Siemens, and it has been widely considered innovative in comparison to its predecessors¹⁵. SAFIRE uses both projection space data and image space data to reconstruct images quickly with high spatial resolution. There are currently five different strengths of SAFIRE that can be utilised, with SAFIRE 5 being the highest¹⁶.

One of the earliest publications (Schulz et al.¹⁷) relating to SAFIRE tested all five of the strengths, for soft and hard kernels, for CT slices of 1 mm and 3 mm. It was suggested that SAFIRE performed best in the bony kernel and that SAFIRE 5 had the greatest noise reduction potential, with noise being reduced by 15-85%. A similar result was found in the publication of Wang et al.⁹, who also found that noise was reduced in SAFIRE images. Furthermore, they compared full-dose FBP images with half-dose SAFIRE 3 images and concluded the noise to be of the same level, suggesting that SAFIRE had a great potential for dose reduction whilst maintaining image quality.

This potential was furthered by a study conducted by Kalmar et al. who investigated the use of SAFIRE for thoracic and abdominal CTs for standard dose FBP and reduced dose IR¹⁸. Subjectively, both images received approximately the same image quality ratings. It was evaluated that an average dose reduction of 64% and 58% was achieved for thoracic and abdominal CTs respectively. Similarly, Baker et al.¹⁹ found that SAFIRE created images with less noise at 70% and 50% dose when compared to FBP at 100%. It was concluded that SAFIRE could create images with higher CNR at lower doses. However, for low-dose and low-contrast images, objects were invisible. Thus, Baker et al. emphasised a need for finding a balance between dose and image quality.

On the other hand, a study by Bratanova et al. concluded that low contrast detectability was higher with SAFIRE than FBP, and it increased with SAFIRE strength. They used two phantoms (low and high contrast), where one part simulated lesion-free background and with another part simulating hypodense lesions. The results showed that not only did SAFIRE produce images with lower noise, but also equal spatial resolution compared to FBP²⁰.

The diagnostic accuracy of SAFIRE was also studied by Moscariello et al. This study used full dose FBP and half dose SAFIRE images. Half dose images were created using 50% of the raw data containing the full dose projections. The results stated that SAFIRE had higher CNR and lower noise. At the same time, image quality was equal or better than that of FBP. This allows for a possible dose reduction of 50% (FBP: 6.4 ± 4.3 mSv and SAFIRE: 3.2 ± 2.1 mSv)²¹.

A phantom-based study by Ghetty et al.¹⁵ suggested that the quality-dose balance recommended by Baker¹⁹ could be achieved by utilising the different strengths of SAFIRE. A noise-power-spectrum (NPS) showed that SAFIRE 4 and SAFIRE 5 performed better at lower frequencies, and concluded that this could be the compromise for dose and image quality in SAFIRE. Furthermore, a study conducted by Yang et al.²² tested all strengths of SAFIRE for low dose lung CT images and determined that a higher strength did not necessarily mean a greater image quality, even though the noise decreased. This was because the higher strengths altered the texture pattern of the image and resulted in unfamiliar image impressions, such as blotchy artefacts in sharp transition zones due to excessive smoothing. Yang et al. concluded that SAFIRE 3 was optimal for the lung. Similarly, a second study²³ investigated SAFIRE 3 and SAFIRE 4 for lung CTs for patients with mean BMI of 22.7 and 25.8 kg/m² respectively, and found that all 120 datasets were feasible for analysis. Diagnostic image quality was assessed as 100% and 98% for SAFIRE at 100 kVp and 80 kVp, an improvement from the 96% and 88% assessed for FBP. Subsequently, doses of 0.7 mSv and 0.4 mSv were deemed acceptable for diagnostic imaging with the use of SAFIRE, further suggesting that individually selecting the strength level for IR is advantageous.

Following this, another experiment performed by Lee et al. tested to see if an ultra low dose CT (ULDCT) of 0.3 mSv reconstructed using SAFIRE was achievable. This was compared with a reduced dose CT (RDCT) of 2.9 mSv. It was found that 91.9% of ULDCT and 100% of RDCT were considered sufficient for diagnosis²⁴. However, patients with a BMI of less than 25 had a greater success rate of 95% for SAFIRE, thus agreeing with the previous study. From the results of the previous study, completed on adults, it could be implied that SAFIRE's ability is greatly affected by selecting the relevant strength depending on patient size or BMI. This could concern paediatric patients due to their smaller sizes and smaller BMI. However, studies assessing SAFIRE's use with children for a range of BMIs or sizes are limited.

Han et al. studied the use of SAFIRE for cardiac CT datasets, for patients with a mean age of 4.1 years²⁵. They adjusted the kVp according to the weight of the patient: 80

kVp if under 65 kg, 100 kVp if above. Their results were in agreement with previous studies; there was little to no difference in diagnostic quality of FBP versus SAFIRE images, and IR images had a decrease in noise and an increase of SNR and CNR. Effective dose and SAFIRE strength used was not reported.

The strength of SAFIRE frequently goes unmentioned in articles, and so it is challenging to predict which strength might be the most efficient for younger patients. Based on aforementioned studies it might be concluded that SAFIRE 2 or SAFIRE 3 would be best, depending on patient size. Kim et al.²⁶ investigated SAFIRE strengths 2, 3 and 4 specifically, for paediatric abdominal CT patients with a range of kVp and mAs. SAFIRE 3 was concluded as optimal for subjective image quality but SAFIRE 4 was optimal for objective image quality, thus agreeing with previously mentioned studies relating to the lung. It is suggested that the mid-strengths (2, 3 or 4) tend to rate higher for physical and visual image quality measures, due to SAFIRE 5 becoming too blurred.

According to the study the possibility of 64.2% dose reduction exists for paediatric abdominal patients.

CONCLUSION

It can be concluded that SAFIRE can significantly reduce noise in images in comparison to FBP. Multiple articles have stated the potential of SAFIRE for significant dose reduction, with most implying a capability of reducing dose by around 50%.

Overall, SAFIRE does have the potential to significantly reduce dose delivered to paediatric patients undergoing CT. However, more research is required to study the extent at which the dose can be reduced, as articles relating to paediatric patients are limited. It is also imperative to further test different strengths of SAFIRE, particularly at lower levels of kVp and mAs, for paediatric patients in order to test the effects on image quality and dose reduction.

REFERENCES

- Pearce MS, Salotti JA, Little MP, McHugh K, Lee C, Kim KP, et al. Radiation exposure from CT scans in childhood and subsequent risk of leukaemia and brain tumours: a retrospective cohort study. *Lancet*. 2012;380(9840):499-505.
- Shah NB, Platt SL. ALARA: is there a cause for alarm? Reducing radiation risks from computed tomography scanning in children. *Curr Opin Pediatr*. 2008;20(3):243-7.
- Brenner DJ, Hall EJ. Computed tomography: an increasing source of radiation exposure. *New Eng J Med*. 2007;357(22):2277-84.
- Brenner DJ, Elliston CD, Hall EJ, Berdon WE. Estimated risks of radiation-induced fatal cancer from pediatric CT. *AJR Am J Roentgenol*. 2001;176(2):289-96.
- Rehani MM. Are children more sensitive to radiation than adults? *Eur Soc Radiol News*. 2013 [cited 2014 Aug 11];(Sep). Available from: http://www.myesr.org/html/img/pool/Radiation_Protection_ESR_Work_Sept_2013.pdf
- Frush DP. Pediatric CT: practical approach to diminish the radiation dose. *Pediatr Radiol*. 2002;32(10):714-7.
- McCullough CH, Primak AN, Braun N, Kofler J, Yu L, Christner J. Strategies for reducing radiation dose in CT. *Radiol Clin North Am*. 2009;47(1):27-40.
- Smith SW. Special imaging techniques. In Smith SW, editor. *The scientist and engineer's guide to digital signal processing* [Internet]. San Diego: California Technical Publishing; 1997. chap. 25. Available from: <http://www.dspguide.com/ch25.htm>
- Wang H, Tan B, Zhao B, Liang C, Xu Z. Raw-data-based iterative reconstruction versus filtered back projection: image quality of low-dose chest computed tomography examinations in 87 patients. *Clin Imaging*. 2013;37(6):1024-32.
- Beister M, Kolditz D, Kalender WA. Iterative reconstruction methods in X-ray CT. *Phys Medica*. 2012;28(2):94-108.
- Hsieh J, Nett B, Yu Z, Sauer K, Thibault JB, Bouman CA. Recent advances in CT image reconstruction. *Curr Radiol Rep*. 2013;1(1):39-51.
- Harrison L. Iterative reconstruction equal to filtered back projection. *Medscape Med News* [Internet]. 2014 May 9 [cited 2014 Aug 10]. Available from: <http://www.medscape.com/viewarticle/824933>
- Schindera ST, Odedra D, Raza SA, Kim TK, Jang HJ, Szucs-Farkas Z, et al. Iterative reconstruction algorithm for CT: can radiation dose be decreased while low-contrast detectability is preserved? *Radiology*. 2013;269(2):511-8.

14. Hu XH, Ding XF, Wu RZ, Zhang MM. Radiation dose of non-enhanced chest CT can be reduced 40% by using iterative reconstruction in image space. *Clin Radiol*. 2011;66(11):1023-9.
15. Ghetti C, Palleri F, Serreli G, Ortenzia O, Ruffini L. Physical characterization of a new CT iterative reconstruction method operating in sinogram space. *J Appl Clin Med Phys*. 2013;14(4):4347.
16. Grant K, Raupach R. SAFIRE: Sinogram Affirmed Iterative Reconstruction [Internet]. 2012 [cited 2014 Aug 11]. Available from: <https://www.healthcare.siemens.com/computed-tomography/options-upgrades/clinical-applications/safire>
17. Schulz B, Beeres M, Bodelle B, Bauer R, Al-Butmeh F, Thahammer A, et al. Performance of iterative image reconstruction in CT of the paranasal sinuses: a phantom study. *AJNR Am J Neuroradiol*. 2013;34(5):1072-6.
18. Kalmar PI, Quehenberger F, Steiner J, Lutfi A, Bohlens D, Talakic E, et al. The impact of iterative reconstruction on image quality and radiation dose in thoracic and abdominal CT. *Eur J Radiol*. 2014;83(8):1416-20.
19. Baker ME, Dong F, Primak A, Obuchowski NA, Einstein D, Gandhi N, et al. Contrast-to-noise ratio and low-contrast object resolution on full- and low-dose MDCT: SAFIRE versus filtered back projection in a low-contrast object phantom and in the liver. *AJR Am J Roentgenol*. 2012;199(1):8-18.
20. Von Falck C, Bratanova V, Rodt T, Meyer B, Waldeck S, Wacker F, et al. Influence of sinogram affirmed iterative reconstruction of CT data on image noise characteristics and low-contrast detectability: an objective approach. *PLoS One*. 2013;8(2):e56875.
21. Moscariello A, Takx RA, Shoenf UJ, Renker M, Zwerner PL, O'Brien TX, et al. Coronary CT angiography: image quality, diagnostic accuracy, and potential for radiation dose reduction using a novel iterative image reconstruction technique: comparison with traditional filtered back projection. *Eur Radiol*. 2011;21(10):2130-8.
22. Yang WJ, Yan FH, Liu B, Pang LF, Hou L, Zhang H, et al. Can sinogram-affirmed iterative (SAFIRE) reconstruction improve imaging quality on low-dose lung CT screening compared with traditional filtered back projection (FBP) reconstruction? *J Comput Assist Tomogr*. 2013;37(2):301-5.
23. Baumueeller S, Winklehner A, Karlo C, Goetti R, Flohr T, Russi EW, et al. Low-dose CT of the lung: potential value of iterative reconstructions. *Eur Radiol*. 2012;22(12):2597-606.
24. Lee SW, Kim Y, Shim SS, Lee JK, Lee SJ, Ryu YJ, et al. Image quality assessment of ultra low-dose chest CT using sinogram-affirmed iterative reconstruction. *Eur Radiol*. 2014;24(4):817-26.
25. Han BK, Grant KL, Garberich R, Sedlmair M, Lindberg J, Lesser JR. Assessment of an iterative reconstruction algorithm (SAFIRE) on image quality in pediatric cardiac CT datasets. *J Cardiovasc Comput Tomogr*. 2012;6(3):200-4.
26. Kim JH, Kim MJ, Kim HY, Lee MJ. Radiation dose reduction and image quality in pediatric abdominal CT with kVp and mAs modulation and an iterative reconstruction technique. *Clin Imaging*. 2014;38(5):710-4.

Experimental article – Maintaining image quality for paediatric chest CTs while lowering dose: FBP versus SAFIRE

Synnøve Borgea, Nina Campbell^b, Ana Gomes^c, Aysha M. Raszkowski^a, Jan Willem Rook^d, Audun Sanderud^a, Anique Vallinga^d, Audrey Vouillamoz^e, Carst Buissink^d

a) Department of Health, Radiography, Oslo and Akershus University College of Applied Sciences, Norway

b) School of Health Sciences, University of Salford, United Kingdom

c) Lisbon School of Health Technology (ESTeSL), Portugal

d) Department of Medical Imaging and Radiation Therapy, Hanze University of Applied Sciences, Groningen, The Netherlands

e) Haute École de Santé Vaud – Filière TRM, University of Applied Sciences and Arts of Western Switzerland, Lausanne, Switzerland



SAFIRE

FBP
CT
Paediatric patients
Chest
Image quality
Dose reduction

ABSTRACT

Objectives: Children have a greater risk from radiation, per unit dose, due to increased radiosensitivity and longer life expectancies. It is of paramount importance to reduce the radiation dose received by children. This research concerns chest CT examinations on paediatric patients. The purpose of this study was to compare the image quality and the dose received from imaging with images reconstructed with filtered back projection (FBP) and five strengths of Sinogram-Affirmed Iterative Reconstruction (SAFIRE).

Methods: Using a multi-slice CT scanner, six series of images were taken of a paediatric phantom. Two kVp values (80 and 110), 3 mAs values (25, 50 and 100) and 2 slice thicknesses (1 mm and 3 mm) were used. All images were reconstructed with FBP and five strengths of SAFIRE. Ten observers evaluated visual image quality. Dose was measured using CT-Expo.

Results: FBP required a higher dose than all SAFIRE strengths to obtain the same image quality for sharpness and noise. For sharpness and contrast image quality ratings of 4, FBP required doses of 6.4 and 6.8 mSv respectively. SAFIRE 5 required doses of 3.4 and 4.3 mSv respectively. Clinical acceptance rate was improved by the higher voltage (110 kV) for all images in comparison to 80 kV, which required a higher dose for acceptable image quality. 3 mm images were typically better quality than 1 mm images.

Conclusion: SAFIRE 5 was optimal for dose reduction and image quality.

INTRODUCTION

Chest CTs are one of the most commonly used diagnostic imaging techniques for paediatric patients¹. Unfortunately, radiation dose delivered during a CT examination is concerning, particularly for children, who have a greater risk per unit dose².

The radiosensitivity of children has been subject to debate and it is currently estimated that for 25% of cancer types, children are more susceptible than adults, and for 20% of tumour types the data is inconclusive³. It has been estimated that a one year old child is as much as ten times more susceptible to cancer than an adult². It is therefore understandable that radiation dose has been a longstanding concern for paediatric patients, particularly when multiple

scans are required.

Various imaging techniques can be used to reduce the radiation dose. Sinogram Affirmed Iterative Reconstruction (SAFIRE), developed by Siemens, is one of the possible new techniques. It is an alternative to conventional filtered back projection (FBP) and has been demonstrated to have significant dose reduction potential for adults. It also has the ability to decrease noise in the images⁴. Images are reconstructed using two correction loops; one occurs in image space to reduce noise, and one utilises sinogram data to correct imperfections⁵.

Iterative reconstruction (IR) techniques typically offer a trade-off between dose and image quality. However, SAFIRE has been reported by numerous studies to have an equal

visual image quality compared to FBP while reducing dose⁶⁻⁸.

This study aims to assess the dose reduction potential of SAFIRE for paediatric chest CTs, as compared to FBP, while maintaining image quality. To quantify image quality, contrast, sharpness, clinical acceptance and image noise were analysed.

MATERIALS AND METHODS

CT protocol

An ATOM® Dosimetry Verification Phantom, modelled on the body of a 5 year old patient, was used for CT imaging⁹. Thorax dimensions were 14 x 17 cm and lung inserts with spherical targets were utilised. Images were taken with a Siemens SOMATOM® Perspective 128 multi-slice CT (MSCT) scanner at 110 kV and 80 kV, with mAs values of 25, 50 and 100. The images were reconstructed with a slice thickness of 1 mm and 3 mm for each mAs value. We chose to use images reconstructed with a soft kernel, as this kernel can increase the low-contrast detectability. FBP images were reconstructed using the B31s kernel, and SAFIRE images using the I31s filter¹⁰.

SAFIRE has five strengths, with SAFIRE 5 being the smoothest. The number of interactions is not dependable on the strength chosen. Each strength has different levels of noise reduction and can create different textures⁵. To ensure that SAFIRE's potential was fully tested, all five strengths were used for reconstruction in this research. Images were also reconstructed using FBP for comparison purposes. This yielded 72 images for analysis in total.

The imaging and reconstruction processes were performed by Siemens, who then provided the images for analysis.

Visual analysis

Ten observers were chosen to review the images, nine of which were graduate or qualified radiographers with varying levels of experience. One observer was a medical physicist.

Images were rated visually based on sharpness, contrast and noise. Each image was reviewed individually and the observers rated contrast and sharpness on a 5 point Likert scale (1 = poor, 2 = fair, 3 = moderate, 4 = good, 5 = extreme). Noise was rated on a 3 point scale (1 = noise affects the interpretation, 2 = acceptable noise, 3 = very little noise). Observers were also asked whether they deemed the image clinically acceptable for diagnostic purposes. Images were displayed using ViewDex, on a 30"

monitor with a resolution of 1440 x 900, for CT images with a matrix of 512 x 512.

Each image was randomised and rated individually; they were not compared with each other. This was done in hopes of achieving a quality score for each image while minimising bias. The observers rated each image twice, in separate sessions.

Dose analysis

Dose was measured using CT-Expo v2.3.1, using a 'child' age group and a scan range of 22 to 44 cm. The scanner model was input as Siemens and scanner as 'perspective series'. The mode was 'spiral mode'. Dose was calculated for each combination of mAs and kV.

Parameters were entered into CT-Expo (kV, mAs, slice thickness) and effective dose (mSv), organ dose, CT dose index (CTDI) and dose length product (DLP) were calculated using the ICRP 103 method.

Statistical analysis data

Statistical analysis was performed using SPSS. Differences between techniques in sharpness and contrast were analysed by means of linear regression analysis. A p-value of less than 0.05 was considered to be statistically significant. The B coefficients (as shown in Tables 1 and 2) were used to create formulae for calculating dose for specific image qualities and visa versa. The equation used for calculation dose was as follows:

$$\begin{aligned} \text{Dose} = & [IQ - (B_1 \times \text{Model}_1) - (B_2 \times \text{Model}_2) \\ & - (B_3 \times \text{Model}_3) \\ & - (B_4 \times \text{Model}_4) \\ & - (B_5 \times \text{Model}_5) - \text{constant}] \\ & / B_{\text{Dose}} \end{aligned}$$

Where model1 was SAFIRE 1, model2 was SAFIRE 2 etc, and B1 was the B coefficient corresponding to SAFIRE 1 etc. Dose could be calculated using image quality.

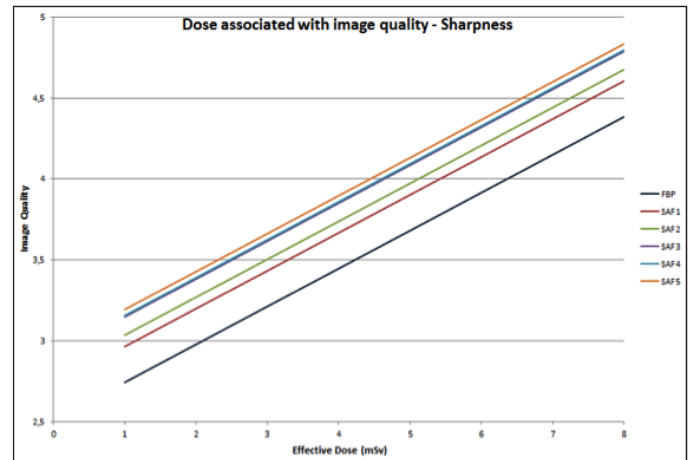
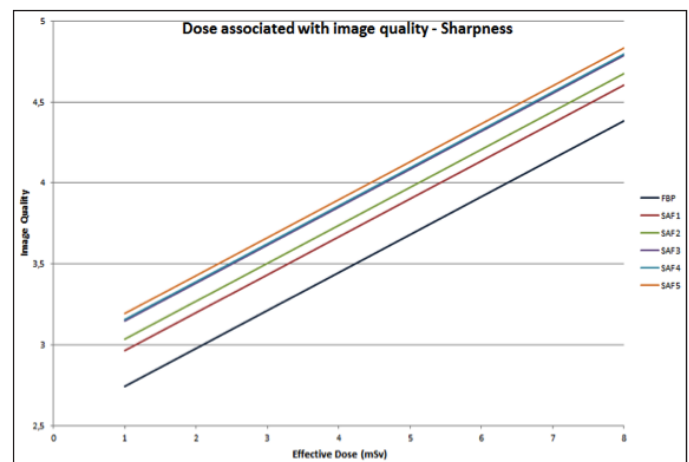
$$\begin{aligned} \text{Image Quality (IQ)} = & (\text{Dose} \times B_{\text{Dose}}) + (B_1 \times \text{Model}_1) \\ & + (B_2 \times \text{Model}_2) + (B_3 \times \text{Model}_3) \\ & + (B_4 \times \text{Model}_4) + (B_5 \times \text{Model}_5) \\ & + \text{constant} \end{aligned}$$

Image noise and clinical acceptability were evaluated using acceptance percentage. Scores of 2 and 3 were counted as acceptable for noise.

Table 1: Statistical significance of SAFIRE for sharpness

Model	Unstandardized Coefficient (B)	Sig.
(Constant)	2,509	<,001
Dose	,234	<,001
SAFIRE 1	,221	,003
SAFIRE 2	,292	<,001
SAFIRE 3	,404	<,001
SAFIRE 4	,412	<,001
SAFIRE 5	,450	<,001

Model	Unstandardized Coefficient (B)	Sig.
(Constant)	2,787	<,001
Dose	,178	<,001
SAFIRE 1	,192	,004
SAFIRE 2	,262	<,001
SAFIRE 3	,383	<,001
SAFIRE 4	,446	<,001
SAFIRE 5	,600	<,001

**Figure 1:** linear regression for sharpness for SAFIRE and FBP.**Figure 2:** linear regression for contrast for SAFIRE and FBP.

RESULTS

Image sharpness and contrast

Linear regression was calculated with respect to both sharpness and contrast. The outcomes of the linear regression are shown in Figures 1 and 2.

An equation to calculate the effect of the dose on image quality for FBP- and all of the SAFIRE-reconstructions was formed using the B-value coefficients. This correlation is shown by Figures 1 and 2. It can be seen that FBP always required a higher dose to achieve the same image quality as SAFIRE. Relating to contrast, an image quality score of 4 required a dose of 3.4 mSv for SAFIRE 5 reconstruction. FBP required a dose of 6.8 mSv. For sharpness-related image quality, a rating of 4 using SAFIRE 5 required 4.4 mSv whereas FBP needed 6.4 mSv.

Table 3 shows the dose reduction potential while

maintaining an image quality of 4 for all reconstruction techniques.

Image noise

The visual ratings regarding image noise are shown in Table 4. Percentages include noise ratings of average and less than average (scores of 2 and 3). The table shows that for 80 kV and 1.2 mSv, 100% of observers evaluated SAFIRE 5 images to have acceptable noise levels. In comparison, only 55% of observers rated FBP reconstructed images as acceptable. It can also be seen that slice thickness generally affects the amount of noise in the images. When comparing FBP images with 80 kV and 2.4 mSv, the acceptance level raised by 45% between 1 and 3 mm.

110 kV greatly improves noise ratings in comparison to 80 kV. The difference between FBP and all strengths of SAFIRE is almost non-existent at this voltage. All 3 mm images were rated to have acceptable noise by at least 90% of observers.

Clinical acceptability

The visual ratings regarding the clinical acceptability are shown in table 5.

It appears that SAFIRE and FBP are equally accepted at

110 kV with doses of 3 and 6 mSv. For 80 kV, SAFIRE consistently has a higher percentage of acceptance than FBP, particularly for the higher doses. Higher strengths of SAFIRE are also generally more clinically acceptable for lower doses, but SAFIRE strengths 2, 3 and 4 also receive good scores for slightly higher doses.

Table 3: Dose reduction (mSv) for SAFIRE strengths compared with FBP

		SAF1	SAF2	SAF3	SAF4	SAF5	FBP
Sharpness	Dose	5,42	5,12	4,64	4,60	4,44	6,36
	Dose reduction (mSv)	0,94	1,24	1,72	1,76	1,92	0
Contrast	Dose (mSv)	5,74	5,34	4,66	4,31	3,44	6,81
	Dose reduction (mSv)	1,08	1,47	2,15	2,5	3,37	0

Table 4: Percentage of observers who scored noise as acceptable or better

	80 kV 1mm			80 kV 3mm			110kV 1mm			110kV 3mm		
	0,6mSv	1,2mSv	2,4mSv	0,6mSv	1,2mSv	2,4mSv	1,5mSv	3mSv	6mSv	1,5mSv	3mSv	6mSv
Acceptable and above noise (%)	%	%	%	%	%	%	%	%	%	%	%	%
FBP	0	25	55	25	75	100	50	85	100	95	95	95
SAF1	5	45	80	55	80	100	75	95	95	95	100	95
SAF2	15	65	95	55	85	100	75	90	95	100	100	95
SAF3	0	70	100	80	95	100	90	100	95	100	95	100
SAF4	35	95	100	80	90	100	95	100	100	100	95	95
SAF5	40	100	100	95	95	100	100	95	95	100	90	95

Table 5: Percentage of observers who scored images as clinically acceptable

	80 kV 1mm			80 kV 3mm			110kV 1mm			110kV 3mm		
	0,6mSv	1,2mSv	2,4mSv	0,6mSv	1,2mSv	2,4mSv	1,5mSv	3mSv	6mSv	1,5mSv	3mSv	6mSv
Clinical acceptance (%)	%	%	%	%	%	%	%	%	%	%	%	%
FBP	5	35	40	15	50	85	55	85	100	65	80	100
SAF1	15	60	65	15	50	90	60	100	100	80	80	100
SAF2	15	60	80	30	65	90	70	95	100	85	85	95
SAF3	15	55	90	50	65	85	85	95	100	80	80	100
SAF4	35	70	90	55	60	90	80	100	95	75	75	95
SAF5	35	90	90	65	70	90	85	100	100	75	75	95

DISCUSSION

It is suggested that SAFIRE 5 can provide a dose reduction of 50% in comparison to FBP, as rated according to image contrast. For image sharpness, the dose reduction is smaller but still significant and is approximately 30%.

Literature suggests that SAFIRE strengths 3 and 4 are best for image quality¹¹⁻¹³. Our results suggest that SAFIRE 5 is optimal

for dose reduction while maintaining image quality. The reason for SAFIRE 5 being optimal could be due to the phantom being child-sized. Research is limited regarding all SAFIRE strengths for paediatric patients and so it is difficult to compare.

Dose reductions for all SAFIRE strengths are shown in Table 3. It shows that dose can be reduced by 0.9 to 3.4 mSv, depending on the strength of SAFIRE used. SAFIRE 5 always has the greatest dose reduction, and also has the best rated clinical acceptance for almost all doses.

Previous studies suggested a potential dose reduction from 15 to 85%⁽¹⁴⁾, depending on parameters, patient size and SAFIRE strength. However, most studies tended to fall in the region of around 50%^{6,12-13,15-17}. Our estimated dose reduction for SAFIRE 5 is approximately 50%, which agrees with other studies.

A linear model was used for data analysis due to measured dose values suggesting a linear trend. For 80 kV it was found that the effective doses were 2.4, 1.2 and 0.6 mSv for 100, 50 and 25 mAs respectively; this shows that although the overall trend might not be linear, for the window of data we were considering it was almost perfectly linear. This trend continued up to our highest measured dose value of 6.1 mSv. In reality, the dose and image quality relationship is not linear, it is asymptotic.

Clinical acceptability was higher for 3 mm image slices than for 1 mm slices, and increased as the SAFIRE strength increased. The higher voltage also had better acceptability overall. 3 mm images contain more data than 1 mm images which allows for greater noise reduction during reconstruction. This might not be true for a clinical CT scan because there is a possibility that pathologies and anatomical structures might be overlooked.

For Tables 4 and 5, percentages that end with 5, for example 85% and 95%, suggest that one or more observers rated images differently during the test and re-test. This could be due to user error or could be a sign of decreased intra-observer reliability. Observers may have rated images differently the second time due to being more acquainted with the image rating procedure. Further research is suggested to investigate this phenomenon.

Noise decreased with increasing dose, and there was less noise in the 110 kV datasets than in the 80 kV images. All of the SAFIRE strengths had acceptable levels of noise for doses of 2.4 mSv and above. For the lower doses at 80 kV, the higher strengths of SAFIRE performed better. SAFIRE 5 received a

90% acceptable noise rating for every dose except 0.6 mSv at 80 kV with 1 mm thickness. SAFIRE 4 was also suitable for most doses, and received a percentage score of 90 and above, excluding 0.6 mSv at 80 kV for 1 mm and 3 mm thicknesses.

Objective data was analysed and then disregarded, based on the fact that results were inconsistent. This is potentially due to the field of view in the received images differing. Changes in the field of view led to the ROI moving and changing in size. This led to different amount of pixels being included which caused anomalous data.

Visual noise rating was evaluated using a three point scale. Linear regression is invalid for a three point scale, meaning that it could not be used during the analysis of signal to noise ratio. It is expected that dose reduction could be calculated if the linear regression was used.

Further research could utilise more observers, or observers with a higher level of experience. Also, real clinical images could be utilised instead of a phantom; lack of anatomical structures makes the evaluation of the images less realistic.

CONCLUSION

Dose reduction increased with higher SAFIRE strengths. SAFIRE 5 was optimal and estimated to have dose reductions of approximately 30% and 50% relating to sharpness and contrast image quality respectively. SAFIRE was most effective for dose reduction at lower kV.

ACKNOWLEDGEMENTS

The authors wish to thank Erasmus for funding this project and Siemens for providing image data. We also wish to thank W. Schaake, R. Visser and P. Hogg for helping analyse our data. Finally, we would like to thank the observers who took the time to participate in this research.

REFERENCES

1. Pearce MS, Salotti JA, Little MP, McHugh K, Lee C, Kim KP, et al. Radiation exposure from CT scans in childhood and subsequent risk of leukaemia and brain tumours: a retrospective cohort study. *Lancet*. 2012;380(9840):499-505.
2. Brenner D, Elliston C, Hall E, Berdon W. Estimated risks of radiation-induced fatal cancer from pediatric CT. *AJR Am J Roentgenol*. 2001;176(2):289-96.
3. Rehani MM. Are children more sensitive to radiation than adults? *Eur Soc Radiol News* [Internet]. 2013 [cited 2014 Aug 11];(Sep). Available from: http://www.myesr.org/html/img/pool/Radiation_Protection_ESR_Work_Sept_2013.pdf
4. Lee SW, Kim Y, Shim SS, Lee JK, Lee SJ, Ryu YJ, et al. Image quality assessment of ultra low-dose chest CT using sinogram-affirmed iterative reconstruction. *Eur Radiol*.

- 2014;24(4):817-26.
5. Grant K, Raupach R. SAFIRE: Sinogram Affirmed Iterative Reconstruction [Internet]. Siemens; 2012 [cited 2014 Aug 11]. Available from: <https://www.healthcare.siemens.com/computed-tomography/options-upgrades/clinical-applications/safire>
6. Moscariello A, Takx RA, Shoenf UJ, Renker M, Zwerner PL, et al. Coronary CT angiography: image quality, diagnostic accuracy, and potential for radiation dose reduction using a novel iterative image reconstruction technique - comparison with traditional filtered back projection. *Eur Radiol*. 2011;21(10):2130-8.
7. Wang H, Tan B, Zhao B, Liang C, Xu Z. Raw-data-based iterative reconstruction versus filtered back projection: image quality of low-dose chest computed tomography examinations in 87 patients. *Clin Imaging*. 2013;37(6):1024-32.
8. Beister M, Kolditz D, Kalender WA. Iterative reconstruction methods in X-ray CT. *Phys Med*. 2012;28(2):94-108.
9. CIRS. ATOM dosimetry verification phantoms [Internet]. Meditron; 2013 [cited 2014 Aug 14]. Available from: <http://www.meditron.ch/medical-imaging/index.php/quality-assurance/phantoms/anthropomorphic-phantoms/product/60-atom-dosimetry-verification-phantoms>
10. Bredenhöller C, Feuerlein U. SOMATOM sensation 10/16 application guide: protocols, principles, helpful hints [Internet]. Siemens; 2005. Available from: http://www.healthcare.siemens.com/siemens_hwem-hwem_sxxa_websites-context-root/wcm/idc/siemens_hwem-hwem_sxxa_websites-context-root/wcm/idc/groups/public/@global/@imaging/@ct/documents/download/mdaw/mje1/~edisp/applicationguide_sensation16_01-00209688.pdf
11. Kim JH, Kim MJ, Kim HY, Lee MJ. Radiation dose reduction and image quality in pediatric abdominal CT with kVp and mAs modulation and an iterative reconstruction technique. *Clin Imaging*. 2014;38(5):710-4.
12. Yang WJ, Yan FH, Liu B, Pang LF, Hou L, Zhang H, et al. Can sinogram-affirmed iterative (SAFIRE) reconstruction improve imaging quality on low-dose lung CT screening compared with traditional filtered back projection (FBP) reconstruction? *J Comput Assist Tomogr*. 2013;37(2):301-8.
13. Baumüller S, Winklehner A, Karlo C, Goetti R, Flohr T, Russi EW, et al. Low-dose CT of the lung: potential value of iterative reconstructions. *Eur Radiol*. 2012;22(12):2597-606.
14. Schulz B, Beeres M, Bodelle B, Bauer R, Al-Butmeh F, Thalhammer A, et al. Performance of iterative image reconstruction in CT of the paranasal sinuses: a phantom study. *AJNR Am J Neuroradiol*. 2013;34(5):1072-6.
15. Schindera ST, Odedra D, Raza SA, Kim TK, Jang HJ, Szucs-Farkas Z, et al. Iterative reconstruction algorithm for CT: can radiation dose be decreased while low-contrast detectability is preserved? *Radiology*. 2013;269(2):511-8.
16. Kalmar PI, Quehenberger F, Steiner J, Lutfi A, Bohlens D, Talakic E, et al. The impact of iterative reconstruction on image quality and radiation dose in thoracic and abdominal CT. *Eur J Radiol*. 2014;83(8):1416-20.
17. Baker ME, Dong F, Primak A, Obuchowski NA, Einstein D, Gandhi N, et al. Contrast-to-noise ratio and low-contrast object resolution on full- and low-dose MDCT: SAFIRE versus filtered back projection in a low-contrast object phantom and in the liver. *AJR Am J Roentgenol*. 2012;199(1):8-18.

Review article – The impact of Sinogram-Affirmed Iterative Reconstruction on patient dose and image quality compared to filtered back projection: a narrative review

Abdulfatah Ahmed^a, André Garcia^b, Astrid Bakker^c, David Tomkinson^a, Julie Salamin^d, René de Lange^c, Sergey A. Buyvidovich^e, Tina Sohrabi^e, Alexandre Dominguez^d, Cosmin Campeanu^d, Paul Plasman^c

a) School of Health Sciences, University of Salford, Manchester, United Kingdom

b) Lisbon School of Health Technology (ESTeSL), Polytechnic Institute of Lisbon, Portugal

c) Department of Medical Imaging and Radiation Therapy, Hanze University of Applied Sciences, Groningen, The Netherlands

d) Haute École de Santé Vaud – Filière TRM, University of Applied Sciences and Arts of Western Switzerland, Lausanne, Switzerland

e) Department of Life Sciences and Health, Radiography, Oslo and Akershus University College of Applied Sciences, Oslo, Norway



KEYWORDS

Comparison
Filtered back projection
Sinogram-affirmed iterative reconstruction
Dose reduction
Paediatric CT
Computed tomography
Image quality

ABSTRACT

Objective: Summarize all relevant findings in published literature regarding the potential dose reduction related to image quality using Sinogram-Affirmed Iterative Reconstruction (SAFIRE) compared to Filtered Back Projection (FBP).

Background: Computed Tomography (CT) is one of the most used radiographic modalities in clinical practice providing high spatial and contrast resolution. However it also delivers a relatively high radiation dose to the patient. Reconstructing raw-data using Iterative Reconstruction (IR) algorithms has the potential to iteratively reduce image noise while maintaining or improving image quality of low dose standard FBP reconstructions. Nevertheless, long reconstruction times made IR impractical for clinical use until recently.

Siemens Medical developed a new IR algorithm called SAFIRE, which uses up to 5 different strength levels, and poses an alternative to the conventional IR with a significant reconstruction time reduction.

Methods: MEDLINE, ScienceDirect and CINAHL databases were used for gathering literature. Eleven articles were included in this review (from 2012 to July 2014).

Discussion: This narrative review summarizes the results of eleven articles (using studies on both patients and phantoms) and describes SAFIRE strengths for noise reduction in low dose acquisitions while providing acceptable image quality.

Conclusion: Even though the results differ slightly, the literature gathered for this review suggests that the dose in current CT protocols can be reduced at least 50% while maintaining or improving image quality. There is however a lack of literature concerning paediatric population (with increased radiation sensitivity). Further studies should also assess the impact of SAFIRE on diagnostic accuracy.

INTRODUCTION

CT is one of the most used radiographic modalities in clinical practice but it also comes with a significant radiation dose to patients. Consequently, this research focused on dose reduction, particularly for paediatric examinations. These patients are more susceptible to long-term effects of radiation exposure, with higher potential for an increased lifetime risk of malignancy. Filtered back projection (FBP) is the standard reconstruction algorithm.

However IT developments in recent years permit iterative image reconstruction (IR) to become compatible with routine clinical practice.

Sinogram-Affirmed Iterative Reconstruction (SAFIRE) is an advanced iterative reconstruction technique recently developed by Siemens that requires less computing power and uses both FBP and raw data-based iterations. SAFIRE estimates the noise caused by fluctuations in neighbouring voxels in the raw-data. It subtracts the noise stepwise

in several validation loops. After the first correction loop, the result is compared with the original raw-data and an updated image is generated for the next iteration leading to further noise reduction. Where IR only uses a single correction loop, SAFIRE uses up to 5 correction loops to further decrease image noise¹. The level of noise reduction and noise texture varies with SAFIRE strength for each reconstruction. SAFIRE strength does not translate the number of iterations and does not affect reconstruction time².

The purpose of this review article is to summarize the current research comparing SAFIRE and FBP. It investigates image quality and the potential of dose reduction provided by SAFIRE, compared to FBP. Data from articles are discussed bearing in mind SAFIRE's potential for dose reduction while maintaining diagnostic image quality.

DATA SOURCES AND SEARCHES

MEDLINE, ScienceDirect and CINAHL data bases were searched, using the following key words: comparison, filtered back projection, sinogram-affirmed iterative reconstruction, dose reduction, paediatric CT, computed tomography, image quality. The research equation was: (Computed tomography AND sinogram-affirmed iterative reconstruction AND radiation dose AND image quality AND filtered back projection) NOT (contrast media). We excluded articles concerning previous generation iterative reconstruction algorithms and articles focusing on cardiac CT on obese patients because of the difference of size between head examination and those patients.

Eleven articles were included in our review article, dating from 2012 to 2014, for examinations of chest, abdomen, head and cardiac on anthropomorphic phantoms and adult or paediatric patients.

MATERIALS AND METHODS

Patients/phantoms

Data came from CT scans performed on patients and phantoms. Patients were mainly adults but some studies focused on paediatric protocols. Scans were performed on physical and anthropomorphic phantoms (chest, head). One study used data from both patients and phantom scans for comparison.

Paediatric vs adult protocols

Three articles focused on paediatric examinations,

“paediatric” denomination including children from 0 to 18 years old. Two explored cardiac CT and one abdomen. What mainly differs from adult studies were tube voltage (70 to 100-120 kVp) and tube current (lower mAs). Both were generally adapted to weight, size and age.

Data acquisition

Since all of the data-sets acquired in these studies had to be reconstructed with the SAFIRE algorithm, almost all exams were performed on the dual-source CT scanner Somatom Definition Flash from Siemens. Filtered back projections were sometimes acquired on other Siemens equipments.

The range of tube voltage explored was usually 100kVp and 120 kVp, sometimes also 80 kVp for ultra low doses. Tube current was variable, either fixed (at 25, 50 and 100 mAs or percentage reduction) or automatically modulated.

Images reconstruction

Acquisitions were reconstructed with FBP and SAFIRE. For SAFIRE, either all strengths (S1-S5) were explored or median strength like strengths S2 to S4 or S3 (recommended by manufacturer)³.

Usually images were reconstructed with a medium smooth kernel or smooth and sharp kernels to compare changes in image quality.

Image quality analysis

For the physics analysis of image quality, noise and Signal-to-Noise Ratio (SNR) were the main criteria calculated. Contrast and Contrast-to-Noise Ratio (CNR) were less often measured. Only one study on phantoms went further by examining the Noise Power Spectrum (NPS), the spatial resolution, the linearity and accuracy of CT numbers.

For visual analysis, in most of the articles, the images were analysed by at least two radiologists with 3 years experience or more in a specific radiological field. Further details about the method of image analysis were often not provided. Visual criteria generally considered image noise (e.g., graininess), quality of contour delineation (i.e., sharpness) and general impression (i.e., overall image quality). Han et al. (2012)⁴ referred to European Image Quality Assessment (i.e., sharpness, noise, noise texture, diagnostic confidence).

For visual analysis, a 4 or 5 point Likert scale is commonly used to evaluate image quality. Furthermore Wang et al. (2012) used a more precise 4 point scale on anatomic

details needed (e.g., level 1: lack of vessel wall definition due to marked motion artefact, poor vessel opacification, prominent structural discontinuity, or high image noise rendering the segment non-diagnostic).

RESULTS

Chest/thorax

Christe et al. (2013)⁶ conclude that while using SAFIRE instead of FBP it was possible to achieve a dose reduction of 30, 52 and 80% for bone, soft tissue and air, respectively. Image quality was verified objectively using signal, noise and contrast measurements. With the same radiation dose, an average of 34% more CNR was achieved by changing respectively from FBP to SAFIRE. For the same CNR, an average of 59% dose reduction was produced for SAFIRE. The visual classification was given by two radiologists. For the same visual image quality, the dose could be reduced by 25% using SAFIRE. This study only used SAFIRE S3.

Wang et al. (2013)⁷ explored SAFIRE strengths S2-S4 after excluding the extremes (S1 and S5), as they were considered to be, respectively, too “noisy” and too “smooth”. The results of this study suggests there was no significant difference in the objective noise and SNR on mediastinal images between full-dose (FD) images reconstructed with FBP and half-dose images reconstructed with SAFIRE. But, on lung images, noise was significantly lower and SNR was significantly higher in half-dose images reconstructed with SAFIRE. Subjective image noise was similar on mediastinal and lung images with half-dose SAFIRE and full-dose FBP reconstruction.

Amongst all strengths, SAFIRE S3 had the best results for physics and visual image quality. Authors conclude that, compared to full-dose CT images reconstructed with the conventional FBP algorithm, SAFIRE with three iterations could provide similar or better image quality at 50% less dose.

Ghetti et al. (2013)¹⁰ explored image quality using 3 phantoms. Noise was analysed on images reconstructed with all 5 SAFIRE strengths and a conventional medium-smooth kernel. Additionally, on images with strength SAFIRE S3, different kernels were selected to evaluate a possible difference in noise reduction due to the filter applied. For the same dose, noise reduction of iterative reconstruction increases with the SAFIRE strength applied in a proportional way.

CT number accuracy and linearity were verified to assess SAFIRE reconstructions influences on them. The different

SAFIRE strengths did not change mean CT values and showed no considerable differences from values obtained with FBP.

Images were reconstructed with three different levels of SAFIRE strength (S1, S3, S5) and FBP at 3 different dose levels. CNR was measured for all images. CNR is always greater for SAFIRE and it increases with the strength of SAFIRE applied. But there is no evidence of a significant difference between the different filters in the SAFIRE outcomes. The spatial resolution was measured through different modules with two dose levels (at 120 kVp). Image texture changes increased with SAFIRE strength, resulting in an overall image quality improvement. Detail edge is sharper with less background noise using SAFIRE.

Abdomen

Greffier et al. (2013)⁸ analysed the data from 10 patients who had a normal dose abdominal CT and who then underwent a second CT scan examination. The first sequence was acquired with 30% less mAs than the original CT and the second acquisition with 70% less mAs. The raw-data of the two scans was reconstructed with FBP and SAFIRE (S1-S5) and medium kernel.

Physics analysis concluded there was no significant difference in the measured signal when using FBP and SAFIRE. Noise significantly decreased (11% between FBP and SAFIRE 1) with SNR and CNR increase after each iteration. Good image quality was obtained with 30% less dose by using SAFIRE S2. Furthermore by using S5, it was possible to achieve up to 70% dose reduction while still maintaining image quality.

In the work of Kim et al. (2014)⁹, a first group of paediatric abdominal patients was scanned with kVp and mAs modulation. Raw-data was reconstructed using SAFIRE (S2-S4). A second group of patients underwent the same exam in emergency room on a CT scanner with only mAs modulation and the raw-data was reconstructed with FBP. Physics and visual analysis of image quality showed that SAFIRE was able to achieve an average 64.2% in dose reduction compared to the control group with FBP. The objective image noise of the SAFIRE S2 and S3 was comparable to that of the control group. For visual image quality analysis, SAFIRE S2 and S3 showed better image quality than the control group in terms of diagnostic acceptability. Moreover, strength S3 scored better in terms of subjective image quality compared to S2.

Head

Schulz et al. (2013)¹ worked on data from a phantom head CT scan at different tube voltages and currents. Each

image was reconstructed using two different kernels with FBP and SAFIRE (S1-S5) algorithms. Image noise was evaluated and showed that compared to FBP, all iterative reconstruction techniques reduced the noise by 15%-85% depending on the iterative strength, rendering kernel, and dose parameters. Visual image quality was evaluated on images acquired at tube currents of 100% (FBP), 50% (SAFIRE), and 25% (SAFIRE). Visual evaluation of the images suggested that FBP images at full dose were preferred to 50% dose SAFIRE reconstruction. Their conclusion was that SAFIRE has a potential in CTs exam since even slight increase in iteration can yield important noise reduction.

Corcuera-Solano et al. (2014)¹¹ aimed to assess dose reduction for patients in the neurosurgical intensive care unit who undergo multiple head CT scans. While maintaining similar image quality and SNR levels, ultra-low-dose CT (ULDCT) reconstructed with SAFIRE represented a 68% lower CTDIvol compared to standard-dose CT (SDCT) with FBP technique in the same patients. SAFIRE reconstruction low-dose CT (LDCT) offered higher image quality than FBP standard-dose CT with no differences in SNR at a 24% lower CTDIvol. Compared with LDCT, ULDCT had significantly lower SNR but demonstrated clinically satisfactory measures of image quality. In visual analyses, there were no major differences in quality between ULDCT and SDCT.

Korn et al. (2013)¹² described an increase of 47% in CNR when using SAFIRE reconstruction instead of FBP in reduced-dose examination, because the degradation of image quality at lower dose was more than compensated by SAFIRE. Through objective measurements of image sharpness, they found that it was similar for FBP and SAFIRE reconstructions. Compared with FBP standard-dose (320 mAs) reconstructions, low-dose (255 mAs) SAFIRE reconstructions also allowed for an improvement in visual grading of noise as well as overall image quality.

Authors concluded that with 20% dose reduction, reconstruction of head CT by SAFIRE provides above standard objective and subjective image quality.

Cardiac

Han et al. (2012)⁴ evaluated the impact of SAFIRE on image quality in paediatric cardiac CT datasets. From a visual point of view, no change was observed in spatial resolution, sharpness improved in 9% of cases, image noise in 63% cases and noise texture in 85% cases when using SAFIRE. The diagnostic confidence was similar in both groups. The improvement and reduction of noise was similar for helical and axial acquisition techniques. Visual image quality analysis resulted on a lower contrast from 1% for SAFIRE but clinically not significant, noise decreased (34%) and CNR (41%) and SNR (56%) increased with SAFIRE.

Wang et al. (2013)⁵ analysed images from patients and phantoms. Data from dual source equipment was reconstructed using FBP and data from single source was reconstructed with SAFIRE and FBP, to assess image quality with only half dose. Images from the phantom suggested that noise proportionally decreased as current increased. No significant difference in SNR and noise was found between full-dose FBP and half-dose SAFIRE neither for phantom nor patients. Similar visual results between full-dose FBP and half-dose SAFIRE were performed in visualising coronary segments. For half-dose FBP, significantly fewer segments were visible. It suggested that with an estimated dose reduction of 50%, there was no significant difference in noise, SNR and overall image quality with SAFIRE reconstruction compared to full-dose standard protocol reconstructed with FBP.

Nie et al. (2014)³ evaluated the impact of SAFIRE on image quality for a tube voltage of 70 kVp. The mean scores of visual analysis were significantly higher with SAFIRE algorithm than with FBP algorithm regarding to graininess, sharpness and overall image quality. Noise was lower and SNR and CNR significantly higher with SAFIRE. Radiologists evaluated the diagnostic accuracy. SAFIRE scored better than FBP algorithm but no significant difference in diagnostic accuracy between FBP and SAFIRE was found ($p > 0.05$).

The authors concluded that, for a same tube current, physical and visual image quality were significantly improved with SAFIRE.

Table 1: Results in dose reduction and image quality (IQ) evaluation

Authors	Part of body examined	SAFIRE Strength	Dose reduction	Image quality results
Christe et al. (2013) ⁶	Chest	S3	80% at same noise 45% at same SNR 59% at same CNR 25% at same subjective IQ	-44 % noise, +36 % SNR, +34 % CNR with SAFIRE Better subjective IQ for SAFIRE with same dose
Wang et al. (2013) ⁷	Chest (low dose)	S3	similar IQ with FBP 100% dose and SAFIRE 50% dose	Full-dose FBP noise comparable to half-dose SAFIRE Subjective IQ evaluation in noise, SNR and lesion detection comparable with full-dose FBP or half-dose SAFIRE
Ghetti et al. (2013) ¹⁰	Chest, Water, Catphan 600 and 3D phantom	S1-S5 S1,S3,S5	Unique dose of 13.4 mGy tested for noise Doses tested for CNR : 20.2, 13.4 and 6.7 mGy	Up to 60% noise reduction with SAFIRE 5 for 2mm slices with same dose Noise decreases and CNR increases when SAFIRE strength rises
Greffier et al. (2013) ⁸	Abdomen	S1-S5	Dose reduced at 30% and 70% from full dose	SNR and CNR improved with the increase in SAFIRE levels
Kim et al. (2014) ⁹	Abdomen (paediatric)	S2,S3,S4	64.2% average dose reduction for similar image quality with SAFIRE	Noise decreases and IQ increases with SAFIRE strengths No significant difference between SAFIRE S4 and FBP
Schulz et al. (2013) ¹	Head: paranasal sinuses	S1-S5	100% FBP, 50% SAFIRE, 25% SAFIRE	Image noise always greater with FBP With 25% dose, mean noise reduction 47.5% for 3mm and 49.4% for 1mm slices with SAFIRE Best IQ with 100% dose level with FBP
Corcuera-Solano et al. (2014) ¹¹	Head	S3	ULDCT 68% dose reduction LDCT 24% dose reduction	Image quality similar with full dose FBP and LDCT reconstructed with SAFIRE S3
Korn et al. (2013) ¹²	Head	S3	20% dose reduction	+ 48% SNR, + 47% CNR with SAFIRE for same dose Similar sharpness IQ SAFIRE scored better than FBP
Han et al. (2012) ⁴	Cardiac	-	-	- 34% noise, + 56% SNR, + 41% CNR using SAFIRE vs FBP using the same dose
Wang et al. (2013) ⁵	Cardiac Water phantom	-	Simulating a 50% radiation dose reduction	No significant noise and SNR difference and equivalent image quality between full dose FBP and half dose SAFIRE
Nie et al. (2014) ³	Cardiac	S3	Same dose 70 kVp	Significantly lower image noise Significantly higher SNR and CNR for SAFIRE Higher scores for subjective IQ with same dose

DISCUSSION

Although specific values differ from one study to another, all studies concluded that SAFIRE allows for a significant dose reduction, while maintaining adequate image quality. Nevertheless some limitations were identified.

The studies included in this review used different parameters to measure image quality. There was no standard way in how both physical and visual image quality was measured. Different sizes of ROI's and different Likert scales were used. Furthermore, not all articles assessed both physical and visual image qualities.

The studies assessing visual image quality only used two radiologists as observers. In order to reduce observer bias, a larger group is needed. Monitor characteristics and display parameters were completely missing as well as the visual acuity performance of the observers.

The images were only classified according to their diagnostic or visual quality, but not their diagnostic accuracy. More studies must be done regarding if SAFIRE provides better diagnostic accuracy than FBP.

In some studies the image sets were acquired using different equipment for FBP and SAFIRE reconstructions.

That implicates possible changes in acquisition protocol and might not allow a proper comparison.

Studies did not always consider all SAFIRE strengths with no clear explanations about exclusion criteria. It doesn't give a complete answer on the potential dose reduction and image quality with SAFIRE.

CONCLUSION

All articles reported an important noise reduction when using SAFIRE reconstruction instead of FBP at equal dose levels. Noise level decreased proportionally when increasing SAFIRE strength. Some articles suggested that a similar visual and physical image quality between FBP and SAFIRE can be achieved when reducing dose to 50%. No significant

difference was measured in CNR between both reconstruction methods. This could suggest the usefulness of SAFIRE in patient radiation protection. Consequently, its use will likely become widespread, allowing exams to be performed using a lower radiation dose, particularly in paediatric examination.

The manufacturer recommended the use of SAFIRE S3 for an optimal image quality and this was confirmed by several articles in general appreciation of the image.

Although from a physics point of view, significant dose reductions are feasible, it is essential to verify the diagnostic accuracy of the image with observer analysis. Studies should also be done regarding other fundamental factors for dose reduction, e.g. detector efficiency and dose modulation (kVp and mAs) and their potentials combined with SAFIRE's ones.

REFERENCES

- Schulz B, Beeres M, Bodelle B, Bauer R, Al-Butmeh F, Thahammer A, et al. Performance of iterative image reconstruction in CT of the paranasal sinuses: a phantom study. *AJNR Am J Neuroradiol*. 2013;34(5):1072-6.
- Grant K, Raupach R. SAFIRE: Sinogram Affirmed Iterative Reconstruction [Internet]. Siemens; 2012. Available from: <https://www.healthcare.siemens.com/computed-tomography/options-upgrades/clinical-applications/safire>
- Nie P, Li H, Duan Y, Wang X, Ji X, Cheng Z, et al. Impact of sinogram affirmed iterative reconstruction (SAFIRE) algorithm on image quality with 70 kVp-tube-voltage dual-source CT angiography in children with congenital heart disease. *PLoS One*. 2014;9(3):e91123.
- Han BK, Grant KL, Garberich R, Sedlmair M, Lindberg J, Lesser JR. Assessment of an iterative reconstruction algorithm (SAFIRE) on image quality in pediatric cardiac CT datasets. *J Cardiovasc Comput Tomogr*. 2012;6(3):200-4.
- Wang R, Schoepf UJ, Wu R, Gibbs KP, Yu W, Li M, et al. CT coronary angiography: image quality with sinogram-affirmed iterative reconstruction compared with filtered back-projection. *Clin Radiol*. 2013;68(3):272-8.
- Christe A, Heverhagen J, Ozdoba C, Weisstanner C, Ulzheimer S, Ebner L. CT dose and image quality in the last three scanner generations. *World J Radiol*. 2013;5(11):421-9.
- Wang H, Tan B, Zhao B, Liang C, Xu Z. Raw-data-based iterative reconstruction versus filtered back projection: image quality of low-dose chest computed tomography examinations in 87 patients. *Clin Imaging*. 2013;37(6):1024-32.
- Greffier J, Fernandez A, Macri F, Freitag C, Metge L, Beregi JP. Which dose for what image? Iterative reconstruction for CT scan. *Diagn Interv Imaging*. 2013;94(11):1117-21.
- Kim JH, Kim MJ, Kim HY, Lee MJ. Radiation dose reduction and image quality in pediatric abdominal CT with kVp and mAs modulation and an iterative reconstruction technique. *Clin Imaging*. 2014;38(5):710-4.
- Ghetti C, Palleri F, Serreli G, Ortenzia O, Ruffini L. Physical characterization of a new CT iterative reconstruction method operating in sinogram space. *J Appl Clin Med Phys*. 2013;14(4):4347.
- Corcuera-Solano I, Doshi AH, Noor A, Tanenbaum LN. Repeated head CT in the neurosurgical intensive care unit: feasibility of sinogram-affirmed iterative reconstruction-based ultra-low-dose CT for surveillance. *AJNR Am J Neuroradiol*. 2014;35(7):1281-7.
- Korn A, Bender B, Fenchel M, Spira D, Schabel C, Thomas C, et al. Sinogram affirmed iterative reconstruction in head CT: improvement of objective and subjective image quality with concomitant radiation dose reduction. *Eur J Radiol*. 2013;82(9):1431-5.

Research article – A comparison of Sinogram Affirmed Iterative Reconstruction and filtered back projection on image quality and dose reduction in paediatric head CT: a phantom study

Abdulfatah Ahmed^a, André Garcia^b, Astrid Bakker^c, David Tomkinson^a, Julie Salamin^d, René de Lange^c, Sergey A. Buyvidovich^e, Tina Sohrabi^e, Alexandre Dominguez^d, Cosmin Campeanu^d, Paul Plasman^c

a) School of Health Sciences, University of Salford, Manchester, United Kingdom

b) Lisbon School of Health Technology (ESTeSL), Polytechnic Institute of Lisbon, Portugal

c) Department of Medical Imaging and Radiation Therapy, Hanze University of Applied Sciences, Groningen, The Netherlands

d) Haute École de Santé Vaud – Filière TRM, University of Applied Sciences and Arts of Western Switzerland, Lausanne, Switzerland

e) Department of Life Sciences and Health, Radiography, Oslo and Akershus University College of Applied Sciences, Oslo, Norway



KEYWORDS

Comparison
Filtered back projection
Sinogram-Affirmed
Iterative reconstruction
Dose reduction
Paediatric CT
Computed tomography
Image quality

ABSTRACT

Background: Computed tomography (CT) is one of the most used modalities for diagnostics in paediatric populations, which is a concern as it also delivers a high patient dose. Research has focused on developing computer algorithms that provide better image quality at lower dose. The iterative reconstruction algorithm Sinogram-Affirmed Iterative Reconstruction (SAFIRE) was introduced as a new technique that reduces noise to increase image quality.

Purpose: The aim of this study is to compare SAFIRE with the current gold standard, Filtered Back Projection (FBP), and assess whether SAFIRE alone permits a reduction in dose while maintaining image quality in paediatric head CT.

Methods: Images were collected using a paediatric head phantom using a SIEMENS SOMATOM PERSPECTIVE 128 modulated acquisition. 54 images were reconstructed using FBP and 5 different strengths of SAFIRE. Objective measures of image quality were determined by measuring SNR and CNR. Visual measures of image quality were determined by 17 observers with different radiographic experiences. Images were randomized and displayed using 2AFC; observers scored the images answering 5 questions using a Likert scale.

Results: At different dose levels, SAFIRE significantly increased SNR (up to 54%) in the acquired images compared to FBP at 80kVp (5.2-8.4), 110kVp (8.2-12.3), 130kVp (8.8-13.1). Visual image quality was higher with increasing SAFIRE strength. The highest image quality was scored with SAFIRE level 3 and higher.

Conclusion: The SAFIRE algorithm is suitable for image noise reduction in paediatric head CT. Our data demonstrates that SAFIRE enhances SNR while reducing noise with a possible reduction of dose of 68%.

INTRODUCTION

Computed Tomography (CT) is fast, precise and one of the most used modalities for diagnostic imaging¹. It is considered the technique of choice both in adult and paediatric population, but it is also associated with high effective dose. 7 million paediatric CT scans were performed in 2007 in the USA and with this value rises almost 10% every year. Dose reduction for paediatric examinations has become a priority, since younger patients have a higher potential for

an increased lifetime risk of radiation-induced malignancy². However, the dose reduction should not compromise diagnostic image quality.

Different CT reconstruction algorithms have been developed over the years. Filtered back projection (FBP) is by far the most used today³. It is fast and applies different filters⁴ and increases spatial resolution. It also increases image noise requiring a higher X-ray tube setting, resulting in a higher radiation exposure⁵.

Iterative reconstruction (IR) techniques have been developed to reduce dose while maintaining or improving objective image quality by reducing noise and consequently improving Signal-to-Noise Ratio (SNR). However, these techniques require a high computing power and have been too time consuming, limiting its clinical application⁶.

Table 1: Acquisition parameters for all the images

Batch	1	2	3
kV	80	110	130
mAs	50	50	50
	100	100	100
	200	200	200

Siemens has recently developed Sinogram-Affirmed Iterative Reconstruction (SAFIRE), an advanced iterative reconstruction technique that requires less computing power and uses both FBP and raw data-based iterations to remove noise and improve image quality. The corrected image is compared with the original and the process is repeated several times. SAFIRE provides 5 strength levels of noise reduction, 1 being the weakest and 5 the strongest⁷. Noise reduction and noise texture vary with the reconstruction strength selected. Strength value does not translate the number of iterations and does not affect reconstruction time⁶. Nonetheless, SAFIRE is still more time consuming than golden standard FBP².

This study aims to compare SAFIRE to FBP and determine whether SAFIRE permits a reduction in dose while maintaining image quality in paediatric head CT.

MATERIALS AND METHODS

CT protocol selection

For this study a simulated examination was performed using the paediatric head phantom ATOM of a five year old child, model 705⁸, to acquire a series of image sets⁹. The equipment used for the simulation was a Siemens SOMATOM perspective 128 CT scanner. Prior to the study, three image sets were created using different settings for kV and mAs, indicated in Table 1.

Data reconstruction

All the image sets were reconstructed using FBP and SAFIRE strengths 1, 2, 3, 4, and 5. The kernels used for

image reconstruction were ‘smooth’ (J30 for SAFIRE and H30 kernel for FBP). This study focused mainly on the soft tissue kernel, as it allows a better representation of soft tissue structures. Sharp kernels, used for bone tissue studies add too much image noise. All images were reconstructed using 1 and 3mm slice thickness but only 3mm thickness were selected for the final three image sets, in order to keep in-line with those used in clinical practice¹⁰⁻¹¹. All reconstructed images were acquired from the same original dataset. Window width 50, window level 100 and field of view were kept constant for visual image quality analysis.

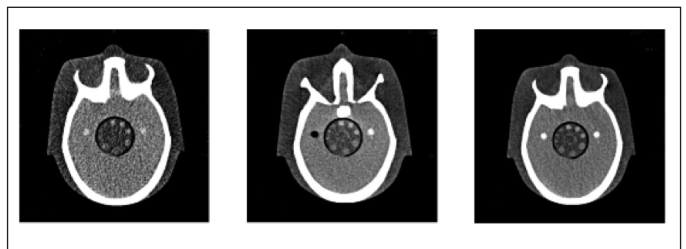


Figure 1: Reference images; FBP 80 kV 100 mAs (left), FBP 110 kV 100 mAs (middle), and FBP 130 kV 100 mAs (right).

Visual assessment of image quality

For visual analysis, a forced choice technique was used for image comparison, using two-alternative forced choice (2AFC) software¹²⁻¹³. Nine sets of parameters and six types of reconstructions totalled 54 images, which were scored by 17 observers. The 54 images were divided into three batches, each batch containing 18 images with the same kVp. In every batch, two duplicated images were included, which allowed for intra observer reliability to be assessed. Slice 18 was chosen for evaluation, through consensus decision, as it was considered that this slice represented a good visualisation of inner structures within the phantom. The SNR was calculated on all FBP images and the one with the average SNR was used as the reference image for each batch, which identified the 100mAs image, for every kVp value (Figure 1).

Eight inexperienced observers (first and second year radiography students and one high school graduate) and nine experienced observers (seven graduate radiographers and one physicist specialized in medical imaging) independently scored the images. All observers took part in a visual acuity test where a series of visibility, depth and contrast perception tests were performed to assess the visual capacity of each observer. These tests were performed to exclude observers with impaired visual acuity.

Table 2: Questionnaire used for evaluation of images

Item 1	The differentiation of contrast within the encircled structure and its immediate background (see image)?
Item 2	The visual sharpness of the bony structure displayed?
Item 3	The sharpness of the circle in the encircled structure (see image)?
Item 4	The overall image quality?
Item 5	The overall noise of the image?

Before visual image quality assessment, each individual observer received verbal instructions and a reference sheet to allow a better understanding of specific image areas evaluated in each question (appendix A). Each image was evaluated separately and compared with the reference image. The questionnaire for this evaluation contained one question for counting the circles in the central area of the phantom and five questions with a 5 point Likert scale which were used for scoring image noise, contrast and overall image quality

as perceived by each individual observer (Table 2)^{10,14-15}. All observers were blinded to acquisition parameters and images were displayed in a randomized fashion.

Light in the room was dimmed and constant; monitor settings (Siemens, 19 inch, resolution: 1280x1024) were kept identical for all observers, in order to further reduce observer bias.

Physical assessment of image quality

For the physical analysis SNR, uniformity and CNR measurements were performed in each image. Using the software ImageJ, three Regions of Interest (ROI's) were drawn with a 10-mm² area for SNR calculation (Figure 2). Two other ROI's were drawn on bone and soft tissue and were used to obtain CNR values (Figure 4). ROI's were drawn in specific areas and in the same place for every image (approximately), in order to obtain better contrast measurements and to facilitate the evaluation of image quality parameters. SNR and CNR were calculated using the following standard equations:

$$CNR = \frac{\text{Mean signal bone} - \text{mean signal tissue}}{\text{Mean SD}}$$

$$SNR = \frac{\text{Mean signal value within ROI}}{\text{SD within ROI}}$$



Figure 2: ROI's used for SNR measurements.



Figure 4: ROI drawn to measure CNR.

CT-EXPO dosimetry software for Monte Carlo modelling for calculating the dose¹⁶.

Statistical Analysis

The data acquired from the visual assessment of image

quality (2AFC) was imported into SPSS software (version 21.0) for statistical analysis. The data was analysed to assess a 95% confidence interval and for each IR. Descriptive statistics were used to determine the participant visual perception of the change in IR and the effect on image quality. Correlations and p-values were calculated using Microsoft Excel (2013).

RESULTS

Physical assessment of image quality

Physical image quality measures indicate the image noise was higher in the FBP compared to the SAFIRE groups (Table 1). Furthermore, a decrease in noise was observed with increasing SAFIRE strength. The decrease in noise with the increase in SAFIRE strength precipitated an increase in SNR. CNR remained constant, with minimal change in standard

deviation. SAFIRE groups 3, 4, and 5 show comparable noise and SNR values.

Dose assessment

Table 3 highlights the increase in mAs within kVp values resulting in a proportional increase in DLP, effective dose (E) and the effective dose to the eyes, with a reduction at low mAs values. Figure 5 illustrates the correlation between DLP and effective dose with an $r^2 = 0.996$, with the effective dose to the eyes displaying a correlation of $r^2 = 1$.

Table 3: The relationship between kVp/mAs and effective dose

kVp	mAs	DLP (mGy*cm)	E(mSv)(103)	E eye (mSv)
80	50	44	0.1	3.4
80	100	88	0.2	6.9
80	200	175	0.5	13.7
110	50	103	0.3	8.1
110	100	207	0.5	16.2
110	200	413	1.1	32.3
130	50	154	0.4	12.1
130	100	309	0.8	24.2
130	200	618	1.6	48.3

Visual assessment of image quality

The division of the observers in terms of experience allowed for comparative analysis between the two groups (Table 4). Table 5 provides the results of the calculated Intra Class Correlation Coefficient (ICC) values for the experienced and non-experienced group of observers. All ICC values have a statistical significance of $p < 0.001$. The values of the intra class correlation (ICC) show weak to moderate agreement within all subject groups, where the group of experienced subjects shows a higher ICC for every criteria. The biggest difference in ICC between experienced and non-experienced observers can be observed in criteria

1, whereas criteria 4 and 5 show similar values.

Figure 6 illustrates the relationship between the mean IQ and the acquisition parameters (kVp/mAs) for FB and the SAFIRE groups with a 95% Confidence Interval (CI). An increase in the mean perceptual IQ is prominently demonstrated with increases in SAFIRE strength.

FBP and SAFIRE 1 are comparable as they display similar mean IQ with increments in parameters; however a stronger confidence interval is displayed within SAFIRE 1. SAFIRE 2 shows an increase in mean IQ at lower parameters, however this increase is more obvious with SAFIRE 3, 4 and 5.

Table 4: Data representing mean value (\pm SD) of image noise, CNR, SNR

	FBP	SAFIRE 1	SAFIRE 2	SAFIRE 3	SAFIRE 4	SAFIRE 5
80 KVP						
Noise	11.1(\pm 3.3)	10.3(\pm 3.1)	9.6(\pm 2.8)	8.9(\pm 2.7)	8.2(\pm 2.5)	7.5(\pm 2.3)
CNR	0.8(\pm 0.4)	0.8(\pm 0.5)	0.8(\pm 0.5)	0.8(\pm 0.5)	0.8(\pm 0.5)	0.8(\pm 0.6)
SNR	5.2(\pm 1.5)	5.7(\pm 1.7)	6.2(\pm 1.9)	6.9(\pm 2.1)	7.6(\pm 2.3)	8.4(\pm 2.6)
110 KVP						
Noise	6.2(\pm 1.6)	5.7(\pm 1.6)	5.3(\pm 1.4)	5.0(\pm 1.4)	4.7(\pm 1.5)	4.2(\pm 1.3)
CNR	0.5(\pm 0.4)	0.5(\pm 0.5)	0.5(\pm 0.5)	0.5(\pm 0.6)	0.5(\pm 0.7)	0.4(\pm 0.7)
SNR	8.2(\pm 2.0)	8.8(\pm 2.1)	9.4(\pm 2.4)	10.2(\pm 2.6)	11.2(\pm 3.0)	12.3(\pm 3.5)
130 KVP						
Noise	4.9(\pm 1.0)	4.6(\pm 0.9)	4.2(\pm 0.9)	3.9(\pm 0.8)	3.6(\pm 0.7)	3.2(\pm 0.7)
CNR	0.5(\pm 0.2)	0.5(\pm 0.2)	0.5(\pm 0.2)	0.6(\pm 0.2)	0.5(\pm 0.2)	0.5(\pm 0.3)
SNR	8.8(\pm 1.1)	9.4(\pm 1.2)	10.2(\pm 1.3)	11.0(\pm 1.3)	12.0(\pm 1.5)	13.1(\pm 1.7)

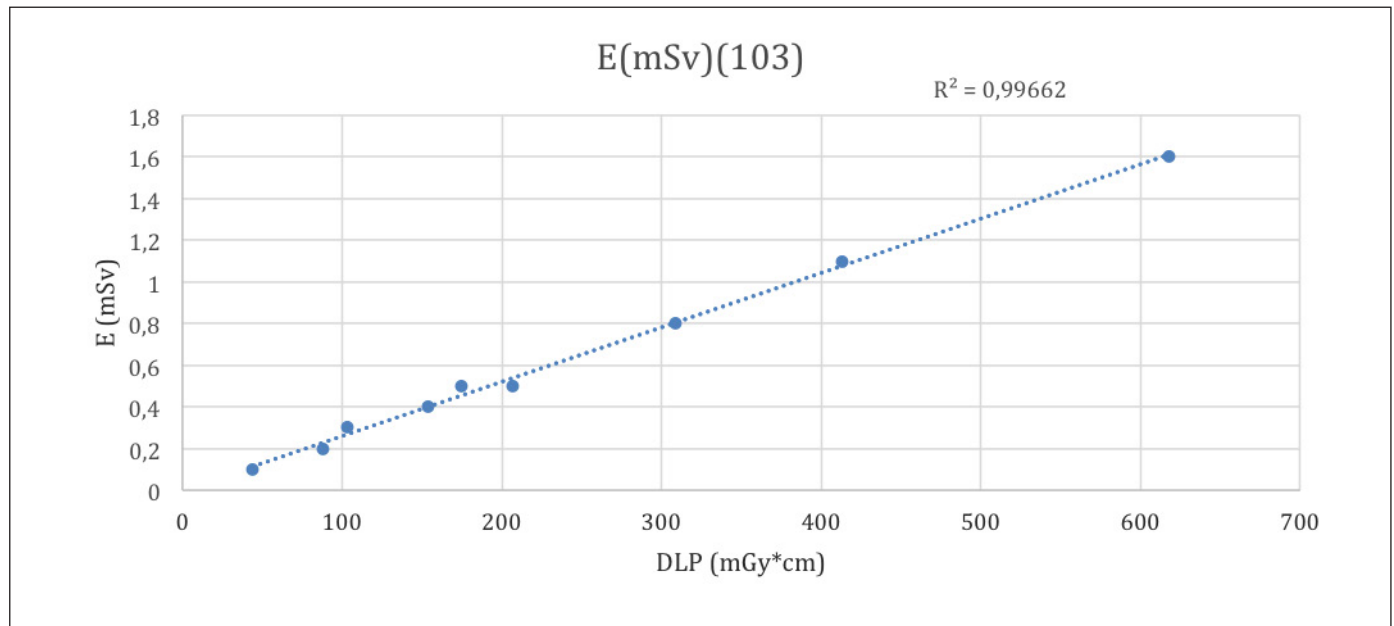
Figure 5: Correlation between the Effective dose (103)(mSv) and DLP (mGy*cm). A strong positive correlation is shown between the effective dose and DLP with a ($r = 0.99$).

Table 5: Calculated values for Intra-class correlation for experience and non-experience observer groups

	Experienced	Non-experienced
Item 1	0.536	0.211
Item 2	0.274	0.18
Item 3	0.531	0.377
Item 4	0.529	0.507
Item 5	0.677	0.624

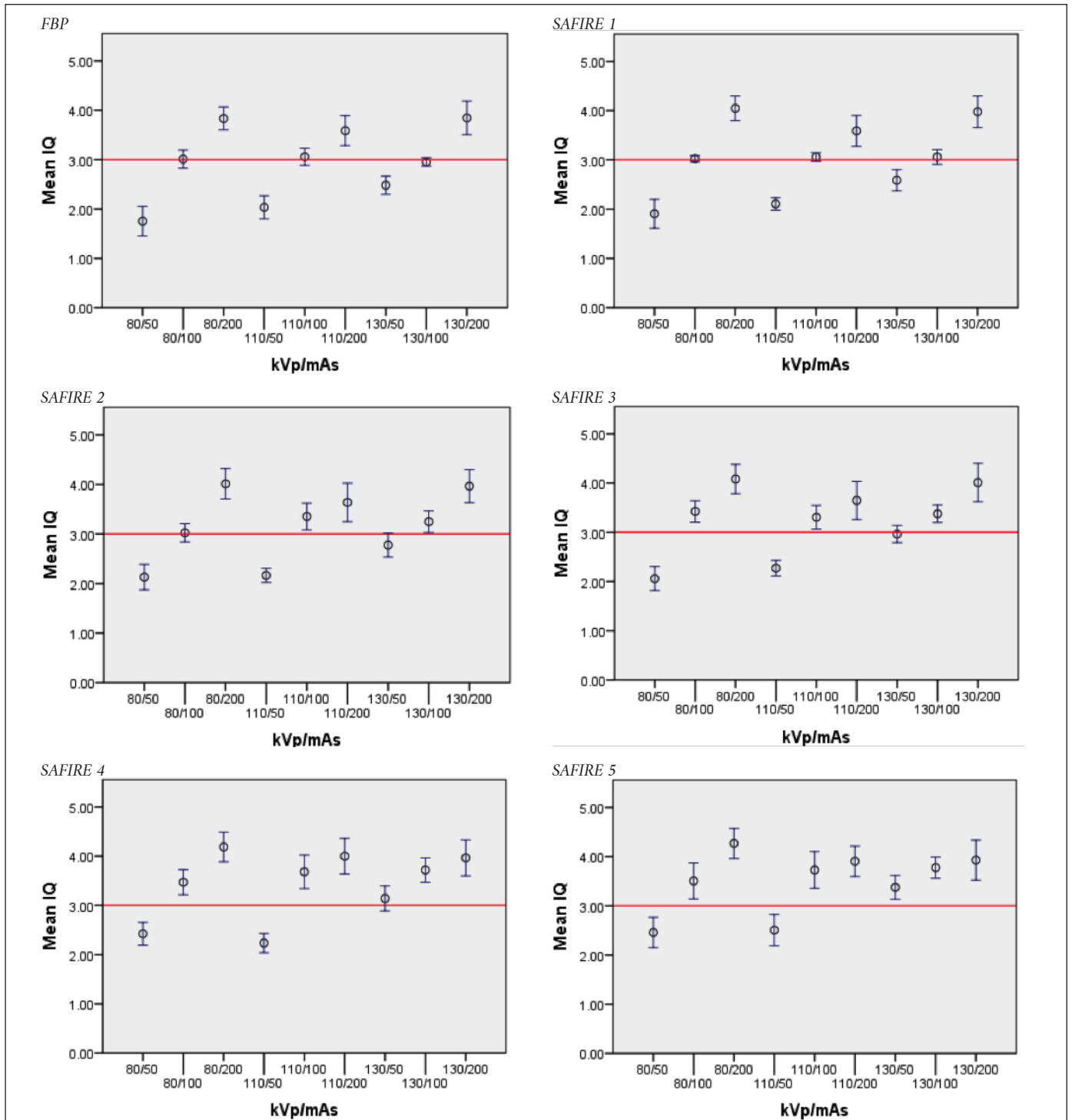


Figure 6: The mean image quality for each IR incorporating a 95% confidence interval, at each acquisition parameter. The reference image intersecting ($y=3$) the y axis represents an average image quality.

The Pearson Product-Moment Correlation Coefficient (r), correlation of determination (r^2), and the p-value were calculated and tabulated (Table 4). This table highlights the lack of correlation between the perceptual image

quality score and the physical image quality measures with $r^2 = 0.20$ and $r^2 = 0.007$ for SNR and CNR respectively. However, the p-value suggests a highly statistical significant relationship.

Mean Image quality		R2	R	P=	P
	SNR	0.2023	0.449778	2.6461E-121	p<0.0001
	CNR	0.0074	0.086023	6.8558E-121	P<0.0001

DISCUSSION

Providing acceptable image quality while reducing the radiation dose remains of paramount importance in CT examinations, more so for paediatric patients. Recent developments in iterative reconstruction technologies such as SAFIRE, shows potential in reducing the dose while improving image quality. However, the application of these techniques are limited for paediatric patients, with insignificant guidelines on the optimal SAFIRE strength for the best image quality.

This study highlights the advantages of using iterative reconstruction for a paediatric head phantom with a reduction of more than 68% in effective dose in comparison to standard Siemens SOMATON perspective 128 Computed Tomography (CT) protocol. The study also found that SAFIRE increases the SNR by an average of 22% with an average reduction in noise of 20%. When comparing the standard FBP reconstruction to SAFIRE 5, an average of 33% reduction in noise and 54% increase in SNR was calculated and the same was appreciated in the mean perceptual image quality scores, with SAFIRE 5 providing the best image quality. However, the item assessing the 'overall image quality' identified SAFIRE 4 as providing the best image quality. A factor most likely influenced by the image blurring or over smoothing reported in several studies¹⁻³ with an increase in SAFIRE strength recognising that a reduction in noise may not directly translate to an improvement in overall image quality¹. Further research is required to identify the dose level at which diagnostic image quality can be achieved.

Observers

Experienced observers showed a higher ICC compared to inexperienced observers, which might be due to the fact that inexperienced observers have a learning effect during the task¹⁷. Buissink et al (2014) found that a statistically significant improvement can be observed post-training. However, all observer groups showed low to moderate ICC in all items of the IQ-criteria. The inclusion of training may

have resulted in smaller difference between the groups¹⁸ and might have increased overall observer reliability.

Limitations

The simulation of paediatric head phantom ATOM five year old child, model 705⁶, ensured no irradiation of human tissue⁷; however this presented a reduction in external validity. The tissue-equivalent epoxy resins present in all aspects of ATOM provided advantages in objective measures, but lacked comparable anatomical representation of a paediatric brain. This further limited the ability to adapt the European guidelines for quality criteria for computed tomography due to its reference to brain anatomy¹⁰. The use of a vetted criteria would have prevented the miss interpretation of the item questioning 'how many circles can you see in the image?' Nonetheless training the observers prior to the perceptual task may have improved their understanding of the question, increasing inter-observer reliability.

Images at 110kVp were acquired at different scan ranges in comparison to 80kVp and 130kVp, limiting the selection of the same slice for all images. Although the method was designed to overcome this restriction the ability to compare the batches may still exist.

CONCLUSION

In summary, the SAFIRE algorithm is suitable for image-noise reduction in paediatric head CT. Our data demonstrate that SAFIRE enhances SNR, while reducing noise, with a possible reduction in effective dose of 68%. The decrease in image quality with dose requires careful consideration of SAFIRE strength application to achieve optimal balance between image quality and noise. Our results suggest a potential for further reduction in dose and encourages an increase in external validity.

ACKNOWLEDGEMENTS

We would like to take this opportunity to acknowledge Carla Lança, for her assistance with the visual acuity tests for the observers, SIEMENS for providing us both the equipment and the reconstructed image sets. We also acknowledge Escola Superior de Tecnologia da Saúde de Lisboa for letting us use their facilities, equipment and time.

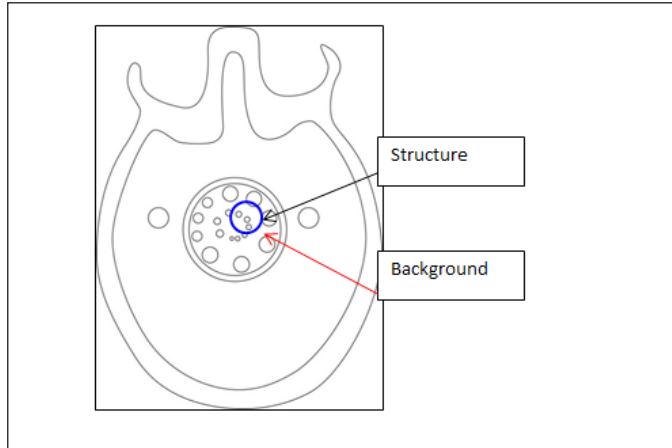
REFERENCES

1. Chang RC, Yu CC, Hsu FY, Chen TR, Hsu SM, Tyan YS. Dose assessment of the patient and the helper in emergency head computed tomography. *Radiat Meas.* 2011;46(12):2048-51.
2. Brenner DJ, Elliston CD, Hall EJ, Berdon WE. Estimated risks of radiation-induced fatal cancer from pediatric CT. *AJR Am J Roentgenol.* 2001;176(2):289-96.
3. Pickhardt PJ, Lubner MG, Kim DH, Tang J, Ruma JA, del Rio AM, et al. Abdominal CT with model-based iterative reconstruction (MBIR): initial results of a prospective trial comparing ultralow-dose with standard-dose imaging. *AJR Am J Roentgenol.* 2012;199(6):1266-74.
4. Korn A, Fenchel M, Bender B, Danz S, Hauser TK, Ketelsen D, et al. Iterative reconstruction in head CT: image quality of routine and low-dose protocols in comparison with standard filtered back-projection. *AJNR Am J Neuroradiol.* 2012;33(2):218-24.
5. Greffier J, Fernandez A, Macri F, Freitag C, Metge L, Beregi JP. Which dose for what image? Iterative reconstruction for CT scan. *Diagn Interv Imaging.* 2013;94(11):1117-21.
6. Han BK, Grant KL, Garberich R, Sedlmair M, Lindberg J, Lesser JR. Assessment of an iterative reconstruction algorithm (SAFIRE) on image quality in pediatric cardiac CT datasets. *J Cardiovasc Comput Tomogr.* 2012;6(3):200-4.
7. Grant K, Raupach R. SAFIRE: Sinogram Affirmed Iterative Reconstruction [Internet]. Siemens; 2012. Available from: <https://www.healthcare.siemens.com/computed-tomography/options-upgrades/clinical-applications/safire>
8. CIRS. ATOM® dosimetry verification phantoms [Internet]. Norfolk-VG: CIRSINC; 2013. Available from: http://www.cirsinc.com/file/Products/701_706/701%20706%20DS%20112613.pdf
9. Department of Health. The ionising radiation (medical exposure) regulations 2000: together with notes on good practice [Internet]. London: Department of Health; 2012. Available from: https://www.gov.uk/government/uploads/system/uploads/attachment_data/file/227075/IRMER_regulations_2000.pdf
10. Menzel HG, Schibilla H, Teunen D. European guidelines on quality criteria for computer tomography [Internet]. Brussels: European Commission; 1999. Available from: http://w3.tue.nl/fileadmin/sbd/Documenten/Leergang/BSM/European_Guidelines_Quality_Criteria_Computed_Tomography_Eur_16252.pdf
11. Haubenreisser H, Fink C, Nance JW Jr, Sedlmair M, Schmidt B, Schoenberg SO, et al. Feasibility of slice width reduction for spiral cranial computed tomography using iterative image reconstruction. *Eur J Radiol.* 2014;83(6):964-9.
12. Gur D, Rubin DA, Kart BH, Peterson AM, Fuhrman CR, Rockette HE, et al. Forced choice and ordinal discrete rating assessment of image quality: a comparison. *J Digit Imaging.* 1997;10(3):103-7.
13. Ledenius K, Svensson E, Stålhammar F, Wiklund LM, Thilander-Klang A. A method to analyse observer disagreement in visual grading studies: example of assessed image quality in paediatric cerebral multidetector CT images. *Br J Radiol.* 2010;83(991):604-11.
14. Yount WR. Developing scales: the Likert scale, the Thurstone scale, the Q-Sort scale, the Semantic Differential. In Yount WR, editor. *Research design and statistical analysis in Christian ministry.* 4th ed. Author; 2006. chap. 12.
15. Båth M, Månsson LG. Visual grading characteristics (VGC) analysis: a non-parametric rank-invariant statistical method for image quality evaluation. *Br J Radiol.* 2007;80(951):169-76.
16. McGreevy RL. Reverse Monte Carlo modelling. *J Phys.* 2001;13(46):R877.
17. Brown CR, Hillman SJ, Richardson AM, Herman JL, Robb JE. Reliability and validity of the Visual Gait Assessment Scale for children with hemiplegic cerebral palsy when used by experienced and inexperienced observers. *Gait Posture.* 2008;27(4):648-52.
18. Buissink C, Thompson JD, Voet M, Sanderud A, Kamping LV, Savary L, et al. The influence of experience and training in a group of novice observers: a jackknife alternative free-response receiver operating characteristic analysis. *Radiography.* 2014;20(4):300-5.

Appendix A. Image test training

Question B

The differentiation of contrast within the encircled structure (see image) and its immediate background (see arrow)?

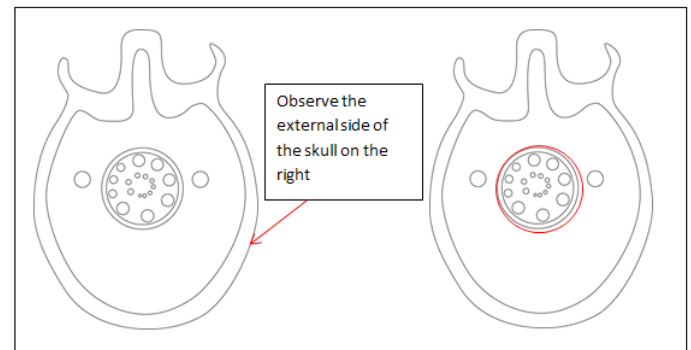


Question C

The visual sharpness of the bony structure displayed?

Question D

The sharpness of the circle in the encircled structure?



Appendix B. Questionnaire

How many circles can you count within the centre of the image?

Image Reference	1	2	4	5	6	7	8	9	10	11	12	13	14	15	16	17	18	19	20
Circles																			

Appendix C

Table 5: The average image quality score incorporating all observers with

80 kVp								
50 mAs	0.1	1.75 (± 0.58)	1.91 (± 0.57)	2.13 (± 0.5)	2.06 (± 0.47)	2.42 (± 0.45)	2.46 (± 0.6)	
100 mAs	0.2	R (± 0.36)	3.02 (± 0.12)	3.02 (± 0.36)	3.42 (± 0.42)	3.47 (± 0.5)	3.51 (± 0.71)	
200 mAs	0.5	3.84 (± 0.45)	4.05 (± 0.49)	4.01 (± 0.6)	4.08 (± 0.58)	4.19 (± 0.59)	4.27 (± 0.6)	
110 kVp								
50 mAs	0.3	2.04 (± 0.45)	2.11 (± 0.25)	2.16 (± 0.28)	2.27 (± 0.31)	2.24 (± 0.38)	2.51 (± 0.62)	
100 mAs	0.5	R (± 0.34)	3.06 (± 0.17)	3.35 (± 0.53)	3.31 (± 0.47)	3.68 (± 0.66)	3.73 (± 0.72)	
200 mAs	1.1	3.59 (± 0.59)	3.59 (± 0.61)	3.64 (± 0.76)	3.65 (± 0.75)	4 (± 0.7)	3.91 (± 0.6)	
130 kVp								
50 mAs	0.4	2.48 (± 0.36)	2.59 (± 0.42)	2.78 (± 0.47)	2.96 (± 0.34)	3.14 (± 0.49)	3.38 (± 0.47)	
100 mAs	0.8	R (± 0.17)	3.06 (± 0.29)	3.25 (± 0.43)	3.38 (± 0.35)	3.72 (± 0.49)	3.78 (± 0.42)	
200 mAs	1.6	3.85 (± 0.66)	3.98 (± 0.62)	3.96 (± 0.65)	4.01 (± 0.76)	3.96 (± 0.71)	3.93 (± 0.79)	

Appendix D

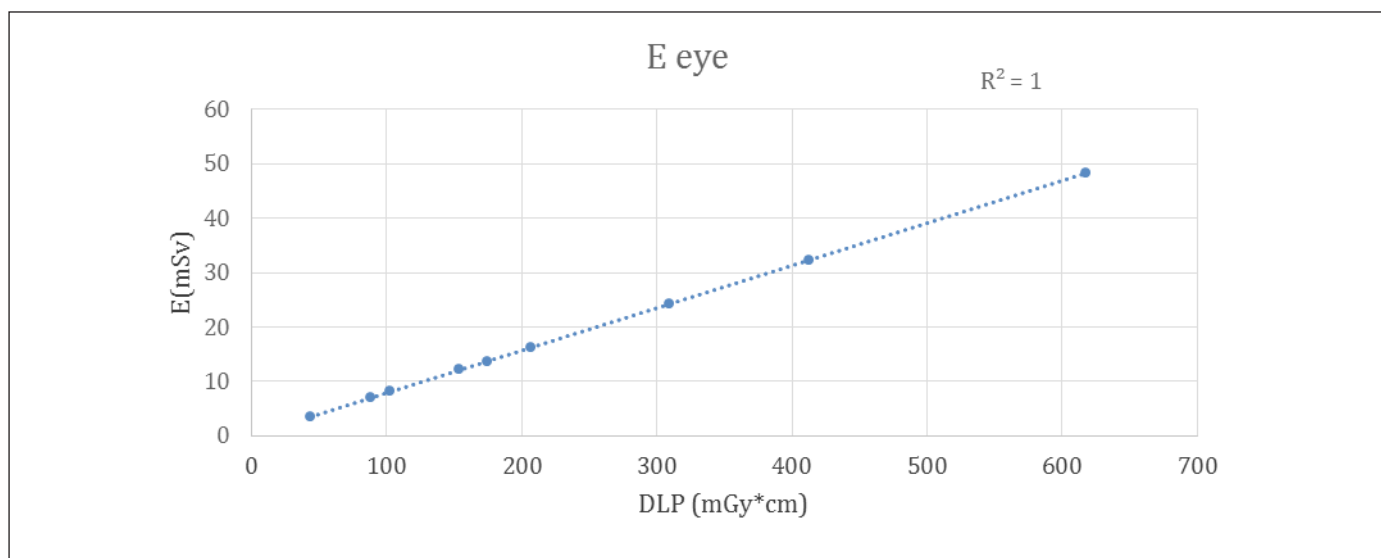


Figure 3: Correlation between effective dose to the eyes (mSv) and the DLP (mGy*cm). A strong linear correlation is shown as the increase in DLP increases the effective dose to the eyes.

COBB ANGLE

Review article – Optimisation of exposure parameters for spinal curvature measurements in paediatric radiography

Cláudia Reis^a, Junior Ndlovu^b, Catarina Serrenho^a, Ifrah Akhtar^b, Seraphine de Haan^c, José Antonio Garcia^d, Daniel de Linde^e, Martine Thorskog^e, Loris Franco^d, Peter Hogg^b

a) Lisbon School of Health Technology (ESTeSL), Polytechnic Institute of Lisbon, Portugal

b) School of Health Sciences, University of Salford, Manchester, United Kingdom

c) Department of Medical Imaging and Radiation Therapy, Hanze University of Applied Sciences, Groningen, The Netherlands

d) Haute École de Santé Vaud – Filière TRM, University of Applied Sciences and Arts of Western Switzerland, Lausanne, Switzerland

e) Department of Life Sciences and Health, Radiography, Oslo and Akerhus University College of Applied Science, Oslo, Norway



KEY WORDS

Optimisation
Spinal curvature
measurements
Effective dose
Image quality
Paediatrics
Phantom
Computed radiography

ABSTRACT

This review aims to identify strategies to optimise radiography practice using digital technologies, for full spine studies on paediatrics focusing particularly on methods used to diagnose and measure severity of spinal curvatures. The literature search was performed on different databases (PubMed, Google Scholar and ScienceDirect) and relevant websites (e.g., American College of Radiology and International Commission on Radiological Protection) to identify guidelines and recent studies focused on dose optimisation in paediatrics using digital technologies. Plain radiography was identified as the most accurate method. The American College of Radiology (ACR) and European Commission (EC) provided two guidelines that were identified as the most relevant to the subject. The ACR guidelines were updated in 2014; however these guidelines do not provide detailed guidance on technical exposure parameters. The EC guidelines are more complete but are dedicated to screen film systems. Other studies provided reviews on the several exposure parameters that should be included for optimisation, such as tube current, tube voltage and source-to-image distance; however, only explored few of these parameters and not all of them together. One publication explored all parameters together but this was for adults only. Due to lack of literature on exposure parameters for paediatrics, more research is required to guide and harmonise practice.

INTRODUCTION

There are several types of spinal deformities that can affect children during their early or late childhood, with scoliosis and kyphosis being the most common¹. Early diagnosis is important to improve prognosis and life expectancy². Diagnosis and follow-up can be performed using physical examinations and/or imaging (e.g., CT, MRI and plain radiography). Imaging is the most common method because it is accurate and it allows the detection and severity assessment. Despite developments in cross-sectional imaging plain radiography remains the mainstay. Plain radiography can be

obtained using analogue or digital systems [computed radiography (CR) or direct radiography (DR)] and is required to measure the degree of spinal curvature, using Centroid, Harrison Posterior Tangent, TRALL and Cobb methods³⁻⁴.

However, plain radiography involves radiation. This can increase stochastic effects, especially for children. Therefore, it should be performed using optimised acquisition parameters to guarantee that Image quality (IQ) is acceptable to analyse the anatomical structures and perform spinal curvature measurements. The European guidelines provided by European Commission (EC)⁵ give information about imaging

on paediatrics with details on technical parameters but only for analogue systems. Also provides general recommendations for paediatrics although not by age.

Several studies⁶⁻⁹ provide information about reducing dose to paediatrics but it is not fully explored for digital systems and age groups. This is important because paediatrics are more radiosensitive than adults, due to the rate of cell division¹⁰, increasing the probability of late radiation effects which can affect life expectancy¹¹. Therefore, it is important to keep doses As Low As Reasonably Practicable (ALARP)¹².

The aim of this review is to identify strategies to optimise radiography practice using digital technologies for spine curvature examinations on paediatrics and provide an overview of the methods available for measuring the degree of spinal curvatures.

Literature review was performed using different resources including databases (PubMed, Google Scholar and ScienceDirect) and websites and guidelines to obtain a range of information on different methodologies available for assessing spinal curvatures. To search for relevant literature, the following keywords were used: optimisation, effective dose, IQ, paediatrics, phantom and Computed Radiography. Other criteria to select the studies were: year of publication for the selection of exposure parameters (most updated) and use of CR/DR.

Spinal deformities in paediatrics

Spinal conditions include scoliosis (curving of the spine), kyphosis (increasing roundback of the spine), lordosis (increasing inward curvature of the spine), spondylolysis (stress fracture of the spine) and spondylolisthesis (movement of one part of the spine on another part). Scoliosis and kyphosis are the most common. These deformities can affect children during their early or late childhood^{1,13}. These may occur due to failure of bone development and are treated depending on the cause. Whilst in adolescence the cause may be unknown, it is more likely to be determined in the early age. To prevent progression of deformity and improve life expectancy early diagnosis is important².

Thoracic kyphosis is the increase of the thoracic curvature in the sagittal plane and indication for treatment is based on kyphosis angular measurement. Normal kyphosis ranges from 20-50° when assessed by modified Cobb's method on lateral radiographs¹⁴.

Scoliosis is a structural three-dimensional deformity of the spine defined by a lateral curvature of more than 10°.

The development and progression of scoliosis is related to growth. Scoliosis can also be classified by cause, into idiopathic or secondary. Idiopathic scoliosis is further classified into infantile, juvenile (4-10 years) and adolescent types or early and late onset. Scoliosis can also be secondary to congenital disorders, neuromuscular conditions, tumors, trauma or syndromic².

Available methodologies to detect spinal curvatures

There are many methods of measuring spinal curvature including: physical examinations (e.g., forward bending) and imaging methods (e.g., CT, MRI and plain radiography). Imaging is the most common and accurate method to determine severity of curvature. Despite the vast development of CT and MRI in terms of cross-sectional imaging, with MRI posing no radiation dose to patient, plain radiography remains the mainstay. It is the most affordable, time efficient, easily accessible (compared to CT and MRI), more patient friendly compared to MRI and provides the least dose when compared to CT¹⁵. It is used to confirm diagnosis, exclude underlying causes, assess the curves and severity, monitor progression, assess skeletal maturing and determine patient's suitability for surgery¹⁶.

Techniques to measure spinal curvature using imaging methods

Many methods are mentioned in the literature for measuring the degree of spinal curvatures using plain radiography. Centroid method is performed on the lateral view by connecting the intersections of 2, 3 or 4 vertebral bodies. This method is easily performed however has less inter-observer reliability and does not provide accurate angles of hypotension or hyperextension³⁻⁴. In addition, the Centroid method uses more points and takes more time to conduct. In comparison to the Cobb method and Harrison posterior tangents method, the Centroid method results in smaller angle measurement of the total spinal curvature³.

In the Harrison posterior tangent method, lines are drawn at two posterior vertebral bodies simultaneously on a lateral radiograph because of the higher density. Despite this method having a smaller standard error compared to other methods, it can only be used on lateral radiographs³.

The TRALL method requires a vertical line drawn from the posterior-superior apex of the 1st Lumbar vertebra (L1) to Sacrum. The largest perpendicular distance (depth) to the posterior longitudinal ligament is used to find the lumbar curve apex. This method only provides one global angle and does not include segmental angles, limiting its usefulness².

The Cobb's method can be used for Antero-posterior (AP)/Postero-anterior (PA) and lateral radiographs, whereas the posterior tangent method is not widely used for assessing both kyphosis and scoliosis. In the modified Cobb method, four lines are drawn to create the Cobb angle. Two parallel to vertebral bodies at the superior aspect of T1 and the inferior aspect of T12 and two perpendicular to those. This method is the most common and can be created by the computer or drawn manually. In clinical practice there may be instances when the Cobb method is not appropriate (e.g., hypolordosis) due to the lack of convergence of lines on the radiograph. In such cases, posterior tangent method is recommended⁴. Several studies¹⁷⁻¹⁹ showed good reliability with the Cobb method. Furthermore, this method represents the standard means of evaluating clinically, spinal curvature and has been adapted traditionally in clinical practice as the most simple, well known and accurate for diagnosis and follow-up²⁰.

Optimisation of radiography for the analysis of spine curvature

To satisfy the needs in paediatric imaging, optimisation must be at the forefront of all techniques. The stochastic effects of radiation are a concern in paediatrics because this population is the most sensitive. Imaging may result in a high cumulative dose because serial imaging is often involved¹. Radiation exposure in the first ten years of life is estimated to cause detrimental effects, with attributable lifetime risk five to seven times greater than exposures between the ages of 50-70⁵.

There are two principles of radiation protection of the patient²¹: justification of practice and optimisation of exposure. Justification is particularly important in paediatrics and is related to the relevance of the examination. This means that an exposure is not justifiable without a valid clinical indication. For every examination benefits must outweigh risks⁵.

The International Commission on Radiological Protection (ICRP) does not recommend the application of dose limits to patient irradiation, dose reference levels (DRL) should be used as an optimisation tool. However, it is always a challenge to minimize the dose to the patient without compromising IQ required for accurate diagnosis^{5,22}. So, during optimisation it is important to consider IQ, the imaging method and technique, to keep doses ALARP¹². Generally, optimisation is focused on examinations that are common and/or give significant dose to patients such as skull, pelvis, spine, abdomen and chest⁵.

To estimate the radiation dose delivered during an

X-ray examination, there are several approaches that can be used such as measurements on phantoms or patients, and also several types of radiation detectors can be used [e.g., Dose-Area product (DAP) dosimeter, thermoluminescent dosimeter (TLD)] and Monte Carlo simulations²³.

The results of the studies can vary according to the methodology that is chosen for dose estimation; however a major overview on dose values can be taken from the literature. A study to optimise lateral thoracic-lumbar images was performed using Monte Carlo simulations. The technical parameters that were used consisted of anode towards the head, broad focus, no Object to Image Distance (OID) or grid, 80kVp, 32mAs and 130cm SID. The estimate effective dose resulted to 0.05 mSv. Yet, this study was performed with adult phantom and patients²⁴.

In order to achieve the adequate balance between IQ and dose, techniques for evaluating IQ should be focused on the clinical aim²⁵. The literature review highlighted many studies on the topic, but this review is focused on more updated studies (after 1990), to have an overview on the strategies for optimisation dedicated to digital technologies.

IQ analysis is difficult to define when there are many aims (e.g., detection only, avoid noise, improve contrast) for different observers, and there are several options to do this. Radiographers and radiologists require images that have quality to ensure a precise diagnosis. Concerning this, observers should share equal standards for visual measures of IQ. IQ is affected by exposure parameters, human characteristics and skills (e.g., eye accuracy, perception and experience) to observe an anatomical region addressing a specific clinical situation. To improve practice, it is desirable that observers have discussions to prevent heterogeneous IQ standards²⁶.

Concerning IQ assessment, there are many different types of recommended tests and these vary within the literature. There are physical methods [e.g., contrast-to-noise ratio (CNR), signal-to-noise ratio (SNR)] and also visual methods. Visual methods found in the literature tend to use several IQ ratings including: absolute or relative scales [(e.g., five-step scale, 1 (worst) to 5 (best); and two-step scale with 1 (criterion was fulfilled) and 0 (criterion was not fulfilled); four-step scale (perfect, good, moderate and inadequate)]. Software also exists to assist in performing visual IQ assessment, for example ViewDEX, 2 Alternative Forced Choice (2AFC), conspicuity index^{25,27}.

ViewDEX (Viewer for Digital Evaluation of X-ray images) allows the validation of new imaging systems, techniques and

research on IQ using observers. This software is DICOM compatible and the features of the interface (tasks, image handling and functionality) are general and flexible²⁸. Also, this software allows observer performance studies with the same fundamental display properties reflected in the clinical reading environment, with less time required to handle the images compared to analogue systems²⁸⁻²⁹.

Studies and guidelines often do not include information on observer training for visual IQ assessment. This could be useful to reduce inter and intra observer variability during the assessment. To select the strategies, human resources, material resources and also the available time to perform the tasks must be considered²⁷.

The literature dedicated to IQ improvement and dose reduction in paediatrics provided general strategies such as raising kVp whilst lowering mAs to reduce dose; and the use of image-processing techniques adapted to the local characteristics, in particular to the noise content, which allows dose reduction. Agfa systems contain MUSICA software that allows different processing methods for 4 different paediatric age/weight groups for a variety of exams⁸.

The first examination on a patient should address IQ but for follow up examinations it may not require the same degree of quality, so dose could be reduced. Main methods to optimise provided by Willis⁷ were: to select a suitable detector (small, higher sensitivity and efficiency), combination of noisy images, scatter reduction with grid or other technique and limit radiation field to anatomy of interest. The same author also provided other options such as increase kVp or SID to reduce dose, increase mAs to improve contrast, increase image processing adopting the best tools, use AEC or manual technique concerning calibrations⁷.

Other studies^{7,30-34} focused on one or two parameters (kVp alone, SID alone), apart from the study performed by Qaroot et al²⁴, which takes into consideration all the above parameters, however relates to adults only. Also, the majority of studies are focused on screen-film systems and measurements accuracy³⁵⁻³⁷.

The studies identified as related to digital technologies are mainly reviews and a protocol to optimise paediatric practice could not be found.

CONCLUSION

The two most common spinal deformities in children are kyphosis and scoliosis. Amongst the many methods used for diagnosis, imaging is the most used as it not only provides diagnosis, but also severity of the condition. Between the many imaging methods, plain radiography is most accurate, cost effective and time efficient. From the various techniques available for measuring the degree of spinal curvature, Cobb measurements are most usual, easily performed and can be used for AP/PA and lateral projections. However, in order to carry out these measurements, X-rays are required, which pose radiation risks, especially for paediatrics as they are more radiosensitive. Moreover, with the serial imaging involved, optimisation of dose is critical along with producing imaging that allows accurate Cobb measurements. Due to the lack of current guidelines for paediatrics using digital equipment, it is important to conduct a study which explores different exposure parameters, in order to conclude the most optimum parameters. This will update information provided by the EC and guidelines by ACR.

REFERENCES

1. Bruce Jr R, Fletcher N. Pediatric spinal deformities [Internet]. Emory Health Care; 2014 [updated 2015; cited 2014 Aug 12]. Available from: <http://www.emoryhealthcare.org/pediatric-orthopedics/conditions/spinal-deformity.html>
2. Rolton D, Nnadi C, Fairbank J. Scoliosis: a review. *Paediatr Child Health*. 2014;24(5):197-203.
3. Harrison DE, Cailliet R, Harrison DD, Janik TJ, Holland B. Reliability of centroid, Cobb, and Harrison posterior tangent methods: which to choose for analysis of thoracic kyphosis. *Spine (Phila Pa 1976)*. 2001;26(11):E227-34.
4. Harrison DE, Harrison DD, Cailliet R, Janik TJ, Holland B. Radiographic analysis of lumbar lordosis: centroid, Cobb, TRALL, and Harrison posterior tangent methods. *Spine (Phila Pa 1976)*. 2001;26(11):E235-42.
5. Kohn M, Moores B, Schibilla H, Schneider K, Stender H, Stieve F, et al. European guidelines on quality criteria for diagnostic radiographic images in paediatrics. Luxembourg: Office for Official Publications of the European Communities; 1996.

6. Hess R, Neitzel U. Optimizing image quality and dose in digital radiography of pediatric extremities [Internet]. Philips Healthcare; 2011. Available from: http://www.healthcare.philips.com/main/about/events/rsna/pdfs/DR_White_paper_Optimizing_image_quality_and_dose_in_digital_radiography_of_pediatric_extremities.pdf
7. Willis CE. Optimizing digital radiography of children. *Eur J Radiol.* 2009;72(2):266-73.
8. Schaetzing R. Management of pediatric radiation dose using Agfa computed radiography. *Pediatr Radiol.* 2004;34 Suppl 3:S207-14
9. Hess R, Neitzel U. Optimizing image quality and dose for digital radiography of distal pediatric extremities using the contrast-to-noise ratio. *Rofo.* 2012;184(7):643-9.
10. Pearce MS, Salotti JA, Little MP, McHugh K, Lee C, Kim KP, et al. Radiation exposure from CT scans in childhood and subsequent risk of leukaemia and brain tumours: a retrospective cohort study. *Lancet.* 2012;380(9840):499-505.
11. Bone CM, Hsieh GH. The risk of carcinogenesis from radiographs to pediatric orthopaedic patients. *J Pediatr Orthop.* 2000;20(2):251-4.
12. Health and Safety Executive. ALARP “at a glance” [Internet]. HSE; 2014 [cited 2014 Aug 12]. Available from: <http://www.hse.gov.uk/risk/theory/alarpglance.htm>
13. SingHealth. Orthopaedic problems in children: spine deformity (scoliosis, kyphosis) and back pain [Internet]. SingHealth Group; 2014 [cited 2014 Aug 12]. Available from: <http://www.singhealth.com.sg/PatientCare/ConditionsAndTreatments/Pages/Orthopaedic-Problems-in-Children-Back-Pain-and-Spine-Deformity-in-Children-and-Adolescents.aspx>
14. Teixeira FA, Carvalho GA. Confiabilidade e validade das medidas da cifose torácica através do método flexicurva [Reliability and validity of thoracic kyphosis measurements using flexicurve method]. *Rev Bras Fisioter.* 2007;11(3):199-204. Portuguese
15. Malfair D, Flemming AK, Dvorak MF, Munk PL, Vertinsky AT, Heran MK, et al. Radiographic evaluation of scoliosis: review. *AJR Am J Roentgenol.* 2010;194(3 Suppl):S8-22.
16. Rajiah P. Idiopathic scoliosis imaging [Internet]. Medscape; 2013 [cited 2014 Aug 7]. Available from: <http://emedicine.medscape.com/article/413157-overview>
17. Hong JY, Suh SW, Modi HN, Lee JM, Park SY. Centroid method: an alternative method of determining coronal curvature in scoliosis. A comparative study versus Cobb method in the degenerative spine. *Spine J.* 2013;13(4):421-7.
18. Chen TR, Tyan YS, Yang JJ, Shao CH, Lin JY, Tung CJ. Measurements and applications of dose indices in radiography. *Radiat Meas.* 2011;46(12):2044-7.
19. Tanure MC, Pinheiro AP, Oliveira AS. Reliability assessment of Cobb angle measurements using manual and digital methods. *Spine J.* 2010;10(9):769-74.
20. Pearsall DJ, Reid JG, Hedden DM. Comparison of three noninvasive methods for measuring scoliosis. *Phys Ther.* 1992;72(9):648-57.
21. ICRP. The 2007 recommendations of the International Commission on Radiological Protection [Internet]. Ottawa: ICRP; 2007 [cited 2014 Aug 20]. Available from: [http://www.icrp.org/publication.asp?id=ICRP Publication 103](http://www.icrp.org/publication.asp?id=ICRP%20Publication%20103)
22. Seeram E, Brennan PC. Diagnostic reference levels in radiology. *Radiol Technol.* 2006;77(5):373-84.
23. International Atomic Energy Agency. Dosimetry in diagnostic radiology: an international code of practice. Vienna: IAEA; 2007. ISBN 9201154062
24. Al Qaroot B, Hogg P, Twiste M, Howard D. A systematic procedure to optimise dose and image quality for the measurement of inter-vertebral angles from lateral spinal projections using Cobb and superimposition methods. *J Xray Sci Technol.* 2014;22(5):613-25.
25. Martin CJ, Sharp PF, Sutton DG. Measurement of image quality in diagnostic radiology. *Appl Radiat Isot.* 1999;50(1):21-38.
26. Ween B, Kristoffersen DT, Hamilton GA, Olsen DR. Image quality preferences among radiographers and radiologists: a conjoint analysis. *Radiography.* 2005;11(3):191-7.
27. Reis C, Pascoal A, Sakellaris T, Koutalonis M. Quality assurance and quality control in mammography: a review of available guidance worldwide. *Insights Imaging.* 2013;4(5):539-53.
28. Håkansson M, Svensson S, Zachrisson S, Svåkvist A, Båth M, Månsson LG. VIEWDEX: an efficient and easy-to-use software for observer performance studies. *Radiat Prot Dosimetry.* 2010;139(1-3):42-51.

29. Börjesson S, Håkansson M, Båth M, Kheddache S, Svensson S, Tingberg A, et al. A software tool for increased efficiency in observer performance studies in radiology. *Radiat Prot Dosimetry*. 2005;114(1-3):45-52.
30. Young KJ. Should plain films of the lumbar spine be taken in the posterior-to-anterior or anterior-to-posterior position? A study using decision analysis. *J Manipulative Physiol Ther*. 2007;30(3):200-5.
31. Guo H, Liu WY, He XY, Zhou XS, Zeng QL, Li BY. Optimizing imaging quality and radiation dose by the age-dependent setting of tube voltage in pediatric chest digital radiography. *Korean J Radiol*. 2013;14(1):126-31.
32. Tinsberg A, Sjöström D. Optimisation of image plate radiography with respect to tube voltage. *Radiat Prot Dosimetry*. 2005;114(1-3):286-93.
33. Saether HK, Lagesen B, Traegde Martinsen AC, Holsen EP, Ovrebo KM. Dose levels from thoracic and pelvic examinations in two pediatric radiological departments in Norway: a comparison study of dose-area product and radiographic technique. *Acta Radiol*. 2010;51(10):1137-42.
34. Olgar T, Onal E, Bor D, Okumus N, Atalay Y, Turkyilmaz C, et al. Radiation exposure to premature infants in a neonatal intensive care unit in Turkey. *Korean J Radiol*. 2008;9(5):416-9.
35. Barnes GT. Contrast and scatter in X-ray imaging. *Radio-graphics*. 1991;11(2):307-23.
36. Mooney R, Thomas PS. Dose reduction in a paediatric department following optimization of radiographic technique. *Br J Rad*. 1998;71(848):852-60.
37. Almén AJ, Mattsson S. Dose distribution at radiographic examination of the spine in pediatric radiology. *Spine (Phila Pa 1976)*. 1996;21(6):750-6.

Research article – Optimisation of paediatrics computed radiography for full spine curvature measurements using a phantom: a pilot study

Cláudia Reis^a, Junior Ndlovu^b, Catarina Serrenho^a, Ifrah Akhtar^b, Seraphine de Haan^c, José Antonio Garcia^d, Daniel de Linde^e, Martine Thorskog^e, Loris Franco^d, Carla Lança^a, Peter Hogg^b

a) Lisbon School of Health Technology (ESTeSL), Polytechnic Institute of Lisbon, Portugal

b) School of Health Sciences, University of Salford, Manchester, United Kingdom

c) Department of Medical Imaging and Radiation Therapy, Hanze University of Applied Sciences, Groningen, The Netherlands

d) Haute École de Santé Vaud – Filière TRM, University of Applied Sciences and Arts of Western Switzerland, Lausanne, Switzerland

e) Department of Life Sciences and Health, Radiography, Oslo and Akerhus University College of Applied Science, Oslo, Norway



KEYWORDS

Optimisation
Spinal curvature Measurements
Effective dose
Image Quality
Paediatrics
Phantom
Computed radiography

ABSTRACT

Aim: Optimise a set of exposure factors, with the lowest effective dose, to delineate spinal curvature with the modified Cobb method in a full spine using computed radiography (CR) for a 5-year-old paediatric anthropomorphic phantom.

Methods: Images were acquired by varying a set of parameters: positions (antero-posterior (AP), postero-anterior (PA) and lateral), kilo-voltage peak (kVp) (66-90), source-to-image distance (SID) (150 to 200cm), broad focus and the use of a grid (grid in/out) to analyse the impact on E and image quality (IQ). IQ was analysed applying two approaches: objective [contrast-to-noise-ratio/(CNR)] and perceptual, using 5 observers. Monte-Carlo modelling was used for dose estimation. Cohen's Kappa coefficient was used to calculate inter-observer-variability. The angle was measured using Cobb's method on lateral projections under different imaging conditions.

Results: PA promoted the lowest effective dose (0.013 mSv) compared to AP (0.048 mSv) and lateral (0.025 mSv). The exposure parameters that allowed lower dose were 200cm SID, 90 kVp, broad focus and grid out for paediatrics using an Agfa CR system. Thirty-seven images were assessed for IQ and thirty-two were classified adequate. Cobb angle measurements varied between $16^{\circ} \pm 2.9$ and $19.9^{\circ} \pm 0.9$.

Conclusion: Cobb angle measurements can be performed using the lowest dose with a low contrast-to-noise ratio. The variation on measurements for this was $\pm 2.9^{\circ}$ and this is within the range of acceptable clinical error without impact on clinical diagnosis. Further work is recommended on improvement to the sample size and a more robust perceptual IQ assessment protocol for observers.

INTRODUCTION

There are several spinal deformities that can affect children, including scoliosis, kyphosis, lordosis, spondylosis and spondylolisthesis. Early diagnosis is paramount to improve life expectancy and quality. Amongst these deformities, scoliosis and kyphosis are identified as most common which can affect children during their early or late childhood¹⁻².

There are many methods of measuring spinal curvature including physical examination and other methods that require imaging (plain radiography, computed tomography (CT) and magnetic resonance imaging (MRI). Imaging

is the most common and most accurate method to determine severity of curvature. Despite the enormous advances in cross-sectional imaging, plain radiography remains the mainstay for assessing spinal curvature³. It is used to confirm diagnosis, exclude underlying causes, assess curve and severity, monitor progression, assess skeletal maturation and determine patient suitability for surgery⁴.

Amongst the techniques that use imaging to measure spine curvature there are Cobb method, Centroid, TRALL & Harrison posterior tangent⁵. Cobb method is considered the gold standard for diagnosis and follow up. Nevertheless, it has been noted to have an error of up to 2° ⁶⁻⁷. However, a

more recent study by Hong et al⁸ showed better reliability with Cobb in comparison to other methods.

When performing Cobb angle measurements plain radiography involves radiation which involves an associated radiation risks. This is a particular concern in paediatrics because they are more sensitive to radiation due to faster cell division. Additionally, this may result to a high cumulative dose because of the series imaging related to the condition, increasing stochastic effects. Thus, it is paramount to keep doses As Low As Reasonably Practicable (ALARP)⁹. Therefore, it is vital to optimise IQ and dose; however, the lack of up-to-date paediatric guidelines makes it a challenge to choose the correct exposure parameters for digital systems. The most complete guideline found in the literature was the European guideline (EC)¹⁰ but it is out-dated as it is based on analogue systems. The most recent guidelines, such as the American College of Radiology (ACR)¹¹, are focussed on digital radiography, but it does not provide detail on exposure parameters for paediatrics. Furthermore, there are no published studies performed on this topic in radiography concerning paediatrics. For these reasons, this study aims to identify a set of exposure factors with the lowest effective dose to delineate spinal curvature using the modified Cobb method in a lateral full spine computed radiography (CR) for a 5-year-old paediatric phantom.

M E T H O D O L O G Y

This section describes the methodology followed in this study for data collection and analysis. It is organised in subdivisions corresponding to the four phases of the study:

- Phase 1: Image acquisition of spine radiographs achieved through manipulating the exposure parameters proposed by European Guidelines¹⁰.
- Phase 2: Effective dose estimation using PCXMC software (Monte Carlo simulation).
- Phase 3: Assessment of IQ using an objective measurement and a perceptual approach.
- Phase 4: Measurement of lateral spine curvature by using the modified Cobb method.

Phase 1 – Image acquisition

To perform image acquisition, a 5 year-old paediatric anthropomorphic phantom (Figure 1a and 1b), SIEMENS General X-ray unit (POLYDOROS IT 30/55/65/80 and OPTILIX 150/30/50C tube - inherent filtration 2.5mm Al @ 75 kVp were used. The images were processed on an AGFA 35-X digitiser using a speed class of 400.

The image acquisition started with a pilot study performed in two stages. First stage was focused on alignment to guarantee that the phantom was placed in the central area of the automatic exposure control (AEC) system. On the second stage, the mAs and exposure time were collected using the AEC system for 70 acquisitions.

The pilot study provided exposure parameters to perform a total of 130 images on the phantom that were acquired in antero-posterior (AP), postero-anterior (PA) and lateral (LAT) positions using the technical exposure parameters recommended by EC guidelines¹⁰ (Table 1).

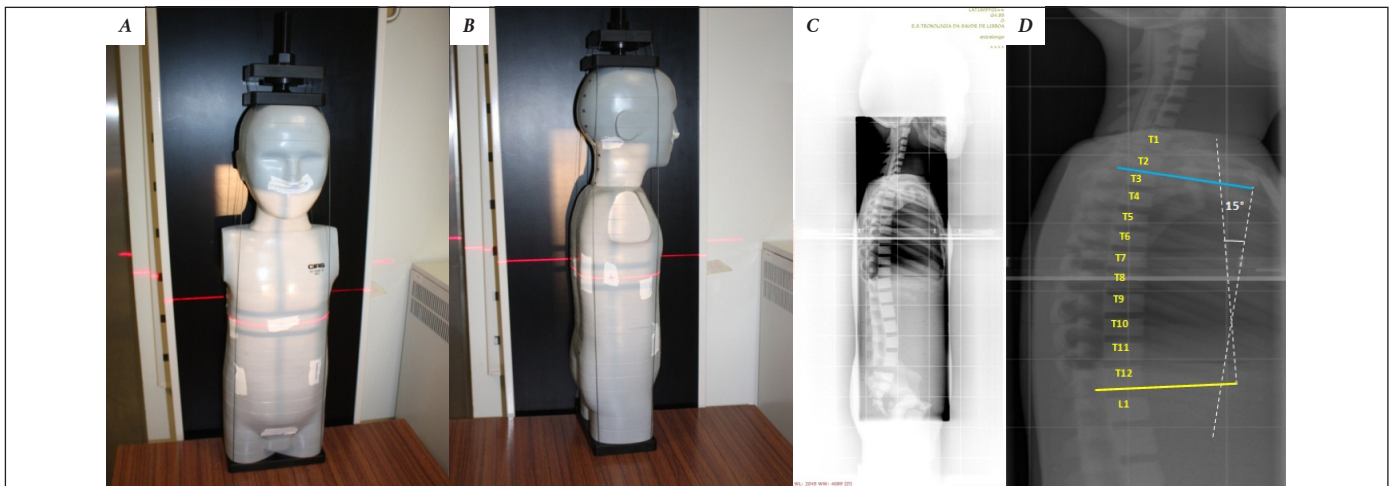


Figure 1: a) The anthropomorphic paediatric phantom in AP, and b) in lateral projection, c) the reference image of the phantom for perceptual image quality analysis, and d) modified Cobb angle measurement.

Table 1: Sets for image acquisition varying voltage (kVp), positioning, grid, source-to-image distance (SID) and focus

Study Phases	Number of exposure performed	Number of images analysed	Manipulated parameters			
			Phantom Position	kVp range	Use Of Grid**	SID range [cm]
Phase 1 (Pilot): Alignment with AEC system	3	3		AEC	In	150
Phase 1 (Pilot): collection of mAs and time (s)	70		AP PA LAT	66 71.5 77 81 85 90	In & Out	150 180 200
Phase 1: Image acquisition	130		AP PA LAT	66 71.5 77 81 85 90	In & Out	150 180 200
Phase 3: Perception of Image Quality		37*	LAT	66 77 90	In & Out	150 180 200
Phase 3: Cobb angle measurements		6*	LAT	66 77 90	Out	150 180 200

Observation: AP: antero-posterior; PA: postero-anterior; LAT: lateral

* Images selected from the 130 acquisitions performed in phase 1

** Grid information: parallel; ratio=8 and absorbing Pb, strips

Phase 2 – Effective dose estimation

Effective dose (E) was calculated using PCXMC software¹. This software uses Monte Carlo simulation for calculating organ dose and E, for those who are examined with X-rays for medical use. By selecting the tissue weighting factors proposed by ICRP103 (mSv)¹², E was estimated using the exposure parameters (kVp, mAs), positioning, focal-skin distance, SID, age and beam size (collimation).

Phase 3 – Image analysis

The images were analysed using two approaches: objective, using the contrast-to-noise ratio (CNR) and perceptual, using observers.

Observers

Five observers performed perceptual image analysis: four radiographers with experience in paediatric radiology and familiar with Cobb angle and a radiography student.

These observers had their visual acuity assessed prior

to participating ((ETDRS chart – CSV 1000 and LogMAR Good-Lite chart), contrast sensitivity (CSV-1000E) and stereopsis (Randot)). Those who normally wore corrective lenses were asked to wear them during the vision testing. Binocular visual acuity for distance was -0.18 ± 0.04 LogMAR (20/13). All subjects had good visual acuity - LogMAR of -0.1 (20/16). All subjects had a normal near visual acuity (0.38 ± 0.04 M – 20/20) and stereoacuity (40.00 ± 0.00). The log average values of contrast sensitivity were similar to the population norms [13]: 3cpd (1.81 ± 0.13), 6cpd (2.20 ± 0.08), 12cpd (1.96 ± 0.07) and 18cpd (1.54 ± 0.02) spatial frequencies.

Image analysis using objective measurements

Thirty images (out of 130) were selected for CNR calculations. The inclusion criteria were the lateral projections in order to measure the Cobb angle (phase 4)¹⁴. The phantom does not present a curvature and for that reason the PA/AP projections were not analysed in this phase. The images acquired at 66, 77 and 90 kVp were selected (minimum, medium and maximum values of the range)¹⁰.

To calculate CNR, two regions of interest (ROI) were

marked on the images using a bespoke software (imageJ). ROI1 was applied mid-way of the vertebral body (maximum density) and ROI2 in the lung region with a homogenous density (minimum density) (Figure 2) and applied to the following formula (equation 1):

$$CNR = \frac{\text{Mean ROI2} - \text{Mean ROI1}}{\text{Standard deviation 1}}$$

The image with the highest CNR was selected as the reference image to perform the fourth phase of the study, which was acquired using fine focus (FF) with the grid inserted to ensure the AEC selected the optimum parameters visualised at 180cm SID.

Perceptual image analysis

To perform perceptual image analysis the previously selected images (30 out of 130) were transferred to a SIEMENS Syngo.via system with a monitor (SCD 1897-M) as used in clinical practice. Four images were selected to repeat the analysis including the reference image.

The images were analysed to determine if five relevant anatomical structures (see Table 2)^{10,14} were identifiable with the selected exposure parameters on a software tool ViewDEX (Viewer for Digital Evaluation of X-ray images). This software has been developed in Java and allows visual grading analysis (VGA) and image criteria scoring (ICS). The results from each observer were saved in a log file to be analysed using Excel and SPSS. It is a software that is DICOM compatible and the interface is easy to use¹⁵⁻¹⁶.

Table 2: Anatomical criteria used for perceptual image quality analysis applying a nominal scale (yes/no)

Criteria	Appraiser combinations	
For the Cobb angle estimation, can you visualize the following?	Not adequate	Adequate
... superior vertebral endplate	Yes/No	Yes/No
... inferior vertebral endplate	Yes/No	Yes/No
... inter-vertebral spaces	Yes/No	Yes/No
... vertebral body	Yes/No	Yes/No
... posterior vertebral body line	Yes/No	Yes/No

Phase 4 – Cobb angle measurements

In this phase, seven digital images were selected (including lowest CNR, medium CNR, highest CNR and the reference) for drawing the Cobb angle stored on the AGFA IPD viewer system (ADC-QS). The lines to determine the Cobb angle were drawn along the superior and inferior vertebrae of the T3 and T12 respectively by each observer and ADC-QS automatically measured the angle (Figure 1d). Literature highlights the thoracic region as the most prominent for a spinal curvature in paediatrics¹⁷.

All images were anonymised to reduce bias. Before the task began, all observers were trained and the images used for the training were discarded from the study. A ten minute interval between this phase and the previous was allocated to minimise error¹⁸.

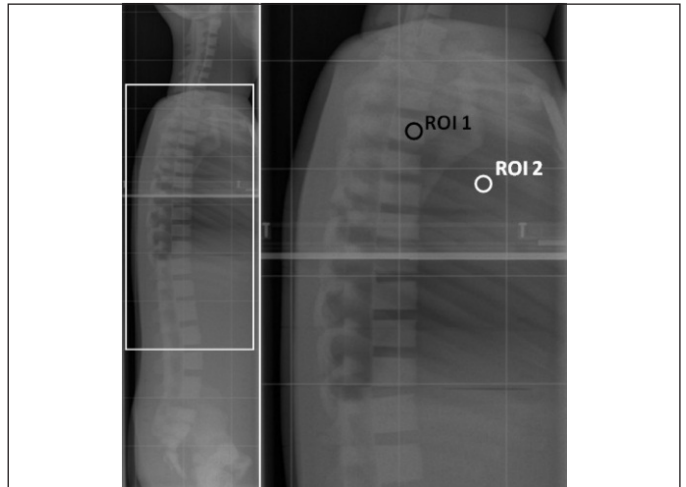


Figure 2: Lateral view showing Regions of Interest [ROI1(vertebrae body) and ROI2(lung)] to perform contrast-to-noise ratio (CNR) measurements.

All equipment is subject to regular quality control (QC). All equipment QC results fall with manufacturer specifications.

Statistical analysis

Data was analysed using Excel and SPSS to perform descriptive statistical analysis. Linear correlations (r^2) and Cohen's Kappa coefficients were also undertaken to observe the relationship between the variables and observers respectively. Five observers were used to determine the reliability for perceptual IQ. Kappa coefficients allow for the nominal scale used in the criteria to give statistical relevance to the study¹⁹. Three of the images were repeated three times to perform an inference sample and attain the standard deviation (StD) of the overall angle measurement. The StD was used to determine the level of accuracy for the angle measurements.

RESULTS

The results were sub-divided according to the dependent variables (E and IQ) and independent variables of position, kVp, the use of a grid and SID (see Table 1).

Effective dose

Under the conditions: 66 kVp, broad focus, no grid and 150cm SID, E was highest at images acquired in the AP position (0.048 mSv) when compared to PA (0.013 mSv). For lateral projection the E was lower than AP (0.025 mSv). When a grid was in use (AP - 0.097 mSv, PA - 0.041 mSv and lateral - 0.061 mSv), E was higher.

The use of a grid showed a moderate negative linear correlation at 150cm SID (-0.770) and a positive linear correlation at 200cm SID (0.7152). No correlation was identified for images acquired at 180cm SID (0.1141). In contrast, the image acquisition without a grid saw a stronger negative linear correlation at 180cm SID (-0.9265) whilst at 200cm SID (-0.7872), a moderate correlation was observed. The correlation weakens at 150cm SID (0.5127). E decreased at the higher kVp for 180cm and 200cm SID, however at 150cm SID, the data showed a moderate increase in E (Figure 3).

Image quality

The highest CNR was achieved at the lowest kVp of 66 consistently across all the categories (see Table 1). A strong negative linear correlation of -0.974 was reached for images acquired at 180cm and 150cm SID without a grid using 66, 77 and 90 kVp. Data also showed the highest SID of 200cm provided the highest CNR from the entire range of images acquired without a grid (Figure 4). Images acquired using a grid showed a similar trend with the highest CNR achieved at the lowest kVp at the SID of 200cm. No correlation was observed at 150cm SID (0.340) (Figure 5).

Concerning the perceptual IQ, thirty two images (out of 37) were classified as adequate because it is possible to visualise the anatomical criteria and five (out of 37) were classified as inadequate because one or more criteria not be identified by at least three observers.

The Kappa coefficient was used to calculate the reliability between each observer. The level of agreement for visualising the range of anatomical regions was good, however for anatomical regions not visualised, the level of agreement was very poor (-0.115 to 0.285) reducing the observer reliability using Kappa. Observer 1 compared to 2 demonstrated a moderate agreement (0.534).

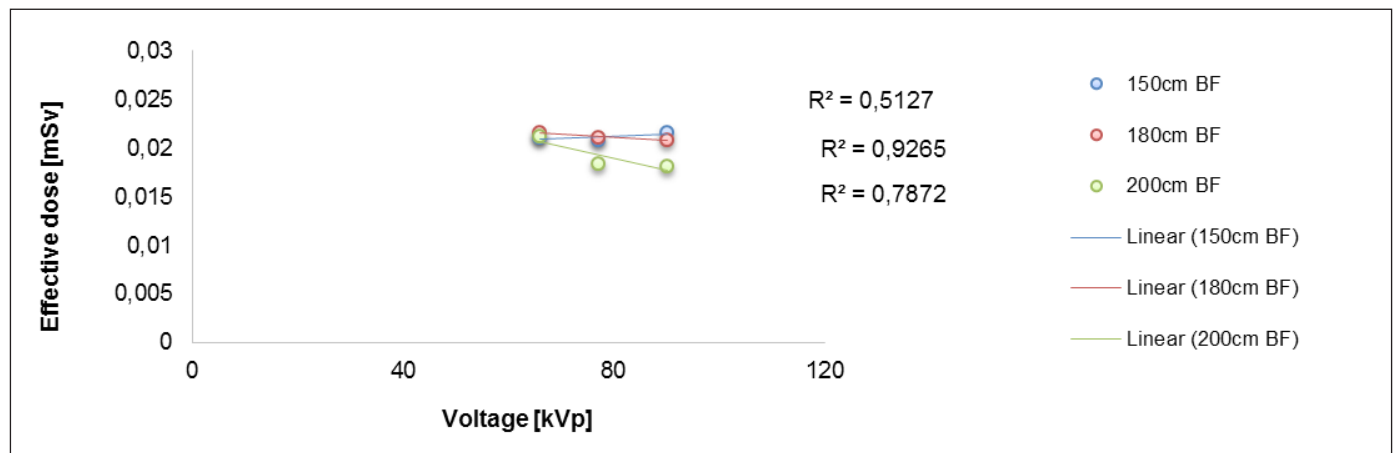


Figure 3: Comparison of effective dose for a range of kVp without grid for three sources to image distance (150, 180 and 200cm).

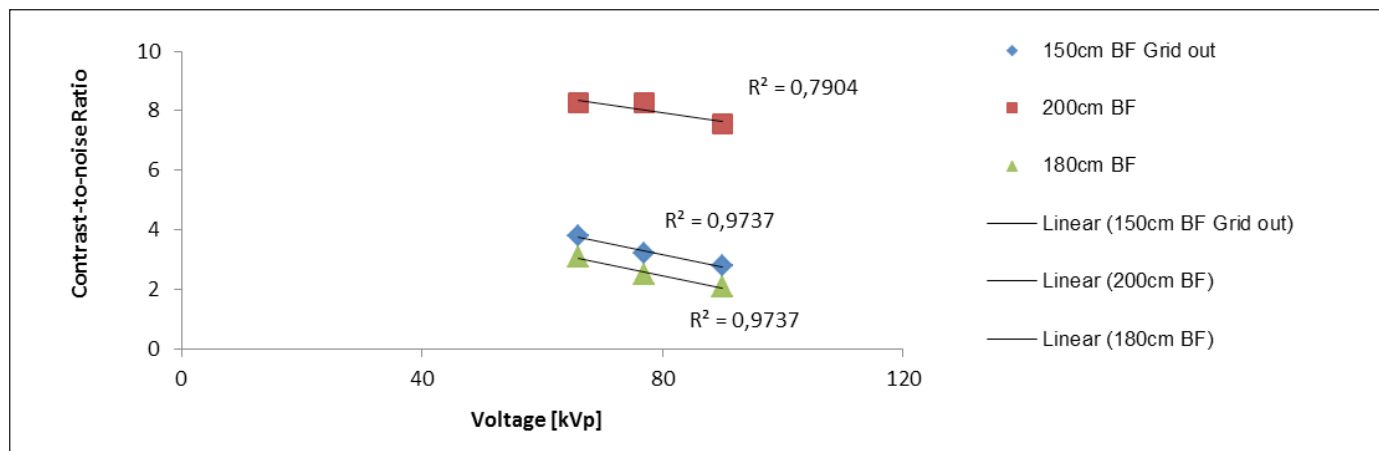


Figure 4: Comparison of contrast-to-noise ratio for images acquired using a range of kVp, broad focus (BF) and without grid for three sources to image distance (150, 180 and 200cm).

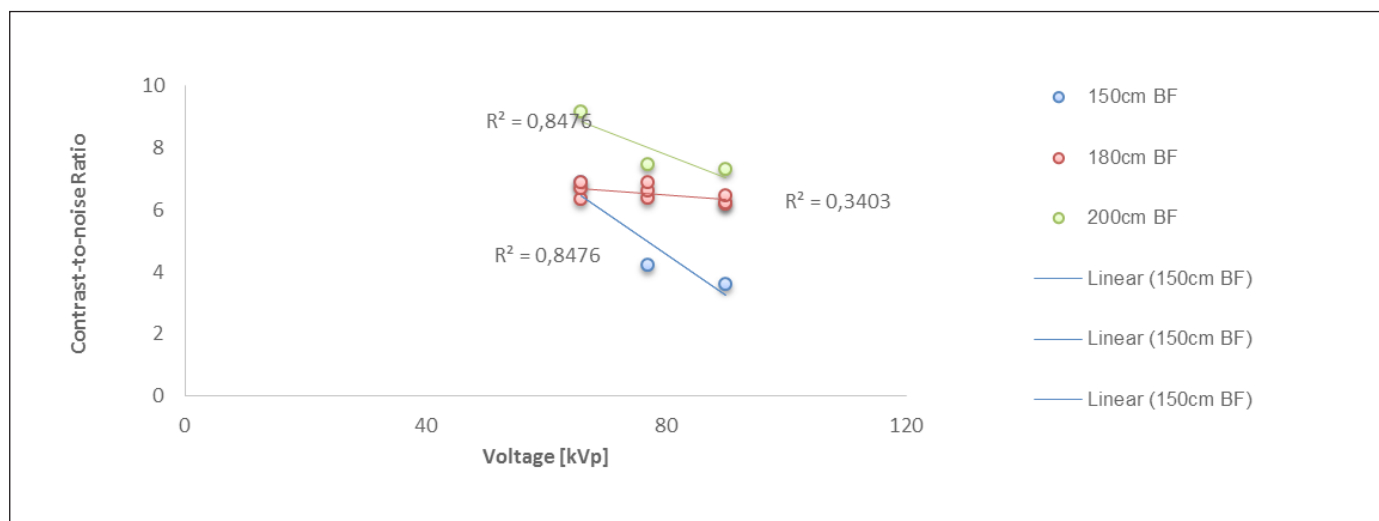


Figure 5: Comparison of contrast-to-noise ratio for images acquired using a range of kVp, broad focus (BF) and with grid for three sources to image distance (150, 180 and 200cm).

Table 3: Observers performance applying modified Cobb's method to measure the spine curvature on lateral projections, the respective Standard-Deviation and image quality data concerning contrast-to-noise ratio and perceptual image quality

Image	Mean Angle	Standard deviation	Contrast-to-noise ratio	Perceptual image quality
85 (Reference)	19.9	0.9	12.829	Accepted
91	16.4	2.3	9.139	Accepted
99	16.0	2.9	8.250	Not accepted
87	17.8	1.6	7.999	Accepted
12	19.0	2	3.611	Accepted
37	16.0	2.9	3.444	Accepted

Cobb angle measurement reliability

The statistical data for Cobb angle measurements are shown in (Table 3). The mean angle measurements showed

for the sampled images scored by the participants ranges from 16 to 19.9°. The mean StD varied between 0.9 to 2.9. The image with highest CNR (reference image) shows the lowest StD (0.9).

DISCUSSION

Many studies have examined the impact of exposure parameters on dose and IQ in spine radiography; however, there is a lack of studies on paediatrics combining several exposure parameters²⁰⁻²².

As noted within the results section, there are variations on E between different positioning, kVp range, grid and SID. The use of grid increased E as expected²³. This was most evident with the AP projection. AP projection had the highest E compared to PA and lateral and for that reason, sensitive organs are more exposed to radiation effects when this projection is used²⁴. Therefore, PA projection should be selected without grid for full spine examination on paediatrics to reduce E to optimise practice²⁰.

Literature suggests using larger SID as a strategy of reducing dose²⁵⁻²⁶. The results of this study are consistent with this as 200cm SID promoted lowest E. Concerning IQ, it was seen that the use of a larger SID increases CNR for the same kVp range because the AEC promotes uniformity of signal reaching the detector by increasing the mAs when kVp is reduced²³. For this reason a higher SID should always be selected for optimisation of the CR system used in this study.

The use of higher kVp is a well-known strategy to reduce dose on paediatrics, but at the same time can decrease CNR^{20,26}. On this study, it was shown that with higher kVp, the E is reduced for 180cm and 200cm SID, although this correlation was not as obvious for 150cm SID. This could be due to the small sample size used for this SID. The highest CNR was achieved at the lowest kVp of 66; this is consistent with Gardner¹⁸. This happens because with lower kVp there is less scatter radiation reaching the detector with increasing mAs due to AEC²³. Using a grid increases CNR as well as E²⁶. Despite this, the observers were able to detect all anatomical structures on an image with the lowest CNR obtained without a grid. This proves that dose can be reduced for this specific context. It also proves that physical (e.g., CNR) and perceptual measures of image quality do not always reflect how well the observer can perform in their diagnostic task.

Table 3 shows that the reference image has the lowest StD. This confirms a good agreement level between the observers. The highest StD was recorded at image with the lowest CNR (99) and medium CNR (37), suggesting disagreement between observers. The StD ranged from 0.9-2.9 and literature highlights that Cobb angle measurement with $\leq 2^\circ$, human error has no clinical impact^{6,27}. It was also noted that image 99 (which did not fulfil all five criteria), the observers

were still able to measure Cobb angle. This proves that Cobb angle can still be measured on images with low E considering this study.

The highest agreement obtained for perceptual IQ was performed by observers 1 and 2. Observer 1 has the longest experience in clinical practice (more than 15 years) and observer 2 have more than five years of paediatric experience with a good understanding of the AGFA system for the perceptual scoring. Observers 4 and 5 had the lowest agreement using the Kappa coefficient when compared against all observers. Observer 4 struggled to understand the task in the initial phase and took the longest time to adapt due to the lack of experience in using the AGFA system. After training, observer 4 assessed one specific region (the coccyx) for intervertebral disc space as opposed to the entire paediatric spine, skewing the data. However, a decision to include the observer's data was taken due to the vast experience in paediatric oncological radiography. Although the paediatric experience was an advantage, the clinical aim of the experiment was different for this observer. Despite the lack of agreement amongst all observers, there is no statistical and clinical method for determining a standard. Further work is recommended.

The agreement on visualising well defined structures is strongest across all observers. This could be related to the perceptual aspect of image quality where contrast impacts the visualisation of structures in imaging, consistent with literature²⁸⁻²⁹. The images varied in contrast detail, confirmed by the variation in the observers ability to not agree on images with less defined anatomical structures. Conversely, although all five observers had normal contrast sensitivity, the sensitivity for observers 1 and 2 was lowest for the "low spatial frequency" (images with low contrast). This suggests that regardless of image quality, the observers were able to accurately draw the Cobb angle within the acceptable clinical limits ($\leq 2^\circ$)^{6,27}, however, the range of experience in assessing paediatric images may be a limiting factor to the lack of agreement. The poor agreement of observer 5 can be explained by their use of tools as they were the only observer to use post processing tools through the use of the window level and the zoom function. These aspects of experience are identified as a limitation to the study and a proposal for more experienced observers and a robust protocol for perceptual IQ assessments are recommended.

Limitations are evident in this study. The sample size is limited on the basis of the high range of parameters (grid, spot size, tube voltage and current, SID and position) that resulted in an inclusion criteria with a reduced sample size.

CONCLUSION

The purpose of this study was to optimise exposure parameters for full spine paediatric radiography. The analysis showed that using higher SID, a dose reduction can be achieved and also an improvement on CNR. Using higher kVp promotes lower E but at the same time can decrease CNR. However, it was possible to verify that when IQ is considered inadequate by the observers the clinical goal can be achieved in this context as the Cobb angle measurements were performed with a lower error. This also confirms that perception of IQ is dependent on the characteristics (e.g. perception, experience and visual characteristics) of the

observer. The optimal exposure parameters for full spine lateral computed radiography applied on paediatrics considering this specific context are 200cm SID, 90 kVp, broad focus and grid out.

ACKNOWLEDGEMENTS

We would like to give acknowledgement to ERASMUS for sponsoring the research project, to the five observers that participated in this study and to Patricia Franco that help to collect the images for this project.

REFERENCES

1. Bruce Jr R, Fletcher N. Pediatric spinal deformities [Internet]. Emory Health Care; 2014 [updated 2015; cited 2014 Aug 12]. Available from: <http://www.emoryhealthcare.org/pediatric-orthopedics/conditions/spinal-deformity.html>
2. SingHealth. Orthopaedic problems in children: spine deformity (scoliosis, kyphosis) and back pain [Internet]. SingHealth Group; 2014 [cited 2014 Aug 12]. Available from: <http://www.singhealth.com.sg/PatientCare/ConditionsAndTreatments/Pages/Orthopaedic-Problems-in-Children-Back-Pain-and-Spine-Deformity-in-Children-and-Adolescents.aspx>
3. Malfair D, Flemming AK, Dvorak MF, Munk PL, Vertinsky AT, Heran MK, et al. Radiographic evaluation of scoliosis: review. *AJR Am J Roentgenol*. 2010;194(s Suppl):S8-22.
4. Rajiah P. Idiopathic scoliosis imaging [Internet]. Medscape; 2013 [cited 2014 Aug 12]. Available from: <http://emedicine.medscape.com/article/413157-overview>
5. Harrison DE, Cailliet R, Harrison DD, Janik TJ, Holland B. Reliability of centroid, Cobb, and Harrison posterior tangent methods: which to choose for analysis of thoracic kyphosis. *Spine (Phila Pa 1976)*. 2001;26(11):E227-34.
6. Tanure MC, Pinheiro AP, Oliveira AS. Reliability assessment of Cobb angle measurements using manual and digital methods. *Spine J*. 2010;10(9):769-74.
7. Chen YL, Chen WJ, Chiou WK. An alternative method for measuring scoliosis curvature. *Orthopedics*. 2007;30(10):828-31.
8. Hong JY, Suh SW, Modi HN, Lee JM, Park SY. Centroid method: an alternative method of determining coronal curvature in scoliosis. A comparative study versus Cobb method in the degenerative spine. *Spine J*. 2013;13(4):421-7.
9. Health and Safety Executive. ALARP “at a glance” [Internet]. HSE; 2014 [cited 2014 Aug 12]. Available from: <http://www.hse.gov.uk/risk/theory/alarplglance.htm>
10. Kohn M, Moores B, Schibilla H, Schneider K, Stender H, Stieve F, et al. European guidelines on quality criteria for diagnostic radiographic images in paediatrics. Luxembourg: Office for Official Publications of the European Communities; 1996.
11. American College of Radiology. ACR – SPR – SSR Practice parameters for the performance of radiography for scoliosis in children [Internet]. Iowa: ACR; 2014 [cited 2014 Aug 12]. Available from: <http://www.acr.org/~media/ACR/Documents/PGTS/guidelines/Scoliosis.pdf>
12. ICRP. The 2007 recommendations of the International Commission on Radiological Protection [Internet]. Ottawa: ICRP; 2007 [cited 2014 Aug 20]. Available from: <http://www.icrp.org/publication.asp?id=ICRP Publication 103>
13. Pomerance GN, Evans DW. Test-retest reliability of the CSV-1000 contrast test and its relationship to glaucoma therapy. *Invest Ophthalmol Vis Sci*. 1994;35(9):3357-61.
14. Al Qaroot B, Hogg P, Twiste M, Howard D. A systematic procedure to optimise dose and image quality for the measurement of inter-vertebral angles from lateral spinal projections using Cobb and superimposition methods. *J XRay Sci Technol*. 2014;22(5):613-25.

15. Håkansson M, Svensson S, Båth M, Månsson LG. ViewDEX: a java-based software for presentation and evaluation of medical images in observer performance studies. In Cleary KR, Miga MI, editors. Medical imaging 2007: visualization and image-guided procedures [Internet]. SPIE; 2007 [cited 2014 Aug 12]. p. 65091R. Available from: <http://proceedings.spiedigitallibrary.org/proceeding.aspx?articleid=1299200>
16. Börjesson S, Håkansson M, Båth M, Kheddache S, Svensson S, Tingberg A, et al. A software tool for increased efficiency in observer performance studies in radiology. *Radiat Prot Dosimetry*. 2005;114(1-3):45-52.
17. Cassidy CR, Calhoun JH. Kyphosis [Internet]. Medscape; 2013 [cited 2014 Aug 20]. Available from: <http://emedicine.medscape.com/article/1264959-overview>
18. Gardner A. Clinical assessment of scoliosis. *Orthop Trauma*. 2011;25(6):397-402.
19. Blackman NJ, Koval JJ. Interval estimation for Cohen's kappa as a measure of agreement. *Stat Med*. 2000;19(5):723-41.
20. Willis CE. Optimizing digital radiography of children. *Eur J Radiol*. 2009;72(2):266-73.
21. Schaetzing R. Management of pediatric radiation dose using Agfa computed radiography. *Pediatr Radiol*. 2004;34 Suppl 3:S207-14.
22. Hess R, Neitzel U. Optimizing image quality and dose for digital radiography of distal pediatric extremities using the contrast-to-noise ratio. *Rofo*. 2012;184(7):643-9.
23. Barnes GT. Contrast and scatter in X-ray imaging. *Radiographics*. 1991;11(2):307-23.
24. Young KJ. Should plain films of the lumbar spine be taken in the posterior-to-anterior or anterior-to-posterior position? A study using decision analysis. *J Manipulative Physiol Ther*. 2007;30(3):200-5.
25. Joyce M, McEntee M, Brennan PC, O'Leary D. Reducing dose for digital cranial radiography: the increased source to the image-receptor distance approach. *J Med Imaging Radiat Sci*. 2013;44(4):180-7.
26. Parry R, Glaze S, Benjamin A. The AAPM/RSNA physics tutorial for residents: typical patient radiation doses in diagnostic radiology. *Radiographics*. 1999;19(5):1289-302.
27. Tung CJ, Tsai HY, Shi MY, Huang TT, Yang CH, Chen IJ. A phantom study of image quality versus radiation dose for digital radiography. *Nucl Instrum Methods Phys Res A*. 2007;580(1):602-5.
28. Shah M. Electronic booking of hospital appointments Hippocrates of Cos and apoptosis For personal use. *The Lancet*. 2003;361(9365):1306.
29. Lança L, Franco L, Ahmed A, Harderwijk M, Marti C, Nasir S, et al. 10 kVp rule – An anthropomorphic pelvis phantom imaging study using a CR system: impact on image quality and effective dose using AEC and manual mode. *Radiography*. 2014;20(4):333-8.

FOREIGN BODIES IN ORBITS

Review article – X Radiation dose implications in screening patients with ferromagnetic IOFBs prior to MRI: a literary review

Sarah Jessop^a, Gabrielle Hart^a, Ana Rita Santiago^b, Abbas Samara^c, Benedicte Markali^d, Yann Cottier^e, Joana Guerreiro^b, Erik Normann Andersen^d, H. Momoniat^a, José Jorge^e, Andrew England^a

a) School of Health Sciences, University of Salford, Manchester, United Kingdom

b) Lisbon School of Health Technology (ESTeSL), Polytechnic Institute of Lisbon, Portugal

c) Department of Medical Imaging and Radiation Therapy, Hanze University of Applied Sciences, Groningen, The Netherlands

d) Department of Life Sciences and Health, Radiography, Oslo and Akerhus University College of Applied Science, Oslo, Norway

e) Haute École de Santé Vaud – Filière TRM, University of Applied Sciences and Arts of Western Switzerland, Lausanne, Switzerland



KEYWORDS

Optimisation
Effective dose
Image quality
Phantom
Computed radiography
Intra orbital foreign bodies

ABSTRACT

Patients scheduled for a magnetic resonance imaging (MRI) scan sometimes require screening for ferromagnetic Intra Orbital Foreign Bodies (IOFBs). To assess this, they are required to fill out a screening protocol questionnaire before their scan. If it is established that a patient is at high risk, radiographic imaging is necessary. This review examines literature to evaluate which imaging modality should be used to screen for IOFBs, considering that the eye is highly sensitive to ionising radiation and any dose should be minimised.

Method: Several websites and books were searched for information, these were as follows: PubMed, Science Direct, Web of Knowledge and Google Scholar. The terms searched related to IOFB, Ionising radiation, Magnetic Resonance Imaging Safety, Image Quality, Effective Dose, Orbits and X-ray. Thirty five articles were found, several were rejected due to age or irrelevance; twenty eight were eventually accepted.

Results: There are several imaging techniques that can be used. Some articles investigated the use of ultrasound for investigation of ferromagnetic IOFBs of the eye and others discussed using Computed Tomography (CT) and X-ray. Some gaps in the literature were identified, mainly that there are no articles which discuss the lowest effective dose while having adequate image quality for orbital imaging.

Conclusion: X-ray is the best method to identify IOFBs. The only problem is that there is no research which highlights exposure factors that maintain sufficient image quality for viewing IOFBs and keep the effective dose to the eye As Low As Reasonably Achievable (ALARA).

INTRODUCTION

Magnetic Resonance Imaging (MRI) is a method of sectional assessment that provides excellent differentiation of many tissues types in different areas of the body with the advantage of using non-ionizing radiation. It is essential for medical diagnosis and has evolved very quickly, providing valuable advances in clinical practice¹⁻².

The main principle of MRI is the interaction of atoms which have a magnetic moment within an applied magnetic field³. Magnetic susceptibility defines the extent to which a material becomes magnetized when placed in a magnetic field. Materials with positive magnetic susceptibility are called paramagnetic; those with negative magnetic susceptibility are called diamagnetic. Ferromagnetic materials, such as iron, cobalt and nickel, are superparamagnetic and so are highly likely to be affected by magnetism. The most

common Intra-Ocular Foreign Bodies (IOFB) are iron particles^{2,4}.

MRI is contraindicated if there are any ferromagnetic foreign bodies present, as the magnetic force emitted may result in movement of the metal, causing serious injuries¹. In relation to the orbits, movement of any metal fragments can cause very serious damage, and even blindness in extreme cases⁵. To prevent damage to the eye, strict pre-assessment protocols have been advocated prior to any MRI scanning, however this is not a legal requirement, only a recommendation¹.

Patients are asked to fill in a questionnaire that helps determine whether they have, or are at high risk of having, any ferromagnetic IOFBs⁶⁻⁸. If a high risk is determined, the patient may be referred for further imaging. There are several imaging options available to confirm the presence or absence of any IOFB including plain film orbital X-ray, CT and ultrasound⁶. The most commonly used method is X-ray of the orbits. However, the lens of the eye is particularly sensitive to ionising radiation. A late onset consequence of ocular radiation exposure is clouding of the lens, known as cataracts⁹. Therefore, it is crucial to ensure that any imaging is justified and radiation dose to the eye is kept ALARA¹⁰.

M E T H O D O L O G Y

Eight investigators searched several online databases and websites for literature. The searches took place on PubMed, Science Direct, Web of Knowledge and Google Scholar. The search terms used were as follows and were searched both alone and in combinations; Radiation Dose, Eye, Orbits, Ocular, X-Ray, Ultrasound, Sonography, MRI, MRI Safety, CT, Epidemiology, Cataracts, Foreign Body, Image Quality, IOFBs, Radiology and Metal. The language searched was English. The years searched ranged from 1986 to the present, due to lack of very recent publications. The inclusion criteria for the selection of the articles for the construction of this literature review were: 1) Comparison between multiple image-related methods for detection of IOFB; 2) Identifying several reports about MRI incidents regarding ocular IOFB. The exclusion criteria applied to articles that referred to use of film in radiography rather than CR, except an article from 1986 that reports the first case of ocular injury on an MRI site. These searches yielded 35 papers, several of which were rejected due to age, irrelevance to the review, and language. This left 28 papers and books that were relevant to the study and were subsequently used.

The importance of screening before MRI

Several published cases of injuries as a result of ferromagnetic IOFBs in MRI scanners exist. The first, in 1986, involved a sheet-metal worker with an occult IOFB. He experienced severe pain as a result of a vitreous hemorrhage. This resulted in subsequent unilateral blindness when he was removed from the 0.35T scanner¹⁰⁻¹². Williamson et al performed various MRI scans with a 0.08T scanner on bovine eyes containing ferromagnetic IOFBs. They concluded that the particles did not move, however they proposed that using a higher field strength may cause intraocular damage¹²⁻¹³. This was confirmed by Gunenc et al when they used a 1.0T scanner. The IOFBs inserted in bovine eyes were shown to move by 7 to 10mm^{12,14}.

Table 1: Range of questions in 78 UK sites⁶

Questions pertaining to IOFBs	Number of sites asking this question
Have you ever had metal in your eyes?	45
Do you have any metal in your eyes?	11
Have you ever had any embedded metal requiring treatment?	3
Have you had an injury to eye involving metal?	8
Have you ever had an intra-orbital foreign body (of any kind)?	4
Have you ever worked with metal?	28
Have you ever worked with metal at speed?	3
Have you ever worked in the iron or steel industry?	1
Have you ever worked in a shipyard?	2
Have you ever had an eye injury?	1
Have you ever attended an eye department?	1

Due to the 1986 report, several measures were recommended to screen patients for MRI examinations before they entered into the MRI controlled area. To decide whether screening is necessary, the patients are asked to complete a written questionnaire. An example of this form can be accessed through www.mrisafety.com⁷. Table 1 provides a list of examples of questions asked to patients at different imaging sites across the UK with regards to IOFB safety. This is provided courtesy of Bailey et al, which they took from a 1996 newsletter published by the British association of MR Radiography¹².

However, the safety questionnaire is not always able to accurately identify patients with IOFBs. According to Bowman et al, a 63 year-old male metal worker requiring a brain MRI denied any history of an IOFB. After MRI he complained of pain and developed hyphema¹². Bailey et al give several reasons why this could happen: “(a) Situations where the patient has no recollection of history of IOFB or occupational exposure to penetrating metallic fragments, (b) the patient forgets a previous history of a metallic penetrating orbital injury, (c) the condition of the patient might inhibit their abilities in answering the screening questionnaire, and/or (d) the patient could fail to disclose relevant information regarding an orbital injury”⁶.

The American College of Radiology (ACR) state that “all patients who have a history of orbital trauma by a potential ferromagnetic foreign body for which they sought medical attention are to have their orbits assessed by either plain X-ray orbit films (2 views) or by a radiologist’s review and assessment of contiguous cut prior CT or MR images, obtained since the suspected traumatic event, if available.”⁶. However, Shellock and Kanal have a different opinion to the ACR and believe only certain patients should be considered “high risk” and should be categorized by size and location of the fragment. Specifically they say that not every metal worker is to be considered a “high risk” patient; only the ones who have a history of eye injury should have radiographic screening prior to MRI. Although, they do consider it important that MR sites have a standardized policy and set guidelines for screening patients with suspected ferromagnetic IOFBs¹⁵.

In summary, it is important that patients who are at “high risk” of ferromagnetic IOFBs must have some form of radiographic screening of which a range of options are available⁶. However, it is essential to consider the radio-sensitivity of the eye and the effects ionizing radiation has on the lens.

The use and optimisation of X-ray

According to the Safety Committee of the Society for Magnetic Resonance Imaging “the use of plain radiography is considered to be an acceptable technique for identifying or excluding intraorbital metallic foreign bodies that represent a potential hazard to a patient about to undergo MRI”⁵.

Imaging protocols for orbital X-ray acquisition vary from hospital to hospital, however the images produced are fairly standardised and usually consist of Postero-anterior (PA) skull radiography¹⁶⁻¹⁷.

The great debate in radiography remains the question

of balance between image quality and radiation dose to the eye. Even different textbooks used worldwide differ in their opinions of the positioning technique, kV, mAs and Source to Image receptor Distance (SID) ranges. For example, Bontranger et al says that by using 75kVp, 18mAs and a SID of 100cm, with a PA axial 30° caudal angle and resting the forehead and nose on the Image Receptor (IR) (Caldwell’s method) the petrous ridge will be projected onto the inferior orbital floor, or even under it, allowing clear visualization of the orbits¹⁷. Ballinger et al. says that for the localization of IOFBs using radiography it should be performed using two perpendicular projections – lateral and PA axial with a 30° caudal angle. This author also says that some physicians prefer to use a modified Waters positioning (25°-37° caudal beam angulation and central ray directed to the nasion instead of the acanthion) instead of Caldwell’s method¹⁸. Richards et al defends that the Parallax motion method can determine if an IOFB is located within the eyeball by acquiring two lateral and two PA modified Waters exposures; one exposure is acquired with the patient looking to the extreme right, and the other one to the extreme left¹⁹. Clark’s textbook (12th edition) says that the parameters should be 70-85kVp, but does not specify mAs or SID. It goes on to say that the patient should rest the chin and nose on the IR and the orbito-meatal line should be positioned at a 35° to the central ray, which is perpendicular to the IR. Clark’s recommends this positioning to “exclude the presence of metallic foreign bodies in the eyes before MRI investigations”¹⁶.

The use of CT in ocular investigation for ferromagnetic IOFBs.

Pinto et al regard CT very highly in terms of IOFB detection, and believe that it is the most sensitive method in IOFB detection, as it can accurately detect and localise many different foreign bodies in the eye including metallic objects²⁰. Saeed et al argue that CT provides better fragment localisation than X-ray and if the IOFB is too small to be seen on X-ray it will be seen on CT²¹. Cullen et al disagree with Saeed et al. Cullen et al conducted research using eyes of rabbits which showed that 3mm x 0.72mm fragments demonstrated some movement but caused no damage. From this, they concluded the much higher level of radiation dose required during CT imaging is unnecessary if the previous X-ray assessment cannot detect the IOFB. If the IOFB is too small to be affected by the electromagnetic field it will not move and cause any damage to the eye; this is particularly true in scanners of 1.5T and below²¹⁻²². It must be considered that these studies were done in dead animals, so there is no blood flow or pressure in the eye, so this may have affected their results.

Although CT is widely regarded by many studies as a good detection tool for IOFBs, the ionising radiation dose to the eye is considered by others to be unreasonably high. This is especially true when considering that Otto et al say that if the particles are so small that they cannot be detected on X-ray, when the patient is submitted to an MRI scan the movement of the IOFBs will not be sufficient to penetrate far enough into the eye to cause any resultant damage²³.

The effect of radiation on the eye

Absorbed ionising radiation can cause biological changes, depending on the area of anatomy exposed. Biological changes vary from stochastic to deterministic. Stochastic effects are changes that are possible when the anatomy is exposed to any amount of ionizing radiation, whereas deterministic effects will occur for certain, once the area has been exposed to a specified amount of radiation. In considering the eye, radiation effects are deterministic. Cataract formation begins after a dose of around 2Gy, and will have become fully opaque after an accumulation of 5.5Gy⁹.

A cataract is a clouding of the lens and is associated with visual impairment. Anatomically, cataracts can be classified into three categories: nuclear sclerosis, cortical cataracts and posterior subcapsular cataracts²⁴. According to numerous studies, which have investigated the association between the formation of cataracts and genetics, hereditary factors play a role in age-related cataract formation in around 50-70% of cases²⁴⁻²⁵. Additionally, ionizing radiation is known to be cataractogenic²⁶⁻²⁷ and the International Commission on Radiological Protection (ICRP) (2012) recognises cataracts are a late stage deterministic effect of radiation exposure²⁸.

The ICRP recommend a reduction in planned exposure to the lens of the eye and so any ionising radiation exposures should be justified and kept ALARA, therefore ruling out use of CT²⁸.

Radiation free alternatives for IOFB identification

Radiation free alternative imaging techniques exist to identify IOFBs, and therefore should be investigated thoroughly. One study compared X-ray, CT and ultrasound of the eye, and their respective detection rates for IOFBs. X-ray was shown to be able to correctly identify size and shape of any metallic IOFBs, CT identified all IOFBs and provided information regarding the relationship to the globe wall. Sonography provided the same detail as CT but gave no ionising radiation dose²⁹. However, a different study has discredited ultrasound in IOFB detection due to its unacceptable negative predictive value (85.2%)³⁰ and due to false detection of IOFB the patient may be denied a scan that could, possibly provide important diagnosis information.

On the whole there is not enough evidence to credit ultrasound as a first line imaging modality, however, for the time being, it can only be used in conjunction with other imaging modalities when looking for IOFBs²⁹.

CONCLUSION

Ferromagnetic IOFBs can be very dangerous for a patient who is undergoing MRI. They need to be identified prior to the MRI scan and there are several imaging modalities that provide varying levels of information on the location, size and shape of the fragments. The lens of the eye is highly radio-sensitive and therefore this needs to be considered when requesting imaging. Ultrasound gives no ionising radiation dose but there is a lack of evidence to use it as a first line modality. CT provides detailed information and detection of the ferromagnetic fragments but the radiation dose is unnecessarily high when X-ray can provide sufficient information using a lower dose. However, there is still controversy regarding the optimal technique and exposure factors that are appropriate and effective for this method of imaging. Further investigations are required to identify the optimal exposure factors to use to provide a diagnostic image whilst keeping the radiation dose ALARA.

REFERENCES

1. Vote BJ, Simpson AJ. X-ray turns a blind eye to ferrous metal. *Clin Experiment Ophthalmol*. 2001;29(4):262-4.
2. Bushberg JT, Seibert JA, Leidholdt Jr EM, Boone JM. The essential physics of medical imaging. 2nd ed. Washington: Lippincott Williams & Wilkins; 2002.
3. Jezzard P, Matthews PM, Smith SM. Functional MRI: an introduction to methods. Oxford: Oxford University Press; 2002.
4. Zhang Y, Cheng J, Bai J, Ren C, Zhang Y, Gao X, et al. Tiny ferromagnetic intraocular foreign bodies detected by magnetic resonance imaging: a report of two cases. *J Magn Reson*

- Imaging. 2009;29(3):704-7.
5. Williamson MR, Espinosa MC, Boutin RD, Orrison WW Jr, Hart BL, Kelsey CA. Metallic foreign bodies in the orbits of patients undergoing MR imaging: prevalence and value of radiography and CT before MR. *AJR Am J Roentgenol*. 1994;162(4):981-3.
 6. Bailey W, Robinson L. Screening for intra-orbital metallic foreign bodies prior to MRI: review of the evidence. *Radiography*. 2007;13(1):72-80.
 7. Shellock FG, Spinazzi A. MRI safety update 2008: part 2, screening patients for MRI. *AJR Am J Roentgenol*. 2008;191(4):1140-9.
 8. Boutin RD, Briggs JE, Williamson MR. Injuries associated with MR imaging: survey of safety records and methods used to screen patients for metallic foreign bodies before imaging. *AJR Am J Roentgenol*. 1994;162(1):189-94.
 9. Chodick G, Bekiroglu N, Hauptmann M, Alexander BH, Freedman DM, Doody MM, et al. Risk of cataract after exposure to low doses of ionizing radiation: a 20-year prospective cohort study among US radiologic technologists. *Am J Epidemiol*. 2008;168(6):620-31.
 10. Kohn M, Moores B, Schibilla H, Schneider K, Stender H, Stieve F, et al. European guidelines on quality criteria for diagnostic radiographic images in paediatrics. Luxembourg: Office for Official Publications of the European Communities; 1996.
 11. Murphy KJ, Brunberg JA. Orbital plain films as a prerequisite for MR imaging: is a known history of injury a sufficient criterion? *AJR Am J Roentgenol*. 1996;167(4):1053-5.
 12. Williamson TH, Smith FW, Forrester JV. Magnetic resonance imaging of intraocular foreign bodies. *Br J Ophthalmol*. 1989;73(7):555-8.
 13. Gunenc U, Maden A, Kaynak S, Pirnar T. Magnetic resonance imaging and computed tomography in the detection and localization of intraocular foreign bodies. *Doc Ophthalmol*. 1992;81(4):369-78.
 14. Ta CN, Bowman RW. Hyphema caused by a metallic intraocular foreign body during magnetic resonance imaging. *Am J Ophthalmol*. 2000;129(4):533-4.
 15. Shellock FG, Kanal E. Re: Metallic foreign bodies in the orbits of patients undergoing MR imaging: prevalence and value of radiography and CT before MR. *Am J Roentgenol*. 1994;162(4):985-6.
 16. Whitley AS, Sloane C, Hoadley G, Moore AD. Clark's positioning in radiography. 12th ed. Koster J, editor. London: CRC Press; 2005.
 17. Bontranger KL. Crânio e ossos do crânio - Incidência PA axial: rotina para crânio. In Bontranger KL, editor. *Tratado de técnica radiológica e base anatômica*. 5a ed. Rio de Janeiro: Guanabara Koogan; 2003. p. 353-78.
 18. Ballinger PW. Skull. In Culverwell D, editor. *Merrill's atlas of radiographic positions and radiologic procedures*. 7th ed. St. Louis, MI: Mosby; 1991. p. 274-81.
 19. Richards G. Localization of foreign bodies in the eye: an additional safeguard. *Am J Roentgenol Rad Ther*. 1927;18:387-9.
 20. Pinto A, Brunese L, Daniele S, Faggian A, Guarnieri G, Muto M, et al. Role of computed tomography in the assessment of intraorbital foreign bodies. *Semin Ultrasound CT MR*. 2012;33(5):392-5.
 21. Saeed A, Cassidy L, Malone DE, Beatty S. Plain X-ray and computed tomography of the orbit in cases and suspected cases of intraocular foreign body. *Eye (Lond)*. 2008;22(11):1373-7.
 22. Cullen C, Kendall E, Cui J, Colleaux K, Grahn B. The effects of exposure to a 1.5-tesla magnetic field on intravitreal metallic foreign bodies in rabbits. *Graefes Arch Clin Exp Ophthalmol*. 2002;240(5):393-402.
 23. Otto PM, Otto RA, Virapongse C, Friedman SM, Emerson S, Li KC, et al. Screening test for detection of metallic foreign objects in the orbit before magnetic resonance imaging. *Invest Radiol*. 1992;27(4):308-11.
 24. Bollinger KE, Langston RH. What can patients expect from cataract surgery? *Cleve Clin J Med*. 2008;75(3):193-200.
 25. Hammond CJ, Snieder H, Spector TD, Gilbert CE. Genetic and environmental factors in age-related nuclear cataracts in monozygotic and dizygotic twins. *N Engl J Med*. 2000;342(24):1786-90.
 26. Blakely EA, Kleiman NJ, Neriishi K, Chodick G, Chylack LT, Cucinotta FA, et al. Radiation cataractogenesis: epidemiology and biology. *Radiat Res*. 2010;173(5):709-17.
 27. Shore RE, Neriishi K, Nakashima E. Epidemiological studies of cataract risk at low to moderate radiation doses: (not) seeing is believing. *Radiat Res*. 2010;174(6):889-94.
 28. ICRP. The 2007 recommendations of the International Com-

- mission on Radiological Protection [Internet]. Ottawa: ICRP; 2007 [cited 2014 Aug 20]. Available from: <http://www.icrp.org/publication.asp?id=ICRP%20Publication%20103>
29. Zhu Y, Zhang XF, Sheng YJ. Combining diagnosis of IOFB and complications with multiple image-related methods. *Zhonghua Yan Ke Za Zhi*. 2003;39(9):520-3.
30. Shiver SA, Lyon M, Blaivas M. Detection of metallic ocular foreign bodies with handheld sonography in a porcine model. *J Ultrasound Med*. 2005;24(10):1341-6.

Experimental article – A balance between image quality and effective dose in orbital X-ray screening for ferromagnetic IOFBs: a pilot study

Gabrielle Hart^a, Sarah Jessop^a, Ana Rita Santiago^b, Abbas Samara^c, Benedicte Markali^d, Yann Cottier^e, Joana Guerreiro^b, Erik Normann Andersen^d, H. Momoniat^{a*}, José Jorge^e, Andrew England^a

a) School of Health Sciences, University of Salford, Manchester, United Kingdom

b) Lisbon School of Health Technology (ESTeSL), Polytechnic Institute of Lisbon, Portugal

c) Department of Medical Imaging and Radiation Therapy, Hanze University of Applied Sciences, Groningen, The Netherlands

d) Department of Life Sciences and Health, Radiography, Oslo and Akerhus University College of Applied Science, Oslo, Norway

e) Haute École de Santé Vaud – Filière TRM, University of Applied Sciences and Arts of Western Switzerland, Lausanne, Switzerland



ABSTRACT

** Acknowledgments to College of Radiographers Industry Partnership Scheme (CoRIPS) for the grant awarded to H. Momoniat.*

Purpose: To investigate whether standard X-ray acquisition factors for orbital radiographs are suitable for the detection of ferromagnetic intra-ocular foreign bodies in patients undergoing MRI.

Method: 35 observers, at varied levels of education in radiography, attending a European Dose Optimisation EURASMUS Summer School were asked to score 24 images of varying acquisition factors against a clinical standard (reference image) using two alternative forced choice. The observers were provided with 12 questions and a 5 point Likert scale. Statistical tests were used to validate the scale, and scale reliability was also measured. The images which scored equal to, or better than, the reference image (36) were ranked alongside their corresponding effective dose (E), the image with the lowest dose equal to or better than the reference is considered the new optimum acquisition factors.

Results: Four images emerged as equal to, or better than, the reference in terms of image quality. The images were then ranked in order of E. Only one image that scored the same as the reference had a lower dose. The reference image had a mean E of 3.31 μ Sv, the image that scored the same had an E of 1.8 μ Sv. **Conclusion:** Against the current clinical standard exposure factors of 70kVp, 20mAs and the use of an anti-scatter grid, one image proved to have a lower E whilst maintaining the same level of image quality and lesion visibility. It is suggested that the new exposure factors should be 60kVp, 20mAs and still include the use of an anti-scatter grid.

INTRODUCTION

A case from the 1980's, highlighted by Kelly et al, saw an American man being blinded by an undetected metal fragment when undergoing a Magnetic Resonance Imaging (MRI) scan. Even though he provided a history of Intra Orbital Foreign Body (IOFB) to the radiographers and underwent a subsequent plain X-ray examination, the fragment was undetected upon first review of the image¹. After the MRI incident the IOFB was seen on the image, suggesting that the technique used was not optimised and the quality of the image was so low that human error meant severe harm to the patient, highlighting the importance of image optimization while maintaining As Low As Reasonably Achievable (ALARA)² principle.

Prior to MRI scan, a safety questionnaire is a good instrument to evaluate whether a patient is at "high risk" of having an IOFB and therefore an orbit X-ray candidate³. Although, there is a case which the patient denied having any IOFB and later he developed hyphema due to a ferromagnetic fragment in the eye⁴.

The lens of the eye is considered to be one of the most radiosensitive tissues of the human body and high or repeated direct exposure causes lens clouding or cataracts, a type of visual impairment⁵. For that reason it is of paramount importance to optimise dose when performing an orbit X-ray.

This study will investigate image quality and dose optimi-

sation in Computed Radiography (CR) in relation to orbital X-rays for MRI screening.

METHODS AND MATERIALS

Equipment and phantom setup

An adult anthropomorphic head phantom was positioned for a postero-anterior (PA) projection of the orbits in accordance with standard radiographic texts⁶⁻⁷ (Figure 1). Images were acquired using a Wollersdorf Acroma X-ray unit (high frequency generator with VARIAN 130 HS standard X-ray tube with a total filtration of 3mm Aluminium equivalent). The source-to-image receptor distance (SID) was set at 100cm and all images were acquired using the same 18 x 24cm CR image receptor (IR). The primary X-ray beam was collimated to include the lateral skull margins and the whole orbital region and was thus fixed at 21.5 x 8.5cm. An Agfa 35-X digitizer (Agfa-Gevaert Corp, Mortsels, Belgium)

was used to process the images using a skull look up table.

IOFB simulation

Five ferromagnetic IOFBs (<1.0mm) were fixed to the anterior aspect of the orbital region of the phantom on the right eye in a pre-determined distribution (Figure 2). The left eye was maintained free from IOFB and would be used to simulate a normal examination.

Image acquisition

A set of images, for the purpose of both image quality and dosemetric analyses, were generated using the phantom and the following acquisition parameters. For peak tube potential, images were acquired at 10kV increments from 60 to 90kVp. For mAs, 5.0, 20.0 and 40.0 were selected. For the first set of images the IR was placed in the vertical bucky which included a secondary radiation grid (ratio 10:1, 40 lines/cm). A second set of images was acquired without a radiation grid using the same kVp and mAs settings.

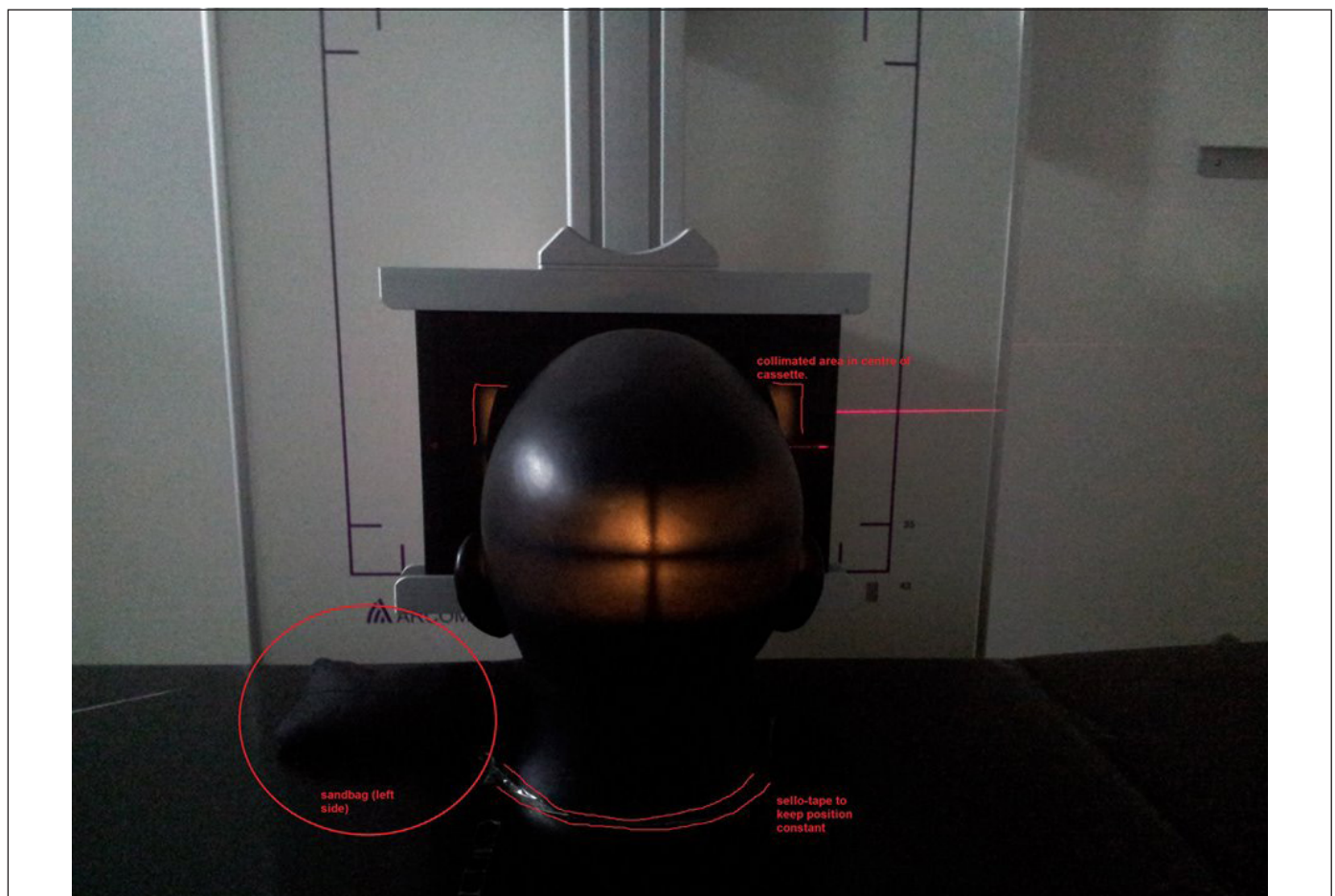


Figure 1: An illustration of the X-ray equipment and phantom setup used in this study. The annotations represent the collimation, the sandbag which steadied the phantom head (to the bottom left) and sellotape used to ensure no movement.

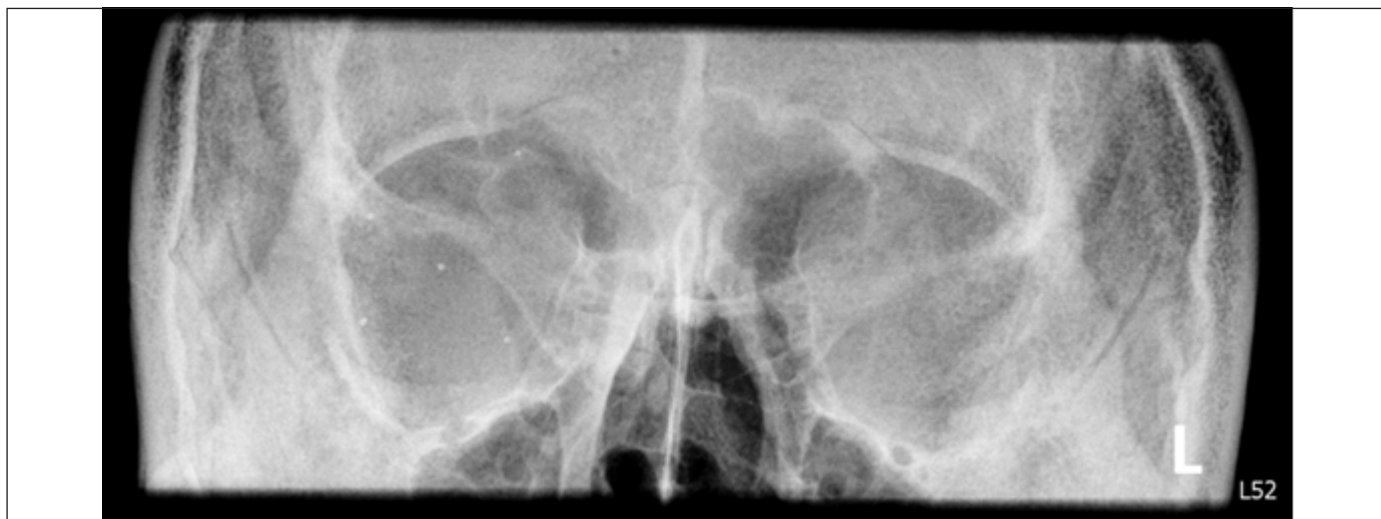


Figure 2: The image sample demonstrates a normal eye (left) and one eye (right) with 5 IOFBs.



Figure 3: A PA orbital radiograph demonstrated the location and size of the two ROIs used in the physical measurement of image quality.

A total of 24 different acquisition factor combinations were selected and acquired. For each of the settings, three X-ray exposures were obtained and the Dose-Area-Product (DAP) values were recorded. At each acquisition parameter combination a single image was sent to an archive and the Exposure Index (LgM) was recorded.

Image quality analysis

Physical measures

Acquired images were first evaluated using physical measures of image quality, to validate the image quality scale and gave an objective measure of image quality. Mean and standard deviation pixel value at two locations were calculated using the ImageJ software (National Institute of Health, Bethesda, MD) using a fixed sized region of interest

(ROI). Two ROIs (S1 and S2) were plotted (Figure 3) and from this signal-to-noise (SNR) and contrast-to-noise (CNR) values were calculated. SNR was defined as the mean pixel value divided by the standard deviation for each ROI, CNR was defined as the difference between the mean pixel values divided by the standard deviation between each ROI. These methodologies have been used in similar experiments⁸⁻⁹.

Perceptual (visual) tests

35 observers from the Netherlands, Switzerland, Portugal, Norway and UK volunteered for the image quality test (mean age = 26.1, range = 19 - 56). All observers had normal to corrected-to-normal vision, although, one participant who would usually wear glasses had forgotten them. The scale was produced through literature review and focus group discussion. Reliability and validation were tested. This approach has been

used in similar radiographic projects reported in the literature^{8,10}. Observers were radiographers (students or qualified practitioners) on a European Dose Optimisation EURASMUS Summer School. Images were initially analysed visually used two alternative forced choice comparisons (2AFC)⁸. 2AFC assesses the psychometric responses of observers who are presented with two separate images and has been used extensively within radiography to compare image quality^{8,11-14}. Limited resources meant 2AFC was as follows, two observers shared one screen and the set up was modified as follows; on the top of the screen, two reference images were fixed, on the bottom the remaining images were presented to each observer in a random order. Selection of a reference image was based on those parameters which reflect typical clinical averages, this was decided by discussions between the study researchers (70kVp, 20mAs and inclusion of an anti-scatter radiation grid). For each image, observers were required to indicate their level of agreement for each scale item against the reference image, where 1 was much worse, 2 worse, 3 the same, 4 better and 5 much better (Table 1). A score of 3 indicated a comparable image to the reference image for that specific criterion.

Table 1: Summary of the perceptual image quality scoring questionnaire (scale) used in the experiment

Contrast between air-filled structures and the surrounding tissues/structures	
Trabecular pattern of the visualised bones	
Sharpness of the orbital rim	
Visibility of the superior orbital fissure	
Quality of noise	
With respect to the visualised lesions:	Brightness
	Contrast
	Visibility
The scale consisted of a total of 12 items.	

Test procedure

Two participants at a time viewed the reference and comparison images on a split screen 30 inch Eizo MX300 (Eizo Corp, Hakusan, Ishikawa, Japan) liquid crystal display (LCD) monitor with a resolution of 2 megapixels, as stated above. Monitors were calibrated to DICOM greyscale standard display function (GSDF) and the ambient lighting conditions were kept constant and dimmed (i.e., 32 Lux) in accordance with the European Guidelines on Quality Criteria for Diagnostic Radiographic Images¹⁵. Noise levels and interruptions to image review were minimised using a sign on the door. Full instructions to observers were given at the start of the visual assessments and observers also were subject to a short

training session prior. Definitions for each image quality criterion were provided in writing together with an anatomy and IOFB location visual aid (Appendix A).

Scale validation

Testing of the scale included the use of both physical measures and scale questionnaires returned from the first 16 participants. Correlations between SNR and mean image quality scores (total per image) have been used previously⁸. Using all data collected in our study, there was almost no correlation between total image quality score and SNR (S_1 $R^2 = 0.022$, $p=0.910$, S_2 $R^2 = 0.031$, $p=0.886$; Figure 4).

For CNR there was a moderate positive correlation $R^2 = 0.302$, $p<0.005$ (Figure 4) against total score.

Validating a scale which includes both normal anatomy and simulated lesions is likely to require metrics other than SNR and CNR. Evidence presented above confirms that image quality scores do have some relationship with SNR and CNR. Time constraints only allowed for one test, re-test. The ICC was 0.508 (95% CI). Rosner (2011) suggested that values in the region of 0.40-0.75 indicate fair to good reproducibility.

Based on a review of SNR and mean image quality scores (IQS) from 35 participants there were still no significant correlations identified with respect to the full image quality scale (S_1 : $R^2 = 0.001$, $p = 0.884$, S_2 : $R^2 = 0.009$, $p = 0.655$).

There was statistically significant correlation between SNR and the average IQS for question 5 (S_1 : $R^2 = 0.595$, $p < 0.001$, S_2 : $R^2 = 0.588$, $p < 0.001$) (Figure 5).

Further validation analyses were undertaken on a per question basis. CNR did demonstrate a moderate positive correlation with mean IQS for question 1 ($R^2 = 0.446$, $p < 0.001$), question 7 ($R^2 = 0.449$, $p < 0.001$), question 8 $R^2 = 0.432$, $p < 0.001$), question 10 ($R^2 = 0.413$, $p = 0.001$), and question 12 ($R^2 = 0.401$, $p = 0.001$). CNR demonstrated a lower positive correlation with mean IQS for question 9 ($R^2 = 0.338$, $p = 0.003$), question 11 ($R^2 = 0.374$, $p = 0.002$) and for the total IQS ($R^2 = 0.380$, $p = 0.001$).

Evidence presented above and in the early stage (n=16) scale validation indicates that IQS do have some relationship with SNR and CNR.

In order to test the reliability of the image scoring system inter-observer variability ICC values were calculated for each image.

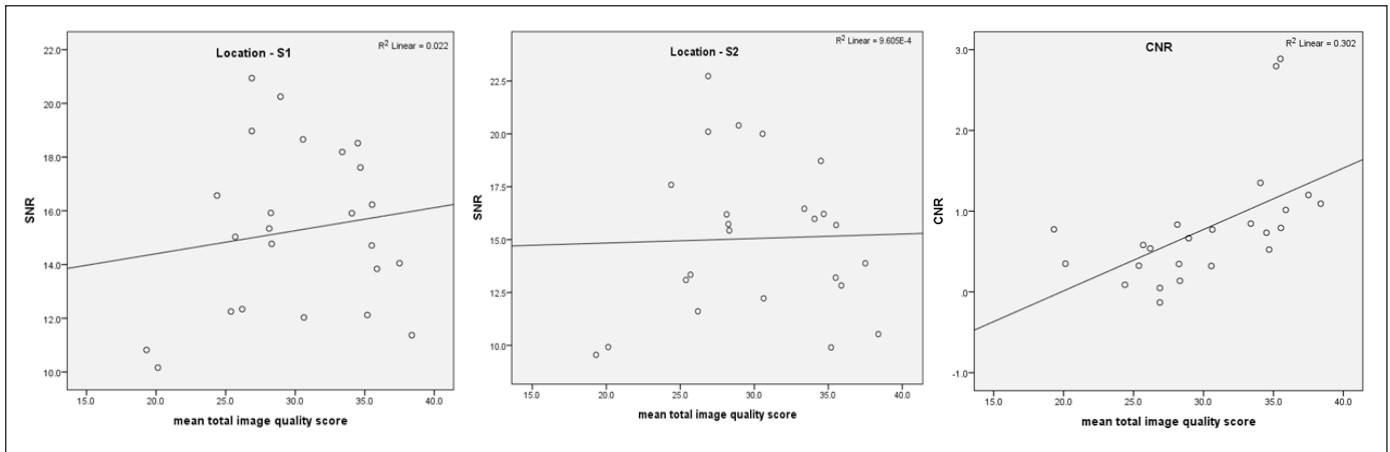


Figure 4: Scatter plots of SNR and CNR when compared to mean total image quality scores of question 5.

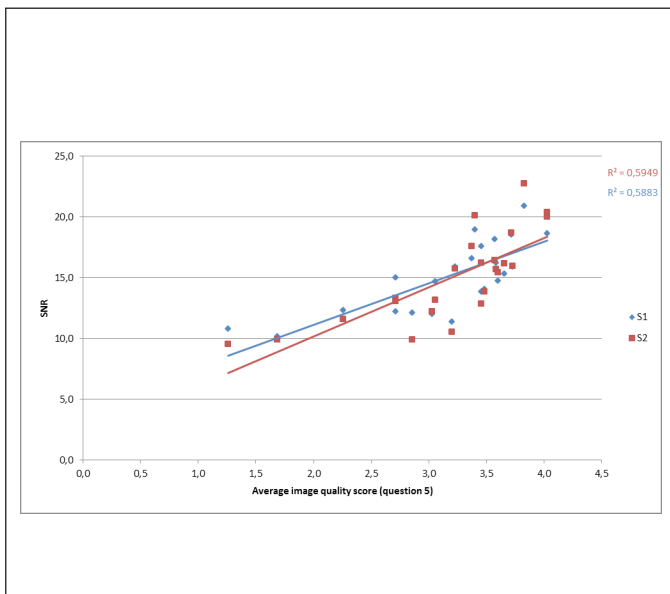


Figure 5: Scatter graphs of SNR compared to average total image quality scores of question 5.

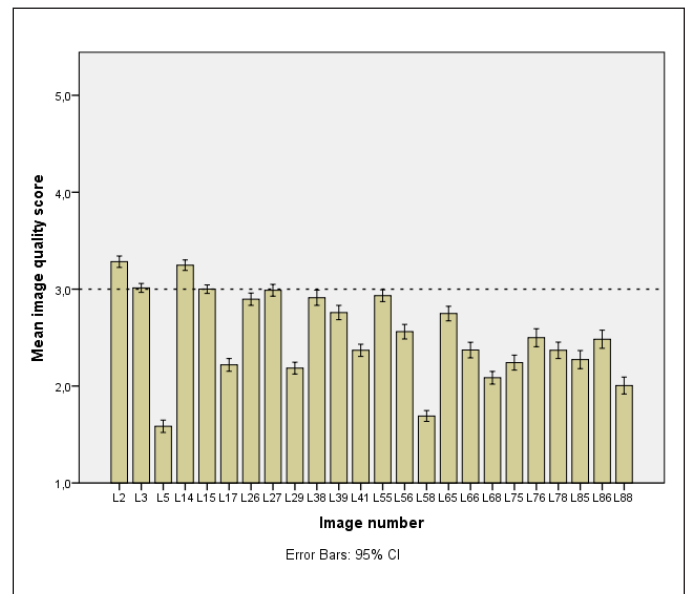


Figure 6: The histogram showing all mean image quality scores for all 24 images.

This used a 2-way mixed effect model for absolute agreement and the SPSS computer software (IBM Corp, 2011). The ICC (N = 35) is 0.456 (95% CI). When interpreting ICC, Rosner, suggested that values in the region of 0.40-0.75 indicate fair to good¹⁶.

Radiation dosimetry

DAP readings were recorded during acquisition. An average of three readings was taken for each image acquisition. Effective dose (E) were calculated from the DAP using Monte Carlo simulation software (PCXMC 2.0). The PCXMC, Monte Carlo base computer software uses computational hermaphrodite phantom defined by mathematical expressions to compute organ and E of patients of different ages and sizes in freely adjustable X-ray projections and

other examination conditions used in radiology¹⁷. PCXMC calculates Es using ICRP, 2007 publication 103 recommendations^{15,18}. The reliability of this software is supported by literature demonstrating results in close agreement with dose measurements and calculations of other phantom models

Statistical analysis

All IQS were transferred to SPSS (IBM Corp., 2011) and mean scores across 11 criteria were calculated, due to an understanding that many observers did not understand question 6. In terms of dose optimization images close to reference IQS (mean L15 = 3.0) were identified. Identified images (4 images) were compared with the reference image by non-parametric Wilcoxon matched-pair signed-rank test (corrected for multiple comparisons).

RESULTS

Perceptual image quality

Figure 6 shows the mean IQS for each of image with a range from 1.584 (St. Dev = 0.456) to 3.283 (St. Dev = 0.340). The mean values which scored above the reference image (represented by the dotted line) suggest better IQS. Several images scored just below the reference image.

Images for further analysis were identified by their mean IQS (compared with the reference image) and E (μSv). Wilcoxon matched-pair signed-rank test showed the mean IQS for images L3 ($P = 0.963$), L27 ($P = 0.945$) and L55 ($P = 0.803$) were not statistically significant from the reference image L15. However, image L2 ($P = .000$) was statistically significant compared to the reference image, L15, the Wilcoxon test is not able to differentiate which direction the mean difference is in. But the difference in the mean IQS for L2 and L15 (Table 2) suggests that observers rate L2 significantly higher than the reference image L15.

Table 2: Describes the descriptive values for each tested image and p

Image Name	kVp	mAs	E (μSv)	Mean IQ score	Std. Dev score	Wilcoxon signed rank (with ref image L15)
L3	60	20	1.821	3.01	0.31	$p > 0.05$
L15 (ref img)	70	20	3.308667	3	0.27	-
L55	60	40	3.531333	2.93	0.31	$p > 0.05$
L2	60	40	3.762667	3.28	0.34	$p < 0.05$
L27	80	20	5.025	2.99	0.33	$p > 0.05$

DISCUSSION

Study findings

The results from this pilot study suggest that using 60kVp 20mAs does not significantly affect the perceived image quality when compared with the clinical average which is 70kVp 20mAs. However the 60kVp 20mAs (1.821 μSv) reduce the E with 45% compared with the reference image (3.308 μSv). Some of the images in the Figure 6 scored slightly higher, lower, or close to the reference image but were excluded from further study based upon their E. One of the images (6.279 μSv) that was excluded had an 89% increase

in E compared with the reference image but scored higher. The perceived image quality of image L2 (60kVp 40mAs, 3.762 μSv) is significantly higher than the reference image but it provides a 13% dose increase when compared with the reference image (see Table 2).

Literature comparison

The results show that, as with kVp decrease, E decreases but IQS remain very similar. This is supported in the work of Allen et al, whose research states that a 10kVp decrease will see a decrease in E with no real compromise in image quality¹⁹. This is supported in the above results as the reference image has an E of 3.30 μSv , and where the mAs stays the same and the kVp decreases from 70 to 60, the E decreases to 1.82 μSv . The mean IQS for both images is very similar, with a small difference of 0.1 in favour of the lower kVp image.

Ma et al also agree that the image quality remains the same while decreasing E between 70kVp and 60kVp. They see similar results in their study where the dose for an acquisition at 70kVp is around 3 μSv , and when it is reduced to 60kVp, the dose is reduced to around 2 μSv ¹¹. This reflects the above results.

Implications on clinical practice

After more in depth research is conducted, presuming the results are similar to the above, implications on clinical practice may be that the new, lower acquisition factors are trialed in only a and the image quality tested by experienced and qualified film readers to see whether they can still see any IOFBs with the lower exposure. If the film readers still maintain a high rate of IOFB identification then the new exposure may become the standard.

Recommendations for improvement

Several factors may have influenced the study, subsequently limiting it. The first was related to the images for analysis. Problems occurred when the observers noticed differences in shuttering throughout the images, which occurred due to a post processing error. This meant that observers found it more difficult to compare the images fully, and the investigators found it harder to place the ROIs. Some observers complained that the LCD screens had a coloured tint and that changed their perception to some degree, although this was an uncommon report. Some observers reported a misunderstanding of question 6, these results were subsequently removed for all observers.

The pre-questionnaire observers were asked to fill out before performing image analysis highlighted the variety in the participants. This meant level of experience within the participants could be monitored. A range of people at different levels in their radiographic education (whether qualified or student) were asked to participate. Students at a lower level may have been less experienced in image evaluation, but this was controlled as much as possible by universal training. Only two participants highlighted this as a problem and subsequently withdrew from the study voluntarily. The experience level could have affected the ICC but we can't discount other variables.

The conditions in the room were controlled as much as possible; however other groups of researchers were using it. This meant that some noise (talking) and light (from the door opening and closing) were exposed to the participants while they graded the images. This may have been distracting but was minimised and was not reported as a problem.

Recommendations for further work

In further studies, the participants asked could be controlled, and invite only qualified radiographers alongside

reporting radiographers and radiologists to grade the images. This change may improve the external validity of the findings due to the increase in relevant experience.

Different projections could be acquired to try and minimise dose such as a caudal angle as suggested by Bontrager et al²⁰.

It may be interesting to repeat the investigation using a Direct Radiography (DR) system. The reduction in exposure from film to CR was drastic (75kVp and 40mAs with a distance of 90cm to 70kVp, 20mAs and a distance of 100cm) and so the E decreased largely, it is likely the dose would decrease with the progression of technology.

CONCLUSION

The results of the study indicate that there is an opportunity in CR radiography to decrease the acquisition factors, namely kVp, in orbital X-rays. The radiograph that demonstrated 60kVp, 20mAs and 100cm SID was rated similarly in image quality to the reference, or clinical average, and provides a dose of 1.8 μ Sv rather than the clinical average of 3.3 μ Sv.

REFERENCES

1. Kelly WM, Paglen PG, Pearson JA, San Diego AG, Solomon MA. Ferromagnetism of intraocular foreign body causes unilateral blindness after MR study. *AJNR Am J Neuroradiol*. 1986;7(2):243-5.
2. Kohn M, Moores B, Schibilla H, Schneider K, Stender H, Stieve F, et al. European guidelines on quality criteria for diagnostic radiographic images in paediatrics. Luxembourg: Office for Official Publications of the European Communities; 1996.
3. Bailey W, Robinson L. Screening for intra-orbital metallic foreign bodies prior to MRI: review of the evidence. *Radiography*. 2007;13(1):72-80.
4. Ta CN, Bowman RW. Hyphema caused by a metallic intraocular foreign body during magnetic resonance imaging. *Am J Ophthalmol*. 2000;129(4):533-4.
5. Chodick G, Bekiroglu N, Hauptmann M, Alexander BH, Freedman DM, Doody MM, et al. Risk of cataract after exposure to low doses of ionizing radiation: a 20-year prospective cohort study among US radiologic technologists. *Am J Epidemiol*. 2008;168(6):620-31.
6. Whitley AS, Sloane C, Hoadley G, Moore AD. Clark's positioning in radiography. 12th ed. London: CRC Press; 2005.
7. Ballinger PW, Frank ED. Merrill's atlas of radiographic positions & radiologic procedures. 10th ed. London: Mosby; 2002.
8. Mraity H, England A, Akhtar I, Aslam A, De Lange R, Momoniat H, et al. Development and validation of a psychometric scale for assessing PA chest image quality: a pilot study. *Radiography*. 2014;20(4):312-7.
9. Lin Y, Luo H, Dobbins JT, Page McAdams H, Wang X, Sehnert WJ, et al. An image-based technique to assess the perceptual quality of clinical chest radiographs. *Med Phys*. 2012;39(11):7019-31.
10. Mraity H, England A, Hogg P. Developing and validating a psychometric scale for image quality assessment. *Radiography*. 2014;20(4):306-11.
11. Ma WK, Hogg P, Tootell A, Manning D, Thomas N, Kane T, et al. Anthropomorphic chest phantom imaging: the potential for dose creep in computed radiography. *Radiography*.

- 2013;19(3):207-11.
12. Fechner GT. *Elemente der psychophysik*. 2nd ed. Leipzig: Breitkopf und Härtel; 1889.
 13. Lança L, Franco L, Ahmed A, Harderwijk M, Marti C, Nasir S, et al. 10 kVp rule – An anthropomorphic pelvis phantom imaging study using a CR system: impact on image quality and effective dose using AEC and manual mode. *Radiography*. 2014;20(4):333-8.
 14. Reis C, Gonçalves J, Klompmaaker C, Bárbara AR, Bloor C, Hegarty R, et al. Image quality and dose analysis for a PA chest X-ray: comparison between AEC mode acquisition and manual mode using the 10 kVp ‘rule’. *Radiography*. 2014;20(4):339-45.
 15. ICRP. The 2007 recommendations of the International Commission on Radiological Protection [Internet]. Ottawa: ICRP; 2007 [cited 2014 Aug 12]. Available from: <http://www.icrp.org/publication.asp?id=ICRP%20Publication%20103>
 16. Rosner B. *Fundamentals of biostatistics*. 7th ed. California: Cengage Learning; 2010.
 17. Tugwell J, Everton C, Kingma A, Oomkens DM, Pereira GA, Pimentinha DB, et al. Increasing source to image distance for AP pelvis imaging: impact on radiation dose and image quality. *Radiography*. 2014;20(4):351-5.
 18. Williams S, Hackney L, Hogg P, Szczepura K. Breast tissue bulge and lesion visibility during stereotactic biopsy: a phantom study. *Radiography*. 2014;20(3):271-6.
 19. Allen E, Hogg P, Ma WK, Szczepura K. Fact or fiction: an analysis of the 10 kVp ‘rule’ in computed radiography. *Radiography*. 2013;19(3):223-7.
 20. Bontrager KL, editor. *Tratado de técnica radiológica e base anatômica*. 5a ed. Rio de Janeiro: Guanabara Koogan; 2003.

Appendix A



Study: Determining exposure factors for the lowest effective dose while maintaining acceptable image quality when identifying IOFB's

Number of Image - _____

- 1) The Contrast between air-filled structures and the surrounding tissues / structures is...
1 - Much worse than 2- Worse than 3 - The same as 4 - Better than 5 - Much better than
- 2) The Trabecular patterns of the bones are visualized...
1 - Much worse than 2- Worse than 3 - The same as 4 - Better than 5 - Much better than
- 3) The sharpness of the orbital rim is
1 - Much worse than 2- Worse than 3 - The same as 4 - Better than 5 - Much better than
- 4) The visibility of the superior orbital fissure is
1 - Much worse than 2- Worse than 3 - The same as 4 - Better than 5 - Much better than
- 5) The amount of noise in this image is
1 - Much worse than 2- Worse than 3 - The same as 4 - Better than 5 - Much better than
- 6) The brightness of the visualized lesions are...
1 - Much worse than 2- Worse than 3 - The same as 4 - Better than 5 - Much better than
- 7) The contrast of the visualized lesions are...
1 - Much worse than 2- Worse than 3 - The same as 4 - Better than 5 - Much better than
- 8) The visibility of Lesion 1:
1 - Much worse than 2- Worse than 3 - The same as 4 - Better than 5 - Much better than
- 9) The visibility of Lesion 2:
1 - Much worse than 2- Worse than 3 - The same as 4 - Better than 5 - Much better than
- 10) The visibility of Lesion 3:
1 - Much worse than 2- Worse than 3 - The same as 4 - Better than 5 - Much better than
- 11) The visibility of Lesion 4:
1 - Much worse than 2- Worse than 3 - The same as 4 - Better than 5 - Much better than
- 12) The visibility of Lesion 5:
1 - Much worse than 2- Worse than 3 - The same as 4 - Better than 5 - Much better than

PRESSURE MAPPING

Review article – The effects of clinical support surfaces on pressure as a risk factor in the development of pressure ulcers, from a radiographical perspective: a narrative literature review

C. Everton^a, S. Bird^a, W. Brito^b, P. Colléc, A.P. Franco^d, S. Lutjeber^c,
K. Nodeland^e, S. Rième^b, M. Siddika^{f-g}, J. Webb^j, S. Angmorter^h

a) School of Health Sciences, University of Salford, Manchester, United Kingdom

b) Haute École de Santé Vaud – Filière TRM, University of Applied Sciences and Arts of Western Switzerland, Lausanne, Switzerland

c) Department of Medical Imaging and Radiation Therapy, Hanze University of Applied Sciences, Groningen, The Netherlands

d) Lisbon School of Health Technology (ESTeSL), Polytechnic Institute of Lisbon, Portugal

e) Department of Life Sciences and Health, Radiography, Oslo and Akershus University College of Applied Sciences, Oslo, Norway

f) Nuffield Foundation

g) The Bluecoat School, Oldham



KEYWORDS

Radiography
Radiology
Pressure ulcer Interface Pressure
Comfort
Supine

ABSTRACT

Purpose: Pressure ulcers are a high cost, high volume issue for health and medical care providers, having a detrimental effect on patients and relatives. Pressure ulcer prevention is widely covered in the literature, but little has been published regarding the risk to patients in the radiographical setting. This review of the current literature is to identify findings relevant to radiographical context.

Methods: Literature searching was performed using Science Direct and Medline databases. The search was limited to articles published in the last ten years to remain current and excluded studies containing participants less than 17 years of age. In total 14 studies were acquired; three were excluded as they were not relevant. The remaining 11 studies were compared and reviewed.

Discussion: Eight of the studies used 'healthy' participants and three used symptomatic participants. Nine studies explored interface pressure with a range of pressure mat technologies, two studies measured shear (MRI finite element modelling, and a non-invasive instrument), and one looked at blood flow and haemoglobin oxygenation. A range of surfaces were considered from trauma, nursing and surgical backgrounds for their ability to reduce pressure including standard mattresses, high specification mattresses, rigid and soft layer spine boards, various overlays (gel, air filled, foam).

Conclusion: The current literature is not appropriate for the radiographic patient and cannot be extrapolated to a radiologic context. Sufficient evidence is presented in this review to support the need for further work specific to radiography in order to minimise the development of PU in at risk patients.

INTRODUCTION

Pressure Ulcers (PUs) are an injury to the skin and deep tissue, mostly occurring over bony prominences, resulting from pressure, or the combination of pressure and shear¹. PUs are a high cost problem for health care providers across

Europe. The number of patients afflicted reaching over 18%² with one UK study as high as 20%³ costing the National Health Service £1.4–£2.1 billion annually (4% of total NHS expenditure)⁴. PUs also have a detrimental effect to the patients physical and psychological wellbeing. It is widely accepted that the action being taken to treat and prevent

PU is outweighed by the size of the problem⁵. Therefore it is imperative that all measures must be taken to identify avoidable instances, where the risk can be reduced or eliminated.

Unrelieved pressure leads to the formation of PUs, and immobility is a significant risk factor in this process⁶⁻⁸. The current literature is focused towards finding the minimum safe time and pressure parameters, before mobilisation is necessary to avoid formation of PU. Pressure ulcer prevention policies and guidelines have been published in Europe and the UK⁹⁻¹⁰. The main focus of these guidelines is repositioning to reduce the time of immobility and the amount of pressure on vulnerable areas. The evidence suggest that high pressures for a short time are just as damaging as low pressures over a long time. In a number of radiological procedures within Nuclear Medicine, Computed Tomography, Magnetic Resonance and Interventional Radiology, the patient is purposefully immobilised for periods of 20 minutes, sometimes in excess of 2 hours. On occasion patients are restrained to inhibit movement for the acquisition of useful images and minimise exposure to ionising radiation.

Table 1: Search terms for databases

Healthy Volunteers	OR	Healthy participant*	OR	Healthy adults	OR	Patient*		
AND								
Pressure Ulcer*	AND	Interface	OR	Average				
AND								
Supine								
AND								
(Cushioned	OR	Mattress)	AND	(Hard	OR	Flat	OR	Rigid)

Within the radiographic field, movement during an examination would cause the resultant images to be diagnostically unacceptable, leading to repeat examinations and increasing the dose to the patient. This review of the literature will identify current pressure ulcer research useful to the field of radiography and possibilities for further work.

M E T H O D S

Literature searching was performed using Science Direct and MEDLINE databases using the search terms as seen in Table 1, from January 2004 to August 2014. Paedi-

atric studies were excluded. Fourteen studies in total were acquired of which three were excluded as one was only available in Japanese, one was a duplicate across the databases and another looked at wheelchair users. This paper will review the remaining 11 studies.

Limit to ≤ 10 years old

Journal articles only

Exclude studies of participants < 18 years age

Seated - Wheelchair

Discussion

All studies were published in peer reviewed journals with a mean impact factor of 1.4059.

Participant demographics

Eight of the eleven studies were performed with 'healthy/able bodied participants'. The remaining three were samples of convenience including acute care, hernia repair and patients at risk of developing PUs. Although using healthy participants is a convenient and acceptable practice for this kind of study, it brings with it a number of limitations. The health of the 'patients' is a determining risk factor for the formation of PUs¹¹, studying 'healthy' participants will affect the external validity of the findings as they cannot be extrapolated to the population at risk.

The samples disclosed are representative of the general population, with ages ranging from 17 to 95. Five of the studies include BMI details of the participants, of these only one analyses the data for comparison as a variable. Of the 308 participants for the 11 studies 52% were female and 47% male, showing no overall gender bias. One study omitted gender information (5 participants).

Pressure measurement tools

Measuring Interface Pressure (IP), as force per unit, is not the recommended gold standard indication for ischemia in tissue. The process of PU development involves a complex interplay of several factors such as shear, blood flow, deep tissue pressure etc. However it is a convenient and widely accepted method. Pressure mats consist of capacitive sensors, placing pressure on these sensors results in potential difference. Nine of the studies used pressure mapping technology from various manufacturers. Rothenberger et al¹² explored skin perfusion dynamics due to external pressure,

for this they used Doppler flowmetry and tissue spectrophotometry. This study is the first to assess micro perfusion and although the justification for this is sound, it results in research that cannot be compared to the existing body of work on PU.

Shear is when two parallel forces act against one another to cause distortion in the body stretching and narrowing blood vessels. Fontaine et al propose a measurement combining pressure and shear, for this they have developed a shear sensor consisting of two parallel plates with an electronic device measuring relative movement between plates. Shear is also explored by Oomens et al¹³ with the use of finite element modelling. This method is complex and lengthy meaning the study only included 3 participants.

Comfort / Pain measurement tools

Of the 11 studies only two mention patient comfort, King et al¹⁴ noted that comfort is not usually taken into account and gave a brief narrative of participant comments but offers no further analysis. Keller et al¹⁵ used a 10-point visual analogue scale to collect participants' assessment of comfort. Visual analogue scales are considered to have good reliability and construct validity but do have some potential for error in interpretation¹⁶. This can be due to participant variation across a group. A published review of alternating pressure air mattresses for preventing PU by Vanderwee et al² found that only 4 of 35 studies reported comfort as a primary outcome. The review goes further, discussing the validity of the methods for collecting comfort data, concluding that more studies are needed to evaluate comfort and better measures need to be devised. A Cochrane review¹⁷ of support surfaces for pressure ulcer prevention excluded two studies in 112 for only measuring 'subjective' outcomes, and included 5 with comfort as a secondary outcome showing a large gap in the current research.

Visual erythema grading tools

Two studies performed visual inspections for erythema, as an indication of tissue damage¹⁸⁻¹⁹. Thorne et al offer no information about the tool used so no further comment can be made. A published grading tool used by Hemmes et al¹⁸ showed a significant number of patients with hyperaemia. No interpretation of the data is offered, so further work is needed to see how this relates to necrosis and ischemia.

RESULTS

The gold standard clinical outcome for PU studies is the measure of pressure ulcer incidence, due to cost, availabil-

ity of resources, and time, intermediate outcomes are often measured in the literature.

Nine studies used IP as the primary outcome. Three of them recorded mean average pressure²⁰⁻²². Miller et al²⁰ noted the capillary occluding measurement of 32mmHg. They compared the average number of red sensors with a reading over 90mmHg across the two surfaces. It was noted that the lab surface with 2-20 red sensors would be less effective at reducing pressure than the surgical table pad with 1-6 red sensors. No further justification is offered for considering the higher mmHg. Moysidis et al compare mean IP with contact surface area and pressure distribution as rate of low pressures (5-33mmHg) for three surfaces. The findings are not statistically significant, but do suggest that the higher specification surfaces produce less IP, and as the specification of the surface increases so does the contact area. Patel et al²² compared 5 existing high specification mattresses against a standard mattress using measures of mean IP, contact area and contact area of pressures above 32mmHg. From the findings the mattresses were 'ranked' according to the ability to reduce interface pressure.

Three studies assessed mean peak pressure of 'jeopardy' sites, the areas more likely to be at risk of developing PUs, including head, scapula, sacrum, and heels^{15,19,23}. Fontaine et al²³ also explored shear as a secondary outcome measure as the right-heel measuring force. Findings were compared for three surfaces in both supine and head of bed (HOB) elevation positions. Whilst the comparisons for supine position are relevant to the radiography setting the HOB elevation results cannot be considered. For the supine position no significant results were obtained for any of the 'jeopardy' areas measured. Three surfaces including two mattresses and a spinal board studied by Keller et al¹⁵ directly compared the mean IP for the 'jeopardy' areas and found the spinal board to have the highest pressure. This finding was also reflected in the mean comfort scores. Thorne et al¹⁹ explored the use of a gel overlay in an ancillary setting and found no significant reduction in mean peak pressure. None of these studies divulged the regions of interest for the mean peak IP.

Two studies also looked at 'jeopardy' areas but recorded the pressure of the single highest sensor (peak)^{14,24}. Chung et al explored the changes in pressure for a standard mattress at various HOB angles, and no comment is made about the peak pressure in the supine position. King and Bridges compared three surgical patient surfaces designed to reduce pressure, all surfaces reported a peak pressure measurement in the 'jeopardy' areas lower than 90mmHg. The use of the 90mmHg benchmark is attributed to previous work by Kosiak⁷. Only one study includes the head in this assessment as most studies

use a pillow to support the head¹⁴. The use of support aids in the radiological setting may not always be appropriate.

One study measured both peak pressure for scapula and heels, and mean peak pressure for the sacrum¹⁸. The single highest sensor readings were taken for the sites with prominent bone near the surface. For the sacrum which is a larger area of high pressure the sensor with the highest value and the 8 adjacent to it were averaged for the peak pressure index. Two spinal boards were compared with these measures and significantly lower readings were reported on the soft layered spinal board compared to the rigid spinal board.

Oomens et al¹³ measured shear, as maximum shear strains for the primary outcome of a comparison of rigid and soft layer spinal boards. A region of interest was selected around the sacrum and the maximum shear strains recorded. The findings on the rigid spinal board exceed the critical range for inducing deformation of tissue, those on the soft layered did not exceed the threshold for damage.

Rothenberger et al¹² measured blood flow and haemoglobin oxygenation as arbitrary units. They used the Oxygen to See (O2C) device to calculate the blood flow. Findings show that there was significant difference in the sacral area between the three mattress surfaces and the hard control surface. This is the only study to compare a hard surface to the support surfaces. Haemoglobin readings showed no significant change.

Overall, three studies found that IP decreases on soft layer spinal boards. Two studies found the results to be body morphology dependant suggesting the need for further work exploring BMI, waist to hip ratio, and body morphology. Both Thorne et al and King and Bridges^{14,19} found no significant differences between surfaces. All studies compare different surface options for the clinical setting giving recommendations on which is best to reduce pressure.

Surfaces

Support surfaces from trauma, surgical and nursing settings are explored in the literature. Spinal boards, both rigid and soft layer were compared by Hemmes et al, and Oomens et al. Keller et al^{13,15,18} also looked at a rigid spinal board in comparison to vacuum mattress, and semisoft overlay mattress. Standard hospital mattresses with a number of pressure reducing overlays; air, gel, fluid, foam, and visco-elastic were explored in four studies (Fontaine et al, King and Bridges, Miller et al, and Thorne et al)^{14,19-20,23}. A range of 'standard', higher specification, vacuum, and visco-elastic hospital mattresses were compared by Myodis et al, Patel et al, and

Rothberger et al. Chung et al^{12,21-22,24} compared HOB elevations on a standard hospital bed and mattress. None of the studies explored the use of ancillary support surfaces.

Time for acquisition

Four of the studies gave no indication of how long the participants were monitored during measurement acquisition. 'Settling in' time to allow for stable pressure measurements is documented in the wider literature as being between 4 and 6 minutes. Three studies allowed settling in time before acquisition, Miller et al²⁰ allowed 4 minutes, Moysidis et al and Rothenberger et al^{12,21} both allowed 6 minutes. Hemmes et al, and Keller et al^{15,18} only disclose the total time on the surface of 15 and 5 minutes respectively giving no information about when during this time the pressure data acquisition occurs. 5 frames in total were collected by Thorne et al at 5 minute intervals over 20 minutes starting at zero. Three frames at 50s, 100s, and 150s were collected by King and Bridges¹⁴ after a 150s settling in period.

Data analysis

Analysis of the data was performed using a range of programmes including SPSS, SAS, Microsoft Excel and Access.

Radiography

No studies include imaging surfaces for comparison. The literature as of 2010 showed only one study of PU development in the radiography field, showing the incidence of PU in patients undergoing radiology procedures was 53.8%²⁵. Sufficient evidence has been found to suggest that ancillary support surfaces can incur high interface pressures. Results from the studies included in this review cannot be accurately interpreted for radiological surfaces. Radiological surfaces are designed by manufacturers to be radiolucent and anything added to the table such as mattresses or overlays would increase dose to the patient. Also patients undergoing radiological examination are required to be immobile. None of these considerations have been taken into account in the current literature.

Validity

Whilst all the studies are valid for their intended clinical audience for example Trauma, Nursing, and Surgery, they cannot be interpreted for the radiographic context. The exclusion of all unnecessary materials, positioning aids, mattresses and the use of immobilisation devices all contribute to a controlled environment. These specific constraints are not yet represented in the literature.

CONCLUSION

This review offers an overview of the current literature that could also be relevant to imaging surfaces in a radiological context. The literature is offered from two main backgrounds, nursing and surgery. Whilst the recommendations from the studies reviewed are applicable to the fields they are designed from they cannot be extrapolated for radiographic context. The need for further work, specific

to radiography, is essential to minimise the development of PU in at risk patients.

ACKNOWLEDGEMENTS

The authors would like to thank, Erasmus for funding and The Nuffield Foundation.

REFERENCES

- Black J, Baharestani M, Cuddigan J, Dorner B, Edsberg L, Langemo D, et al. National pressure ulcer advisory panel's updated pressure ulcer staging system. *Dermatology Nurs.* 2007;19(4):343-9.
- Vanderwee K, Clark M, Dealey C, Gunningberg L, Defloor T. Pressure ulcer prevalence in Europe; a pilot study. *J Eval Clin Pract.* 2007;13(2):227-35.
- Clark M, Bours G, Defloor T. The prevalence of pressure ulcers in Europe. In Clark M, editor. *Pressure ulcers: recent advances in tissue viability.* Salisbury: Quay Books; 2004.
- Bennett G, Dealey C, Posnett J. The cost of pressure ulcers in the UK. *Age Ageing.* 2004;33(3):230-5.
- Butler F. Essence of care and the pressure ulcer benchmark: an evaluation. *J Tissue Viability.* 2008;17(2):44-59.
- Woodward M. Risk factors for pressure ulcers: can they withstand the pressure? *Prim Intent.* 1999;7(2):52-61.
- Kosiak M. Etiology and pathology of ischemic ulcers. *Arch Phys Med Rehabil.* 1959;40(2):62-9.
- Barbenel JC. Pressure management. *Prosthet Orthot Int.* 1991;15(3):225-31.
- National Institute for Health and Care Excellence. Pressure ulcers: prevention and management of pressure ulcers [Internet]. NICE; 2014. Available from: <http://www.nice.org.uk/guidance/CG179>
- Haesler E, editor. National Pressure Ulcer Advisory Panel, European Pressure Ulcer Advisory Panel and Pan Pacific Pressure Injury Alliance. *Prevention and treatment of pressure ulcers: quick reference guide.* Perth: Cambridge Media; 2009.
- Defloor T. The risk of pressure sores: a conceptual scheme. *J Clin Nurs.* 1999;8(2):206-16.
- Rothenberger J, Krauss S, Held M, Bender D, Schaller HE, Rahmanian-Schwarz A, et al. A quantitative analysis of micro-circulation in sore-prone pressure areas on conventional and pressure relief hospital mattresses using laser Doppler flowmetry and tissue spectrophotometry. *J Tissue Viability.* 2014;23(4):129-36.
- Oomens CW, Zenhorst W, Broek M, Hemmes B, Poeze M, Brink PR, et al. A numerical study to analyse the risk for pressure ulcer development on a spine board. *Clin Biomech (Bristol, Avon).* 2013;28(7):736-42.
- King C, Bridges E. Comparison of pressure relief properties of operating room surfaces. *Perioper Nurs Clin.* 2006;1(3):261-5.
- Keller BP, Lubbert PHW, Keller E, Leenen LP. Tissue-interface pressures on three different support-surfaces for trauma patients. *Injury.* 2005;36(8):946-8.
- Bijur PE, Silver W, Gallagher EJ. Reliability of the visual analog scale for measurement of acute pain. *Acad Emerg Med.* 2001;8(12):1153-7.
- McInnes E, Jammali-Blasi A, Bell-Syer SE, Dumville JC, Cullum N. Support surfaces for pressure ulcer prevention. *Cochrane Database Syst Rev.* 2011;(4):CD001735.
- Hemmes B, Brink PR, Poeze M. Effects of unconsciousness during spinal immobilization on tissue-interface pressures: a randomized controlled trial comparing a standard rigid spine-board with a newly developed soft-layered long spineboard. *Injury.* 2014;45(11):1741-6.
- Thorne S, Sauv   K, Yacoub C, Guitard P. Evaluating the pressure-reducing capabilities of the gel pad in supine. *Am J Occup*

- Ther. 2009;63(6):744-50.
20. Miller S, Parker M, Blasiolo N, Beinlich N, Fulton J. A prospective, in vivo evaluation of two pressure-redistribution surfaces in healthy volunteers using pressure mapping as a quality control instrument. *Ostomy Wound Manage.* 2013;59(2):44-8.
 21. Moysidis T, Niebel W, Bartsch K, Maier I, Lehmann N, Nonnemacher M, et al. Prevention of pressure ulcer: interaction of body characteristics and different mattresses. *Int Wound J.* 2011;8(6):578-84.
 22. Patel UH, Jones JT, Babbs CF, Bourland JD, Graber GP. The evaluation of five specialized support surfaces by use of a pressure-sensitive mat. *Decubitus.* 1993;6(3):28-37.
 23. Fontaine R, Risley S, Castellino R. A quantitative analysis of pressure and shear in the effectiveness of support surfaces. *J Wound Ostomy Continence Nurs.* 1998;25(5):233-9.
 24. Chung CH, Lau MC, Leung TY, Yui KY, Chan SH. Effect of head elevation on sacral and ischial tuberosities pressure in infirmity patients. *Asian J Gerontol Geriatr.* 2012;7(2):101-6.
 25. Messer M. Pressure ulcer risk in ancillary services patients. *J Wound Ostomy Continence Nurs.* 2010;37(2):153-8.

Experimental article – An experimental study to compare the interface pressure and experience of healthy participants when lying still for 20 minutes in a supine position on two different imaging surfaces

C. Everton^a, S. Bird^a, W. Brito^b, P. Collé^c, A. P. Franco^d, S. Lutjeber^e,
K. Nodeland^e, S. Rième^b, M. Siddika^{f-g}, J. Webb^a, S. Angmörter^h

a) School of Health Sciences, University of Salford, Manchester, United Kingdom

b) Haute École de Santé Vaud - Filière TRM, University of Applied Sciences and Arts of Western Switzerland, Lausanne, Switzerland

c) Department of Medical Imaging and Radiation Therapy, Hanze University of Applied Sciences, Groningen, The Netherlands

d) Lisbon School of Health Technology (ESTeSL), Polytechnic Institute of Lisbon, Portugal

e) Department of Life Sciences and Health, Radiography, Oslo and Akershus University College of Applied Sciences, Oslo, Norway

f) Nuffield Foundation

g) The Bluecoat School, Oldham



ABSTRACT

Introduction: Pressure ulcers are a high cost, high volume issue for health and medical care providers, affecting patients' recovery and psychological wellbeing. The current research of support surfaces on pressure as a risk factor in the development of pressure ulcers is not relevant to the specialised, controlled environment of the radiological setting.

Method: 38 healthy participants aged 19-51 were placed supine on two different imaging surfaces. The XSENSOR pressure mapping system was used to measure the interface pressure. Data was acquired over a time of 20 minutes preceded by 6 minutes settling time to reduce measurement error. Qualitative information regarding participants' opinion on pain and comfort was recorded using a questionnaire. Data analysis was performed using SPSS 22.

Results: Data was collected from 30 participants aged 19 to 51 (mean 25.77, SD 7.72), BMI from 18.7 to 33.6 (mean 24.12, SD 3.29), for two surfaces, following eight participant exclusions due to technical faults. Total average pressure, average pressure for jeopardy areas (head, sacrum & heels) and peak pressure for jeopardy areas were calculated as interface pressure in mmHg. Qualitative data showed that a significant difference in experiences of comfort and pain was found in the jeopardy areas ($P < 0.05$) between the two surfaces.

Conclusion: A significant difference is seen in average pressure between the two surfaces. Pain and comfort data also show a significant difference between the surfaces, both findings support the proposal for further investigation into the effects of radiological surfaces as a risk factor for the formation of pressure ulcers.

INTRODUCTION

Many medical imaging procedures, especially interventional procedures, can take up to 20 minutes or more¹. During imaging, patients are required to lie completely still as movement during acquisition could make the resultant procedure diagnostically unacceptable. Whitley et al² argued that movement during X-ray procedures is a major contributor to loss of diagnostic value, leading to repeat examinations. Repeating an X-ray examination carries further risk, not just

in terms of the patient experience but also because of the risk of the additional dose of radiation².

Studies have shown that sustained interface pressure for more than 20 minutes can cause tissue breakdown². Lack of movement, as in the radiographical context, will increase the length of time the interface pressure between the patient and the imaging surface is maintained. Interface pressure is defined as the pressure exhibited between the body and a contact surface³. This could heighten the probability of

developing Pressure Ulcers (PU)².

A search of the available literature reveals that there are currently no studies which investigate the relationship between radiological surfaces and interface pressure, and how these could affect the formation of PUs in at risk patients. Using healthy participants, this experimental study will therefore:

- Identify and compare the interface pressure of healthy participants on two imaging surfaces;
- Identify and compare the average and peak interface pressures of three areas of interest (head, sacrum and heels) of healthy participants on the two imaging surfaces;
- Compare the level of comfort of healthy participants on the two imaging surfaces;
- Explore the level of pain experienced by healthy participants on the two imaging surfaces.

Hypothesis

- The average interface pressure will be higher on the imaging surface without the mattress;
- The areas of interest (head, sacrum, heels) will have a higher interface pressure on the imaging surface without the mattress;
- The overall comfort will be higher on the mattress surface;
- The participants will experience higher pain when the interface pressure is higher in the three areas of interest.

M E T H O D O L O G Y

Ethical approval

This study was approved by the ethics committee of the College of Health and Social Care of the University of Salford, Manchester, UK.

Study design and setting

This study used pressure mapping equipment and software to measure interface pressures of 38 healthy participants whilst lying still on two medical imaging surfaces.

The experiment was conducted in the medical imaging laboratory of the Escola Superior de Tecnologia da Saúde de Lisboa (ESTeSL) in Portugal during the Erasmus OPTIMAX 2014 Summer School.

Sample

A convenience sample of 38 healthy participants aged 19-51 was taken from a population of 65. These participants were from different countries in the European Union, with different academic backgrounds, attending the OPTIMAX summer school.

Inclusion criteria

- Healthy adults, 18 years or older were recruited to the study and therefore the findings of the study can be generalised to an adult population. Gelis et al⁵ stated that adult populations constitute the majority of all PU cases and recommended that studies into measuring interface pressures should be targeted at this population group, so that the findings will be beneficial for clinical practice.

Exclusion criteria

- Participants with a height of 177cm or more were excluded from the study, due to the limitations of the pressure mat dimensions.
- Participants with any health condition, such as back pain, that prevents them from lying still for 20 minutes were excluded from the study. This was to ensure that participants can lie still during the acquisition of the interface pressure as excessive movement would render the data unusable in the study⁴.
- Participants who could not participate on the grounds of religious beliefs.

Surfaces

Two imaging surfaces available at the Escola Superior de Tecnologia da Saúde de Lisboa were used for the study.

- Norland XR-36 bone density scanner with a mattress;
- Siemens MULTIX Pro X-ray table without a mattress.

The Siemens X-ray table is typical of many systems available in radiographical departments throughout Europe. The Norland density scanner is not in regular use, but the mattress was designed for radiographic practice, as such the

findings of this study should be representative of available equipment.

Measurement tools

Pressure Mat – This study used the XSENSOR PX100:48.144.02 pressure mat from Sumed International. Various clinical studies⁵ and academic studies⁶ used the XSENSOR to perform pressure mapping on humans. Fader et al⁷ stated that XSENSOR appears to be the gold standard technology for pressure mapping. Manufacturer calibration and quality control data, prior to sales, confirm a high level of precision and reliability⁸.

The pressure mat is flexible, has a 61cm x 183cm sensing area, 12.7mm resolution, 6,912 sensing points, and 5-50mmHg and 10-200mmHg pressure ranges⁸, and an accuracy rate of ± 10 percent of the calibrated values⁵. The XSENSOR has been calibrated to manufactures specification. The pressure mat transmits individual pressure measurement from each sensor to a computer for analysis⁵.

The pressure mat was linked to XSENSOR X3 Medical v5.0 software, which according to Trewartha and Stiller⁶ has excellent calibration stability leading to consistent data collection with high reliability, high accuracy and low creep, defined as the increase in pressure with constant force.

Questionnaire – A 5-point Likert scale questionnaire was used to assess participants' level of comfort and pain. The Likert scale is the most widely used format for designing a questionnaire⁹. The questionnaire was checked for validity and unethical questions. Preston and Colman¹⁰ suggested that scales ranging from 5-101 response categories show little difference in validity and reliability. Open-ended questions were asked in order to explore the experience of the participants, providing responses in their own terms⁷. This qualitative questionnaire was filled out after each pressure measurement to provide subjective information in a standardised design¹¹. Brace¹¹ discussed that by using a questionnaire one can assure all participants are asked the appropriate questions and that they are always asked in the same way, thus standardising the acquisition. Furthermore time constraints made it impractical to conduct verbal interviews with the participants; therefore a questionnaire was desirable.

Pilot

A pilot study was performed with a participant representative of the target population to assess the validity and reliability of the equipment and method. The height limi-

tation of the XSENSOR mat was discovered and exclusion criteria were implemented. During acquisition in the pilot the participants feet were immobilised to prevent movement. However this was not carried forward in to the main study so participants' feet were in their natural position. This was to better assess their level of comfort, and get a true baseline reading.

Data collection

Quantitative – The XSENSOR equipment was securely fixed onto the imaging surface with tape to ensure that it remained in place during data acquisition. Once secure, the pressure mat was not removed or repositioned until the full sample had been acquired. The pressure mat was checked to ensure that it worked to the manufacturer's specifications, at this time some artefacts in the data were noted and recorded for further evaluation. Participants signed up at a mutually convenient time to participate in the study. The participants were given the opportunity to read the information sheet, and to ask questions or seek clarification. Subsequently, participants were asked to sign a consent form.

Participants were asked to change into a pair of leggings and two t-shirts. This was to respect participants' privacy and standardise clothing. Fader et al¹² established that different clothing has different impacts on interface pressure and advised that studies involving interface pressure measurements should have standardised clothing. The height and weight of the participants were measured and recorded prior to acquisition. Participants were then asked to lie supine on the pressure mat with their hands pronated. Positioning of participants was checked to ensure they were lying straight, in the centre of the mat.

A similar study by Stinson et al³ measured interface pressure over a 20 minute sitting period and established that the pressure values change significantly over the first 6 minutes, this increase in pressure values may be due to creep. Six minutes were anticipated by Stinson et al to be an optimal settling time prior to interface pressure measurement. A settling time of 6 minutes was used in this study, to reduce measurement error.

A supervisor from the research team was present at each acquisition to monitor participants and equipment.

Qualitative – The patient experience in the clinical setting is of paramount importance, and a number of studies and reviews recommend that further work should be done in this area to explore personal opinions¹³. Following pressure data acquisition participants were asked to complete a question-

naire devised by the research team, it included five questions, two of which were on a five-point Likert scale. These two questions consisted of numerical descriptions with verbal anchors. In a cross-national setting, there is the potential for reliability error due to differences in knowledge, perceptions and familiarity with research instruments¹⁴. In this study the participants were assisted in completing the questionnaire by a member of the research team to assist in definitions and clarity.

Data analysis

From the data acquired for participants on each of the surfaces the average pressure and the peak pressure in mmHg of the whole body and the areas of interest (head, sacrum and heels) were calculated. When taking the average readings, of the sacrum, the lower limit of the pressure was set to 32mmHg, as this represents the value from which the pressure may influence the formation of Pus¹⁵. Objective data analysis was achieved by selecting and averaging 30 frames per person on both surfaces in order to ensure the reliability of results therefore verifying the non-existence of data changes obtained due to the performance of the equipment. The peak pressure measurements, of the sacrum, were collected by selecting an area of 3x3 cells with the highest pressure value in the centre, in order to calculate the mean peak value¹⁶. SPSS version 22 was used to assess normal distribution of data using histograms and Shapiro-Wilk tests. In the second phase, the average pressures of both the mattress and the X-ray table were compared using a paired t-test. Measures of the average and peak pressures were taken at the triple jeopardy areas and a comparison between the three individual areas on both surfaces were made using a paired t-test. Finally, a qualitative analysis was made in order to verify the relationship between the pain experience in the triple jeopardy areas during the experiment and the average pressure obtained in those areas. A Wilcoxon test was used to compare the level of pain in each of the triple jeopardy areas and the overall comfort of the participants.

RESULTS

Quantitative -

The data sample of 30 healthy participants was analyzed. The sample included 24 females (80%) and 6 males (20%) with an age range from 19 to 51 (mean=25.77; SD=7.72) and a BMI range from 18.7 to 33.6 (mean 24.12; SD=3.29). The

average pressure of both surfaces is presented in Table 1. The results indicate a significant difference ($P<0.001$) in average IP between the different imaging surfaces showing a higher average pressure on the X-ray table with a mean difference of 11.95mmHg (Figure 1). In the measurements of average and peak pressures of the triple jeopardy areas (Table 1, Graphic 1 and 2) the pressure reduction was found to be statistically significant in all three areas for the different surfaces ($P<0.001$). In both the peak and average pressure measurements, it was found that the pressure is higher on the X-ray table than in the density scanner with a mattress (Figure 2). For peak pressure the mean differences achieved for each area were 96.06mmHg (head), 117.61mmHg (sacrum) and 85.30mmHg (heels) and the differences obtained for the average pressures were 53.19mmHg, 19.18mmHg and 38.11mmHg respectively. There was no correlation between BMI and average pressure ($r^2=0.029$).

Table 1: Interface pressure measurements on the whole body, average and peak values for the triple jeopardy areas

	Siemens MULTIX Pro X-ray table without a mattress	Norland XR-36 bone density scanner with a mattress	P value
Total Average Pressure	43.04 ± 3.75	31.09 ± 2.34	<0.0001
Peak pressure measurements			
Peak Head	159.72 ± 45.88	255.77 ± 1.18	<0.0001
Peak Sacrum	97.65 ± 36.14	215.26 ± 54.6	<0.0001
Peak Heels	161.56 ± 63.02	246.87 ± 32.51	<0.001
Average Pressure measurements			
Average Head	53.92 ± 14.42	107.11 ± 19.29	<0.0001
Average Sacrum	48.83 ± 5.25	68.01 ± 10.09	<0.0001
Average Heels	58.36 ± 19.54	96.48 ± 26.28	<0.0001

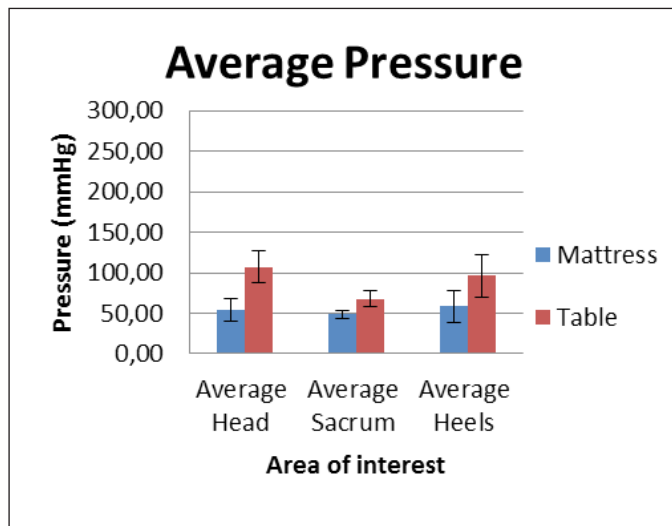


Figure 1: Graph comparing average pressure in mmHg for each of the jeopardy areas for both the mattress and the x-ray table. Inc standard deviation.

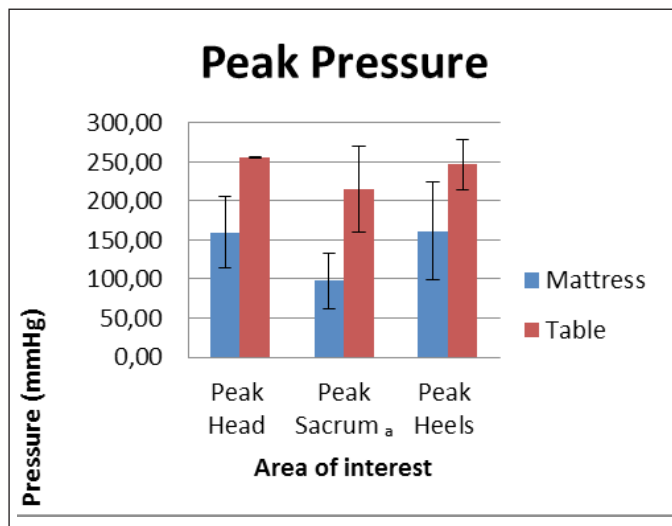


Figure 2: Graph comparing peak pressure in mmHg for each of the jeopardy areas for both the mattress and the x-ray table. Inc standard deviation. ^a Mean peak of the 3x3 area.

Qualitative -

The comfort levels between the mattress and the X-ray table varied, 50% of the participants found the surface with a mattress was comfortable or very comfortable, compared to the X-ray table where only 23% found the mattress comfortable or very comfortable. 10% of participants described the X-ray table as very uncomfortable, whereas none of the participants scored the mattress as very uncomfortable.

There is a significant difference in the pain experienced in the sacrum and head ($P < 0.001$) between the two surfaces. The participants experienced more pain in the head when lying on the X-ray table compared to the other areas of inter-

est. For the other jeopardy areas the pain experienced by the participants was higher for the hard surface as well.

DISCUSSION

The results obtained in our study confirm that the average IP for whole body and average of the triple jeopardy areas were higher in the hard surface. All of the IP values recorded for the mattress surface showed an improvement when compared to the hard surface. From this we can say that with the inclusion of radiolucent mattresses average pressure of the jeopardy areas can be reduced below the accepted benchmark of 90mmHg, the bony prominences may need a thicker or higher specification mattress¹³. Although most jeopardy area values recorded from both surfaces still exceed the standard for a hospital mattress (60mmHg). The mattress surface provides a more even distribution of pressure in the jeopardy regions; this is comparable to a previous study that found greater distribution to be in agreement with the conclusion, that higher specification surfaces reduce the incidence of PUs, proposed in a recent Cochrane analysis (Moysidis).

The open-ended questions revealed themes of movement and loss of sensation, a number of the participants highlighted that they had 'twitched' or were 'shocked', suggesting that they had moved during the 20 minutes which in practice may have a negative impact on image quality. More participants had a sensation of 'numbness' on the mattress surface, this is an issue that needs further work as loss of sensation is another risk factor for the formation of PUs (NICE CG 179, Cochrane review).

The participants found the mattress surface to be overall more comfortable ($P = 0.015$) and less painful in the head and sacrum, this is comparable with the findings of King and Bridges. When asked if the participants felt like moving 22 said yes on the mattress surface, whereas only 19 said yes on the hard surface, implying that although the mattress appears to reduce discomfort and interface pressure participants were more inclined to move. More research needs to be done to look at the movement of patients, on various surfaces, during radiography image acquisition.

Limitations

This study included only healthy participants; it is recommended that further work be undertaken with samples including at risk patients.

The Norland XR-36 bone densitometry scanner is out-

dated equipment and may not be found in most radiology departments. Nevertheless the findings of this study are likely to be comparable to imaging surfaces with thin radiolucent mattresses. Further research exploring interface pressure on other surfaces often used in radiology is recommended.

CONCLUSION

A significant difference in average interface pressure is demonstrated between imaging surfaces, justifying the need for further investigation into pressure reducing surfaces and overlays in the radiographic context. A mattress surface reduces both average and peak interface pressures on the whole body and the three jeopardy areas. Therefore

it can be assumed that the use of a mattress will reduce the probability of developing pressure ulcers. There is a significant difference in pain and comfort assessment between the two surfaces, which also supports the findings in favour of using radiolucent mattresses or supports (pillows, props, foam pads) where possible.

ACKNOWLEDGEMENTS

The authors would like to thank, Erasmus for funding, The Nuffield Foundation, and Sumed International for the loan of the pressure mat. Thanks are also extended to all participants who gave their time.

REFERENCES

- Westbrook C, Roth CK. MRI in practice. 4th ed. Wiley-Blackwell; 2011.
- Dharmarajan TS, Ugalino JT. Pressure ulcers: clinical features and management. *J Am Med Assoc.* 2006;296:974-84.
- Stinson MD, Porter-Armstrong AP, Eakin PA. Pressure mapping systems: reliability of pressure map interpretation. *Clin Rehabil.* 2003;17(5):504-11.
- Gil-Agudo A, De la Peña-González A, Del Ama-Espinosa A, Pérez-Rizo E, Díaz-Domínguez E, Sánchez-Ramos A. Comparative study of pressure distribution at the user-cushion interface with different cushions in a population with spinal cord injury. *Clin Biomech (Bristol, Avon).* 2009;24(7):558-63.
- Peterson MJ, Gravenstein N, Schwab WK, van Oostrom JH, Caruso LJ. Patient repositioning and pressure ulcer risk: monitoring interface pressures of at-risk patients. *J Rehabil Res Dev.* 2013;50(4):477-88.
- Trewartha M, Stiller K. Comparison of the pressure redistribution qualities of two air-filled wheelchair cushions for people with spinal cord injuries. *Aust Occup Ther J.* 2011;58(4):287-92.
- Lewis-Beck MS, Bryman A, Liao TF. Encyclopedia of social science research methods. Sage; 2013.
- Rugg G, Petre M. A gentle guide to research methods. London: Sage; 2006.
- Wakita T, Ueshima N, Noguchi H. Psychological distance between categories in the Likert scale: comparing different numbers of options. *Educ Psychol Meas.* 2012;72(4):533-46.
- Preston CC, Colman AM. Optimal number of response categories in rating scales: reliability, validity, discriminating power, and respondent preferences. *Acta Psychol (Amst).* 2000;104(1):1-15.
- Brace I. Questionnaire design. London: Kogan Page; 2004.
- Fader M, Bain D, Cottenden A. Effects of absorbent incontinence pads on pressure management mattresses. *J Adv Nurs.* 2004;48(6):569-74.
- King C, Bridges E. Comparison of pressure relief properties of operating room surfaces. *Perioper Nurs Clin.* 2006;1(3):261-5.
- Parameswaran R, Yaprak A. A cross-national comparison of consumer measures. *J Int Bus Stud.* 1987;18:35-49.
- Kosiak M. Etiology of decubitus ulcers. *Arch Phys Med Rehabil.* 1961;42:19-29.
- Hemmes B, Brink PR, Poeze M. Effects of unconsciousness during spinal immobilization on tissue-interface pressures: a randomized controlled trial comparing a standard rigid spineboard with a newly developed soft-layered long spineboard. *Injury.* 2014;45(11):1741-6.

PAEDIATRIC PELVIS – CU FILTRATION

Review article – A narrative review on the reduction of effective dose to a paediatric patient by using different combinations of kVp, mAs and additional filtration whilst maintaining image quality

Charlotte Bloomfield^a, Filipa Boavida^b, Diane Chabloz^c, Emilie Crausaz^c, Elsbeth Huizinga^d, Hanne Hustveit^e, Heidi Knight^a, Ana Pereira^b, Vanja Harsaker^e, Wouter Schaake^d, Ruurd Visser^d

a) School of Health Sciences, University of Salford, Manchester, United Kingdom

b) Lisbon School of Health Technology (ESTeSL), Polytechnic Institute of Lisbon, Portugal

c) Haute École de Santé Vaud – Filière TRM, University of Applied Sciences and Arts of Western Switzerland, Lausanne, Switzerland

d) Department of Medical Imaging and Radiation Therapy, Hanze University of Applied Sciences, Groningen, The Netherlands

e) Department of Life Sciences and Health, Radiography, Oslo and Akershus University College of Applied Science, Oslo, Norway



KEYWORDS

Paediatric pelvis
Additional filters
Low kVp, mAs
Dose
CR

ABSTRACT

This paper reviews the literature for lowering of dose to paediatric patients through use of exposure factors and additional filtration. Dose reference levels set by The International Commission on Radiological Protection (ICRP) will be considered. Guidance was put in place in 1996 requires updating to come into line with modern imaging equipment. There is a wide range of literature that specifies that grids should not be used on paediatric patients. Although much of the literature advocates additional filtration, contrasting views on the relative benefits of using aluminium or copper filtration, and their effects on dose reduction and image quality can vary. Changing kVp and mAs has an effect on the dose to the patient and image quality. Collimation protects adjacent structures whilst reducing scattered radiation.

INTRODUCTION

It is the responsibility of the radiographer to select the correct exposure factors to produce an image that is diagnostically acceptable whilst maintaining a reasonably low dose to the patient¹. Ionising radiation has been shown to cause cancer since early in the use of medical imaging². Whilst children are developing, their cells are rapidly dividing, making them more predisposed to increased DNA damage and malignant changes later in life³. It has been estimated that radiation exposure in the first 10 years of life has an attributable lifetime risk⁴, therefore dose is of high consideration especially in paediatric examinations. It is important to ensure dose is kept as low as reasonably achievable (ALARA)⁵ as stated in the ICRP guidance⁶, whilst maintaining acceptable image quality.

Due to the associated risks of ionising radiation, it is essential to try and find optimal exposure / acquisition factors and if required additional filtration to reduce dose. Research has shown that additional filtration of 0.2mm of copper (Cu) can reduce dose by up to 40%⁷. Filtration works by hardening the beam, meaning more useful X-rays reach the image receptor and the low energy X-rays are filtered out without being detrimental to image quality. Uffmann and Schaefer-Prokop state that standard tube filtration in diagnostic radiology, as required by regulations, is 2.5mm of the aluminium (Al) equivalent⁵.

Diagnostically acceptable image quality does not mean as good as possible, but rather as good as is needed. Exposure factors can be manipulated to achieve a low dose with diagnostically acceptable image quality; this can be achieved by

altering kVp and mAs. This review article concentrates on literature relating to analysing ionising radiation dose and diagnostic image quality in paediatric pelvis imaging.

This paper reviews evidence about cancer risks, the effects of changing acquisition parameters (eg kVp, mAs, grid, collimation and copper filtration) and the influence this has on patient dose. Visual and physical evaluation of image quality, dose estimation (Monte Carlo) and diagnostic reference level will be discussed.

The search strategy for literature was peer reviewed journal articles from PubMed. Additional material used was Grey literature, professional guidelines, and international standard documents

Key Words			
Paediatric pelvis	Low kVp, mAs	PCXMC	Collimation
Paediatric cancer	Dose	2AFC	Dose
Additional filters	Image quality	ImageJ	CR
Copper			

Cancer risks in paediatric imaging

Since the discovery of the risks of using X-ray imaging there has been a debate on optimising the image quality and minimising dose. Because of this, the concept of ALARA was developed. This is to protect the patient so that an image is obtained that is adequate for diagnostic purposes, whilst the radiation dose is kept as low as reasonably achievable⁸. In paediatric imaging there can be a higher risk of developing cancer from X-ray imaging through stochastic effects, because children are expected to live longer than adults. In addition they have a more rapid cell division, which makes them more sensitive to radiation⁹. This causes an awareness of lowering the radiation dose in X-ray imaging, especially for children. The necessity of the image needs to be higher than the risks of taking it^{5,10}, that is, the examination needs to be justified. The pelvis examination is a common region with high dose, compared to other radiographic exposures. One pelvis image has the same effective dose as 35 chest images⁸, causing more concern in children, particularly of dose to the gonads. The pelvis area has organs and tissues that are highly radio-sensitive⁶.

Changing parameters to lower the dose – kVp, mAs and grid

Radiographers can change a number of exposure factors, including kVp and mAs; these regulate the X-ray beam quantity, thereby affecting the patient dose and quantity of radiation received by the image receptor¹. Changes in these

factors must be performed cautiously because it is important to perform examinations according to the philosophy of ALARA. Therefore optimisation is a balance between the risk of the ionising radiation exposure and the advantage of the diagnostic imaging to the patient¹⁰. The increase of kVp and mAs result in an overall increase of patient dose and also result in more signal reaching the detector that should reduce the noise in the image and improve the SNR¹⁰. According to European Guidelines the parameters advised for paediatric pelvis X-ray in AP projection are 60 – 70 kV and < 10ms¹¹. The anti-scatter grid is used to filter out the scattered photons, thereby improving the quality of the image by increasing the contrast. However, the dose to the patient can be increased by a factor of two compared with not using a grid^{10,12}. In paediatrics, the use of a grid is not recommended, the proportion of diffused radiation is much lower and therefore has no impact on the quality of the image¹². In cases where high voltages are used then a grid must be used; it is suggested the grid be composed of materials with low attenuation such as carbon fibre or non-metallic materials¹¹. In practice, the proportion of diffused radiation is so small that the grid is not used for paediatric patients, as dose increases unnecessarily¹⁰.

*In previous studies, a steep increase in dose was observed in a group of children aged 3–7 years due to the use of the grid*⁴. However, for children over 15 a significant increase in image quality is seen when a grid is used. *On younger children, the quality of images without grid is considered to be of an acceptable diagnostic level*¹³.

Collimation

Collimation restricts the X-ray beam to the body part that is to be examined, protecting the adjacent structures from being exposed unnecessarily. It also reduces the scattered radiation that arrives to the detector contributing to an improved contrast resolution and image quality. As the collimation field is reduced so too is the tissue volume irradiated and, as a result, the overall integral dose reduces at the same time as the radiation risks^{14–15}.

Diagnostic reference level and dose lowering

To keep the radiation dose under a maximum level, The ICRP has developed a diagnostic reference level (DRL). There are difficulties developing these levels because all patients are different. Even though the patients' age, gender and thickness of the anatomy being X-rayed is the same, there can be other variations that need to be considered. Furthermore, a child will have tissue with a higher water content than an adult, therefore radiation is absorbed differently. A higher kVp is needed to penetrate an adult for the same thickness¹².

Considering these factors, a scale was devised showing that for a 5 year old child in an AP pelvis examination, there is a maximum of 0.9 mGy expressed in entrance surface dose per image. Some of the factors that can be alternated in lowering the dose is kVp, mAs and filters⁶.

Filtration – Copper 0.1mm and 0.2mm

In most radiological facilities found in practice, there is a recommended filtration of at least 2.5mm of aluminium inside the tube¹¹. Adding an additional filtration can harden the photon beam and reduce the proportion of lower energy radiation. Part of the low-energy radiation is completely absorbed by the patient and is not used for the production of the X-ray image whilst also increasing the dose to the patient unnecessarily. This is why thin sheets of metal such as copper or aluminium are used as additional filtration^{7,11}. Several authors recommend the use of additional filtration rather than decreasing the kVp to reduce patient dose⁵.

Using thin layers of copper can reduce the dose at the entrance to the patients by up to 40% following the body part that is considered⁷. Using 0.1 and 0.2mm copper is suggested and is commonly used in practice for radiographs in paediatric departments⁵. The use of copper is recommended compared to the aluminium because it can absorb a larger proportion of lower energy radiation. However, the disadvantage of the use of copper is the need to increase kVp to compensate for the additional attenuation produced by the filter⁷. According to a previous study, the use of copper provides additional filtration to reduce the dose at the entrance of the skin of the patient, without reducing the image quality. However, the SNR and CNR are affected by the additional copper filtration¹⁶. Yet Brosi et al state that the potential consequences due to reduced contrast from the use of copper filtration are minor in digital imaging systems as contrast can be changed in post-processing¹⁷.

Evaluation of image quality

The ALARA principle states that although dose needs to be kept low, it is important to maintain an image quality that is diagnostically acceptable. Image quality is based on the sharpness of the details, the contrast, the presence or not of noise, the luminance, the distortion, the presence of artefacts or not and most importantly whether the pathology can be seen. Some of these factors can be measured physically and others visually. One of the most commonly used measurable indicators is SNR⁵ which, aside positioning the region of interest, is not dependent on human observer³. Although the SNR is quite basic, it is useful as it includes the noise level, which gives an indication of image quality. High noise

indicates a low quality image and a large SNR indicates an image of high quality. In the literature, the SNR is one of the most used factors⁵.

It is written in the literature that for the comparison of a pelvis X-ray, the most common method is achieved by asking questions about the visibility of a part of an images, such as femoral neck, sacral foramina, sacro-iliac joint and more^{13,18}. The answers often use a Likert scale from 1 to 5: much worse, worse, same, better, much better^{7,13}. It is also possible to rate the image from -2 to +2, in much the same way as the 1 to 5 scale¹⁸. Every image can be evaluated one by one asking every question on each image or to get a reference image and compare each image to it. That last option is adapted to evaluate a large range of images and showing the differences between the two¹⁹.

Estimating dose

Monte Carlo simulations can provide estimates of organ and effective dose (E) for a range of radiographic examinations. Such simulations calculates the patients' organ doses by using the acquisition parameters – tube potential, filtration, focus skin distance, geometry of the X-ray beam – and also the air kerma at the point where the central axis of the X-ray beam enters the patient²⁰. One example is PCXMC software; this provides an accurate estimation of the effective dose to the patient and their potential risks of cancer¹⁷.

Measuring image quality

ImageJ is a program that can display, edit, analyse, process, save and print 8-bit, 16-bit and 32-bit images. This program can calculate area and pixel value statistics of user-defined selections. It can measure distance, angle, create density histograms and line profile plots. It also supports standard image processing functions, such as contrast manipulation, sharpening, smoothing, edge detection and median filtering. ImageJ can also calculate SNR or CNR by choosing one or more specific regions of interest (ROI) in the image. The program uses one ROI for calculating the SNR and two ROIs to measure the CNR²¹.

CONCLUSION

Because of the relative high dose in a paediatric pelvis exam, and the stochastically high risk of developing cancer, this is an important area of interest in research. In radiographic imaging, there will always be an ionising radiation dose, but the goal is to keep this as low as reasonably achievable. With a combination of kVp, mAs, collimation and

additional copper filtration, this can be achieved. It is shown in previous studies that when adding copper filtration, the image quality remains the same or better, with a lower dose.

This is a reason to test dose and image quality in paediatric pelvis exams. To prove that the image quality remains acceptable, it is important to do a visual and physical evaluation.

REFERENCES

- Allen E, Hogg P, Ma WK, Szczepura K. Fact or fiction: An analysis of the 10 kVp “rule” in computed radiography. *Radiography*. 2013;19(3):223-7.
- Parkin DM, Darby SC. Cancers in 2010 attributable to ionising radiation exposure in the UK. *Br J Cancer*. 2011;105 Suppl 2:S57-65.
- Perks TD, Trauernicht C, Hartley T, Hobson C, Lawson A, Scholtz P, et al. Effect of aluminium filtration on dose and image quality in paediatric slot-scanning radiography. *Conf Proc IEEE Eng Med Biol Soc*. 2013;2013:2332-5.
- Gogos KA, Yakoumakis EN, Tsalafoutas IA, Makri TK. Radiation dose considerations in common paediatric X-ray examinations. *Pediatr Radiol*. 2003;33(4):236-40.
- Uffmann M, Schaefer-Prokop C. Digital radiography: the balance between image quality and required radiation dose. *Eur J Radiol*. 2009;72(2):202-8.
- Khong PL, Ringertz H, Donoghue V, Frush D, Rehani M, Applegate K, et al. ICRP publication 121: radiological protection in paediatric diagnostic and interventional radiology. *Ann ICRP*. 2013;42(2):1-63.
- Martin CJ. Optimisation in general radiography. *Biomed Imaging Interv J*. 2007;3(2):e18.
- Linnet MS, Slovis TL, Miller DL, Kleinerman R, Lee C, Rajaraman P, et al. Cancer risks associated with external radiation from diagnostic imaging procedures. *CA Cancer J Clin*. 2012;62(2):75-100.
- Hess R, Neitzel U. Optimizing image quality and dose in digital radiography of pediatric extremities [Internet]. Philips Healthcare; 2011. Available from: http://www.healthcare.philips.com/main/about/events/rsna/pdfs/DR_White_paper_Optimizing_image_quality_and_dose_in_digital_radiography_of_pediatric_extremities.pdf.
- Willis CE. Optimizing digital radiography of children. *Eur J Radiol*. 2009;72(2):266-73.
- Kohn M, Moores B, Schibilla H, Schneider K, Stender H, Stieve F, et al. European guidelines on quality criteria for diagnostic radiographic images in paediatrics. Luxembourg: Office for Official Publications of the European Communities; 1996.
- Alzen G, Benz-Bohm G. Radiation protection in pediatric radiology. *Dtsch Arztebl Int*. 2011;108(24):407-14.
- Martin L, Ruddlesden R, Makepeace C, Robinson L, Mistry T, Starritt H. Paediatric X-ray radiation dose reduction and image quality analysis. *J Radiol Prot*. 2013;33(3):621-33.
- Lança L, Silva A. Digital imaging systems for plain radiography. New York: Springer-Verlag; 2013.
- UPSTATE. Collimation effects [Internet]. New York: State University of New York; 2014 [cited 2014 Aug 19]. Available from: <http://www.upstate.edu/radiology/education/rsna/fluoro/collimation/>
- Hansson B, Finnbogason T, Schuwert P, Persliden J. Added copper filtration in digital paediatric double-contrast colon examinations: effects on radiation dose and image quality. *Eur Radiol*. 1997;7(7):1117-22.
- Brosi P, Stuessi A, Verdun FR, Vock P, Wolf R. Copper filtration in pediatric digital X-ray imaging: its impact on image quality and dose. *Radiol Phys Technol*. 2011;4(2):148-55.
- Tingberg A, Sjöström D. Optimisation of image plate radiography with respect to tube voltage. *Radiat Prot Dosimetry*. 2005;114(1-3):286-93.
- Reis C, Gonçalves J, Klompaker C, Bárbara AR, Bloor C, Hegarty R, et al. Image quality and dose analysis for a PA chest X-ray: comparison between AEC mode acquisition and manual mode using the 10 kVp ‘rule’. *Radiography*. 2014;20(4):339-45.
- Zenone F, Aimonetto S, Catuzzo P, Peruzzo Cornetto A, Marchisio P, Natrella M, et al. Effective dose delivered by conventional radiology to Aosta Valley population between 2002 and 2009. *Br J Radiol*. 2012;85(1015):e330-8.
- Ferreira T, Rasband W. ImageJ User Guide, IJ 1.46r. 2012. Available from: <http://imagej.nih.gov/ij/docs/guide/user-guide.pdf>

Experimental article – Reducing effective dose to a paediatric phantom by using different combinations of kVp, mAs and additional filtration whilst maintaining image quality

Charlotte Bloomfield^a, Filipa Boavida^b, Diane Chabloz^c, Emilie Crausaz^c, Elsbeth Huizinga^d, Hanne Hustveit^e, Heidi Knight^a, Ana Pereira^b, Vanja Harsaker^c, Wouter Schaake^d, Ruurd Visser^d

a) School of Health Sciences, University of Salford, Manchester, United Kingdom

b) Lisbon School of Health Technology (ESTeSL), Polytechnic Institute of Lisbon, Portugal

c) Haute École de Santé Vaud – Filière TRM, University of Applied Sciences and Arts of Western Switzerland, Lausanne, Switzerland

d) Department of Medical Imaging and Radiation Therapy, Hanze University of Applied Sciences, Groningen, The Netherlands

e) Department of Life Sciences and Health, Radiography, Oslo and Akershus University College of Applied Science, Oslo, Norway



KEY WORDS

Paediatric
Pelvis
Additional filters
Dose
Low kVp mAs
CR

ABSTRACT

Purpose: To determine whether using different combinations of kVp and mAs with additional filtration can reduce the effective dose to a paediatric phantom whilst maintaining diagnostic image quality.

Methods: 27 images of a paediatric AP pelvis phantom were acquired with different kVp, mAs and additional copper filtration. Images were displayed on quality controlled monitors with dimmed lighting. Ten diagnostic radiographers (5 students and 5 experienced radiographers) had eye tests to assess visual acuity before rating the images. Each image was rated for visual image quality against a reference image using 2 alternative forced choice software using a 5-point Likert scale. Physical measures (SNR and CNR) were also taken to assess image quality.

Results: Of the 27 images rated, 13 of them were of acceptable image quality and had a dose lower than the image with standard acquisition parameters. Two were produced without filtration, 6 with 0.1mm and 5 with 0.2mm copper filtration. Statistical analysis found that the inter-rater and intra-rater reliability was high.

Discussion: It is possible to obtain an image of acceptable image quality with a dose that is lower than published guidelines. There are some areas of the study that could be improved. These include using a wider range of kVp and mAs to give an exact set of parameters to use.

Conclusion: Additional filtration has been identified as a major tool for reducing effective dose whilst maintaining acceptable image quality in a 5 year old phantom.

INTRODUCTION

It is the responsibility of the radiographer to select the correct exposure factors to produce an image that is diagnostically acceptable whilst maintaining a reasonably low dose to the patient¹. Ionising radiation has been shown to cause cancer from its early use². Whilst children are developing, their cells are rapidly dividing compared to adults, making them more predisposed to increased DNA damage and malignant changes later in life³. It has been estimated that radiation exposure in the first 10 years of life has an attributable lifetime risk⁴ therefore dose is of high consideration especially in paediatric examinations. It is important to

ensure dose is kept as low as reasonably achievable (ALARA)⁵ as stated in the International Commission on Radiological Protection (ICRP) guidance⁶, whilst maintaining image quality.

Due to the associated risks of ionising radiation, it is essential to optimize image quality. This can be achieved by altering exposure factors and using additional filtration. Filtration works by hardening the beam, meaning more useful X-rays reach the image receptor and the low energy X-rays are filtered out without reducing image quality⁵. Using copper filtration has been shown to be more efficient and filter more lower energy photons than by using aluminium

filtration⁷. Research also demonstrates that additional filtration of 0.2mm Cu can reduce dose up to 40%⁸.

Dose reference level have been set by the ICRP⁶ because of the wide variations in patients’ habitus. However the guidance was put in place in 1996 and requires updating to come into line with modern imaging and acquisition equipment.

This article investigates dose and image optimization in relation to use of copper filtration, for paediatric pelvis imaging.

MATERIALS AND METHODS

Material

To simulate a paediatric pelvis a phantom (ATOM Dosimetry Verification Phantom Model 705)¹⁰, was used with the characteristics of a 5 year old child.

The images were produced by varying kVp and mAs in set combinations based on European guidelines¹⁰. Copper filtration was also varied: none; 0.1mm; and 0.2mm⁹ (Table 1). In total 27 images were acquired.

Table 1: Set combinations with kVp, mAs and copper filtration

kVp Filters	50	60	70
None	5/ 3.6/ 2.2 mAs	5/ 3.6/ 2.2 mAs	5/ 3.6/ 2.2 mAs
0.1mmCu	5/ 3.6/ 2.2 mAs	5/ 3.6/ 2.2 mAs	5/ 3.6/ 2.2 mAs
0.2mmCu	5/ 3.6/ 2.2 mAs	5/ 3.6/ 2.2 mAs	5/ 3.6/ 2.2 mAs

A SIEMENS POLYDOROS IT 30/55/65/80 X-ray unit combining an OPTILIX 150/30/50C X-ray tube with an inherent filtration of 1.0mm aluminium were used. Images were acquired using an Agfa CR 24 x 30 image receptor and processed in an Agfa CR 35-X digitizer. All equipment was subject to regular quality control tests and the results fell within manufacturer specifications.

Images were acquired in the AP standing position without using air gap technique. An SID of 115cm was used and the collimation field size 21.8cm by 18.6cm at the image receptor. The phantom was not moved throughout the image acquisition to ensure the positioning and tube parameters

remained the same. No grid was used as this is not standard practice in paediatric imaging⁸.

Ten participants (5 experienced and 5 student radiographers) took part in the image appraisal using the 2 Alternate Forced Choice (2AFC) software. Images were displayed on a dual LCD colour monitors system (SIEMENS DSC 1904-D) at 1280 X 1024 resolution. The reference image remained fixed on one monitor and the 27 acquired images were viewed randomly on the second monitor. Each participant performed the image appraisal twice. Image appraisal was performed with a low level of ambient light, in accordance with the European Guidelines¹⁰.

Visual image quality analysis

The reference image was agreed by a small focus group as being the lowest acceptable image quality so that any image that scored below the reference image could be excluded. The criteria for choosing the reference image were selected from the European Guidelines¹⁰ (Table 2).

Table 2: Pelvis image criteria

Item	Pelvis image criteria
1.	Symmetrical reproduction of the pelvis
2.	Visualization of the sacrum and its intervertebral foramina
3.	Reproduction of the necks of the femora which should not be distorted
4.	Visualization of the trochanters consistent with age
5.	Reproduction of spongiosa and cortex

To evaluate visual image quality, 2AFC software was used with a series of three questions for each image, with the purpose of observing three separate areas of the pelvis and scoring them. The questions focused on the right hand side of the pelvis as this was the location of the ROI. The questions were selected from previous research that used similar methods^{8,11} excluding the soft tissue questions because the phantom did not contain tissue (Table 2).

A 5 point Likert scale was used so that each of the five responses had a numerical value which was used to score each image (Table 3). To measure image quality an average score was obtained from each image.

Table 3: Criteria used for evaluation

Questions	
How well can you visualize the right femoral neck?	
How well can you visualize the right sacro iliac joint?	
How well can you visualize the sacral foramina?	
Likert Scale	Numerical Scale
Much worse than	1
Slightly worse than	2
Equal to	3
Better than	4
Much better than	5

Physical image quality assessment

To measure physical image quality, SNR and CNR calculations were performed. Both programs used the right side of the pelvis to perform the calculation as it was clearer to visualise the structures and place the region of interest (ROIs).

SNR and CNR calculations were made using ImageJ software, by placing a ROI on two contrasted homogeneous structures of the simulated soft tissue and femoral head. The ROI was placed in the same location on all 27 images to get a true value for comparison.

To compare the dose of each image, a DAP reading was taken and the PCXMC software was used to calculate the effective dose as a comparison with image quality.

Visual acuity

Adequate eyesight is essential to make accurate interpretations for optimal patient care and cannot be compensated with technology¹². Although the observers' training, experience, viewing time and distance from the image are important variables, visual acuity is relatively easily to measure and correct¹³. Therefore, to ensure the ten participants had normal visual function, eye tests were performed before the image appraisal. Participants received a visual assessment, including visual acuity (ETDRS chart – CSV 1000 and LogMAR Good-Lite chart), contrast sensitivity (CSV-1000E) and stereopsis (Randot). As it is shown on appendix 1, all participants were within the normal stand-

ards, therefore all qualify to participate in the research.

Statistical analysis

To investigate the intra-rater reliability the data for the different assessments for each observer were compared by means of the Intraclass Correlation Coefficient (ICC). To investigate the inter-rater reliability the mean scores of both assessments for each observer were compared with the mean scores of the other observers by means of the ICC.

Intra-rater reliability (timepoint 1 vs. timepoint 2)	Intraclass correlation coefficient	P-value
Observer 1	0.587	0.001
Observer 2	0.890	0.001
Observer 3	0.905	0.001
Observer 4	0.945	0.001
Observer 5	0.786	0.001
Observer 6	0.840	0.001
Observer 7	0.850	0.001
Observer 8	0.925	0.001
Observer 9	0.849	0.001
Observer 10	0.916	0.001
Mean	0.849	0.001
Inter-rater reliability	0.872	0.001

R E S U L T S

Intra- and inter-rater reliability

The intra-rater reliability of all observers was high (ICC > .79), except for observer 1 (ICC=0.587). The inter-rater reliability, the agreement between observers, was also high (ICC=0.872) (Table 4).

Image quality

Figures 1 to 5 have points that have specific meanings, the blue points represent the experimental images, the red point represents the image with the lowest acceptable image quality and the green point represents the image with the standard parameters.

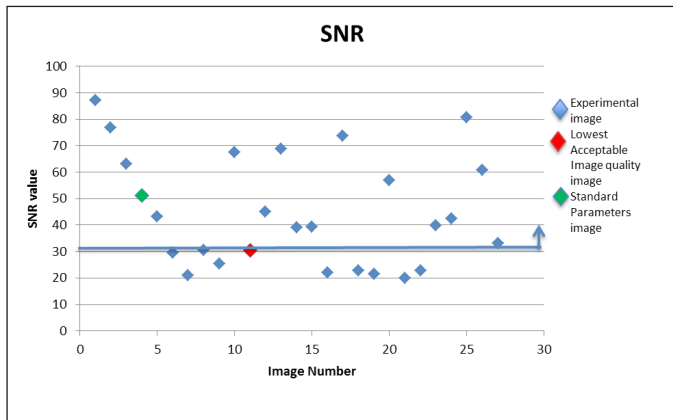


Figure 1: SNR from each image. The images above the line have acceptable image quality. The green (I) is the standard parameter image and the red (I) is the lowest acceptable image quality level.

Figure 1 shows that 18 out of the 27 images (66.7%) have a SNR score above or the same as the lowest acceptable image quality level.

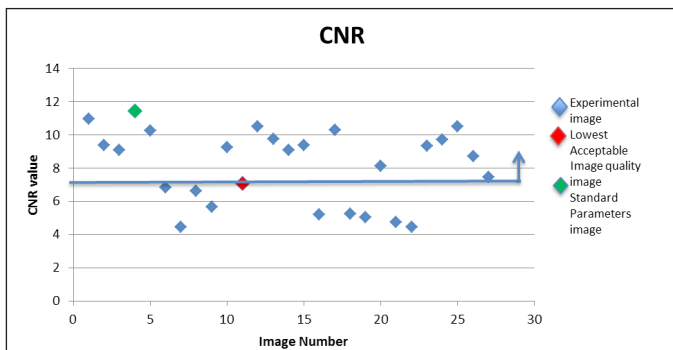


Figure 2: CNR from each image. The images above the line have acceptable image quality. The green (I) is the standard parameter image and the red (I) is the lowest acceptable image quality level.

Figure 2 shows that 18 out of the 27 images (66.7%) have a CNR score above or the same as the lowest acceptable image quality level.

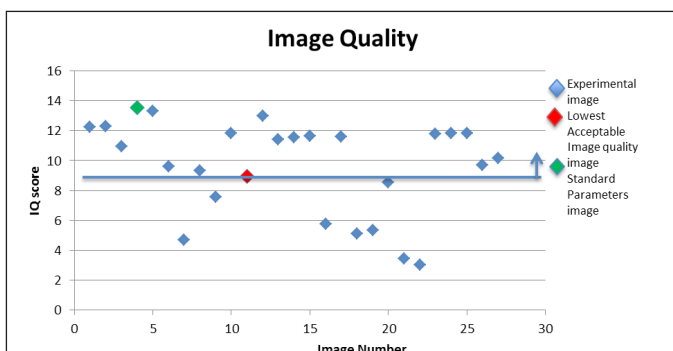


Figure 3: Image quality scores for each image. The green (I) is the standard parameter image and the red (I) is the lowest acceptable image quality level.

Figure 3 shows that 19 out of the 27 images (70.35%) have an image quality score above or the same as the lowest acceptable level, as scored using the visual evaluation. Two images have very low image quality, numbers 21 (70 kVp, 5 mAs and 0.2mm Cu filter) and 22 (70 kVp, 3.6 mAs and no filter).

Dose

Figure 4 shows that 23 out of the 27 images (85.2%) have an effective dose below or the same as that of the image acquired with the standard parameters.

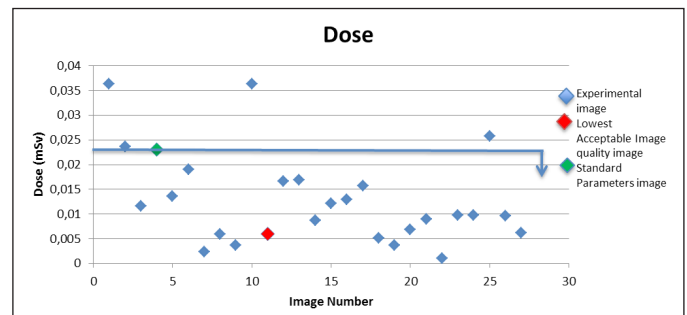


Figure 4: Effective dose (mSv) for each image. The green (I) is the standard parameter image and the red (I) is the lowest acceptable image quality level.

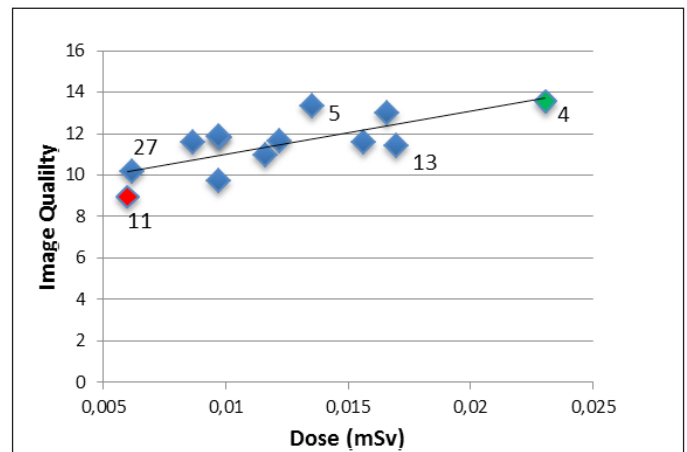


Figure 5: How the dose in mSv increase, in relation to how the image quality increase at the same time.

Using figures 1 to 4, images that were acceptable in every category were identified and only these images were expressed in figure 5.

Figure 5 shows that when dose increases, the image quality also increases, with a correlation coefficient of $R=0.745$. This means that there is a strong relationship between the dose and image quality. This is demonstrated by the image with the standard parameters, produced without any additional filter, having the highest dose

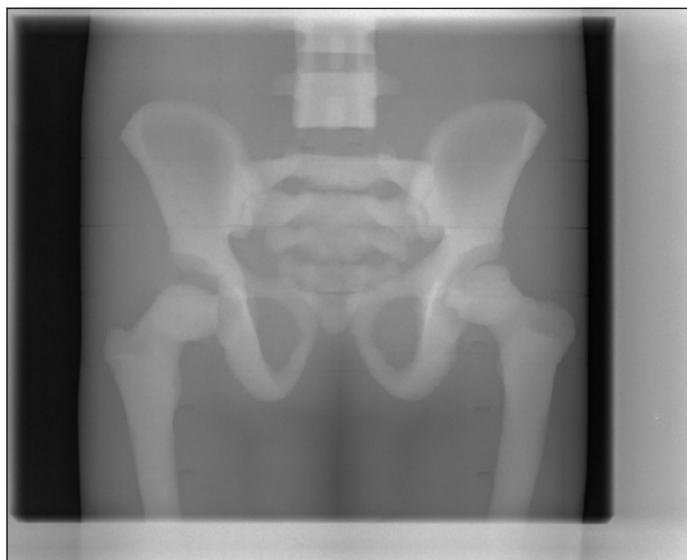


Figure 6: Image with the standard parameters.

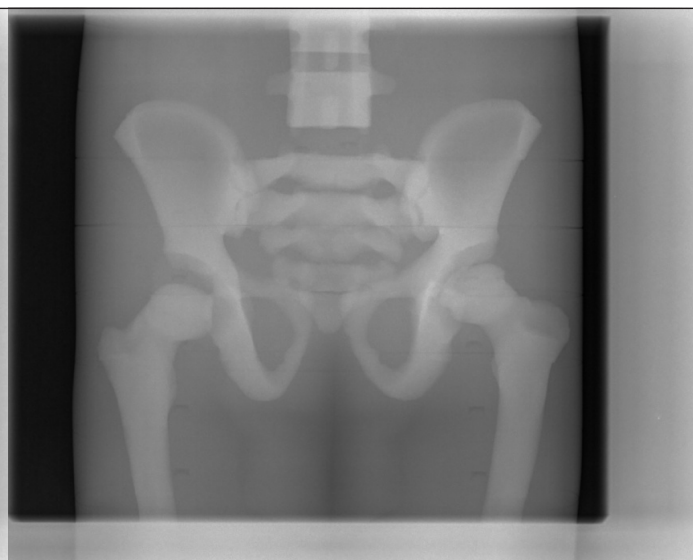


Figure 7: Image 5 (60kVp/3.6mAs/0.1mmCu).

and image quality level. The divergence of the line is not straight. Figure 5 (60 kVp / 3.6 mAs / 0.1mm Cu) has a similar image quality to image 4 (60 kVp / 3.6 mAs / 0mm Cu), but with a lower dose. These images were obtained with the same parameters, with the addition of a 0.1mm filter on figure 5.

Image 27 (70 kVp / 2.2 mAs / 0.2mm Cu) has a better image quality than the lowest acceptable image, image 11 (50 kVp / 5 mAs / 0.1mm Cu) and only a slight increase in dose.

Finally, it is interesting to see that of all the images in figure 5, only 2 of these were produced without additional filtration, images 4 (60 kVp / 3.6 mAs / 0mm Cu) and 13 (50 kVp / 3.6 mAs / 0mm Cu). However, image 4 represents the standard parameters.

DISCUSSION and CONCLUSION

The aim of this study was to reduce effective dose to a paediatric phantom by using different acquisition parameters and additional filtration whilst maintaining image quality. These results suggest that dose reduction is possible by changing kVp, mAs and additional filtration. The final graph shows that 85% of the images that were accepted in all categories were produced using additional filtration.

This research has shown that in practice the use of 50 kVp and filtration instead of 60 kVp and no filtration allows enough image quality (visualized and measured) and decreases the dose.

As expected, the results show that copper filtration is helpful in reducing dose without reducing image quality to an unacceptable standard⁸. From the results it is also clear that 0.1mm of copper filtration is similarly useful to 0.2mm. It can be seen that it is possible to obtain an image of acceptable image quality (13.55 vs 13.3) with a dramatically reduced dose by nearly two (23.05 μ Sv vs 13.55 μ Sv), this is image 5 (60 kVp / 3.6 mAs / 0.1mm Cu). This has important implications for clinical use, as the European Commission guidelines¹⁰ published in 1996 have the potential to be updated to accommodate the possibility of dose reduction by routinely using 0.1mm of Cu filtration on patients of this size. The parameters used to produce this image were 50 kVp and 3.6 mAs with 0.1mm of copper filtration. These are below the recommended parameters¹⁰ in the guidelines with the addition of copper filtration, further suggesting the need for an update of the guidelines.

Another point on the graph that has been highlighted represents an image of higher image quality than the lowest acceptable (10.15 vs 8.95), with only a minor increase in dose (6.18 μ Sv vs 5.98 μ Sv). This is image 27 (70 kVp / 2.2 mAs / 0.2mm Cu). The clinical implications of this are that, for a small increase of 0.2 μ Sv, there is an increase in image quality that is justified. This means that higher quality images can be obtained with an acceptably low dose reducing the potential for repeated examinations due to poor visualisation. In children this is especially relevant, due to their higher risk of malignancy^{2,9} and the gonads in the region of the examination⁶.

Some areas of the study have been identified that could be improved upon. These include using a wider range of kVp

and mAs to give an exact set of parameters to use, rather than a suggestion, which is given here. Another point is that the limits of the kVp tested were quite close together, only altering by 20 kVp. It is possible that another set of parameters outside of these limits produces a diagnostically acceptable image, with a dose lower than ICRP guidelines. Another area for future work is to have a group of observers that includes professionals with higher levels of experience, such as radiologists and reporting radiographers. Their experience may cause them to rate the images differently to the group of observers used here. It would be beneficial to know whether student radiographers can identify poor and good image quality as well as professionals with years of clinical experience.

In conclusion, additional copper filtration has been identified as a major tool for reducing effective dose whilst maintaining an acceptable image quality in a 5 year old phantom. It is suggested that the European Commission guidelines be updated to recommend lower parameters and 0.1mm of copper filtration in patients of this size.

ACKNOWLEDGEMENTS

Carla Lança for eye tests, Elsa Loureiro for laboratory support, Erasmus for funding, participants of the visual evaluation for their time.

REFERENCES

1. Allen E, Hogg P, Ma WK, Szczepura K. Fact or fiction: An analysis of the 10 kVp “rule” in computed radiography. *Radiography*. 2013;19(3):223-7.
2. Parkin DM, Darby SC. Cancers in 2010 attributable to ionising radiation exposure in the UK. *Br J Cancer*. 2011;105 Suppl 2:S57-65.
3. Perks TD, Trauernicht C, Hartley T, Hobson C, Lawson A, Scholtz P, et al. Effect of aluminium filtration on dose and image quality in paediatric slot-scanning radiography. *Conf Proc IEEE Eng Med Biol Soc*. 2013;2013:2332-5.
4. Gogos KA, Yakoumakis EN, Tsalafoutas IA, Makri TK. Radiation dose considerations in common paediatric X-ray examinations. *Pediatr Radiol*. 2003;33(4):236-40.
5. Uffmann M, Schaefer-Prokop C. Digital radiography: the balance between image quality and required radiation dose. *Eur J Radiol*. 2009;72(2):202-8.
6. Khong PL, Ringertz H, Donoghue V, Frush D, Rehani M, Applegate K, et al. ICRP publication 121: radiological protection in paediatric diagnostic and interventional radiology. *Ann ICRP*. 2013;42(2):1-63.
7. Martin CJ. The importance of radiation quality for optimisation in radiology. *Biomed Imaging Interv J*. 2007;3(2):e38.
8. Martin CJ. Optimisation in general radiography. *Biomed Imaging Interv J*. 2007;3(2):e18.
9. Hess R, Neitzel U. Optimizing image quality and dose in digital radiography of pediatric extremities [Internet]. Philips Healthcare; 2011. Available from: http://www.healthcare.philips.com/main/about/events/rsna/pdfs/DR_White_paper_Optimizing_image_quality_and_dose_in_digital_radiography_of_pediatric_extremities.pdf
10. Kohn M, Moores B, Schibilla H, Schneider K, Stender H, Stieve F, et al. European guidelines on quality criteria for diagnostic radiographic images in paediatrics. Luxembourg: Office for Official Publications of the European Communities; 1996.
11. Tingberg A, Sjöström D. Optimisation of image plate radiography with respect to tube voltage. *Radiat Prot Dosimetry*. 2005;114(1-3):286-93.
12. Safdar NM, Siddiqui KM, Qureshi F, Mirza MK, Knight N, Nagy P, et al. Vision and quality in the digital imaging environment: how much does the visual acuity of radiologists vary at an intermediate distance? *AJR Am J Roentgenol*. 2009;192(6):W335-40.
13. Straub WH, Gur D, Good BC. Visual acuity of radiologists: is it time ? *AJR Am J Roentgenol*. 1991;156(5):1107-8.

Appendix A

<i>Visual Function¹</i>	<i>Standard/Average</i>	<i>Participants Results</i>
1. Visual acuity		
<i>Distance</i>	<i>0.0 LogMAR</i>	<i>-0.13 ± 0.07 (20/15) LogMAR²</i>
<i>Near Distance</i>	<i>1 M</i>	<i>0.40 ± 0.00 (20/20) M</i>
3. Contrast Sensitivity		
<i>3 cpd</i>	<i>1.61 ± 0.21</i>	<i>1.84 ± 0.10</i>
<i>6 cpd</i>	<i>1.66 ± 0.23</i>	<i>2.08 ± 0.20</i>
<i>12 cpd</i>	<i>1.08 ± 0.32</i>	<i>1.92 ± 0.11</i>
<i>18 cpd</i>	<i>0.56 ± 0.35</i>	<i>1.45 ± 0.14</i>
2. Stereoacuity	60	40 ± 0.0
¹ All subjects who normally wore corrective lenses were asked to wear them during vision testing.		
² All subjects had best visual acuities LogMAR of 0.0 (20/20) or better for distance		

